Ph.D. Dissertation of Natural Science

Differential functions of the dorsal and intermediate hippocampus in encoding place and its value

장소와 그 가치를 저장하는 배측과 중간 해마의 차별적 역할

August 2021

Graduate School of Natural Sciences

Seoul National University

Brain and Cognitive Sciences Major

Seung-Woo Jin

Differential functions of the dorsal and intermediate hippocampus in encoding place and its value

Inah Lee

Submitting a Ph.D. Dissertation of Natural Sciences

August 2021

Graduate School of Natural Sciences

Seoul National University

Brain and Cognitive Sciences Major

Seung-Woo Jin

Confirming the Ph.D. Dissertation written by

Seung-Woo Jin

August 2021

Chair	이석호
Vice Chair	이인아
Examiner	정민환
Examiner	이상아
Examiner	이도윤

ABSTRACT OF THE DISSERTATION

Differential functions of the dorsal and intermediate hippocampus in encoding place and its value

By

Seung-Woo Jin

Graduate School of Natural Sciences

Seoul National University

Brain and Cognitive Sciences Major

It has long been postulated that the hippocampus is vital for memorizing autobiographical episodic events. Because an episodic event often entails memories for certain places associated with their emotional and motivational significance, it is promising that the hippocampus processes spatial information in conjunction with its associated valence. Among the hippocampal subregions (i.e., dorsal, intermediate, and ventral), the amygdala, which plays key roles in processing valence information, sends direct axonal projection to the intermediate and ventral hippocampus. Also, there are extensive recurrent collaterals and associational projections (presumably spatial information) from the dorsal hippocampus to the intermediate hippocampus. Thus, the intermediate hippocampus may integrate emotional/motivational information in association with locational information. However, it is largely unknown that how the intermediate hippocampus process value-associated spatial information processing. Therefore, I hypothesized that encoding the value of an event at a specific location takes priority in the intermediate hippocampus, compared to the dorsal hippocampus, whose priority resides in representing the precise location of an animal, presumably in the cognitive map. To test this hypothesis, I simultaneously recorded single units from the dorsal and intermediate hippocampus while rats performed a battery of tasks in which the level of motivational significance of a place was controlled by foods with different palatability.

In this dissertation of *Chapter 1*, I examined the changes in spatial firing patterns along

the dorsoventral axis while rats foraged in an open field maze. Specifically, spatially selective firing was more eminent in the dorsal than in the intermediate hippocampus, and spatial signals were hardly observed in the ventral hippocampus. In *Chapter 2*, after changes in reward value during non-mnemonic tasks, differential global remappings of place cells were found between the dorsal and intermediate hippocampus. When more-palatable reward (i.e., sunflower seeds) were replaced with less-palatable one (Cheerios) in a given location, place cells in the intermediate hippocampus remapped immediately. In contrast, place fields recorded from the dorsal hippocampus maintained their spatial representations stably in the same manipulation. In *Chapter 3*, value-dependent remappings were further investigated in hippocampal-dependent tasks. During the place-preference task in the T-maze, place fields obtained from the intermediate hippocampus accumulated near the arm associated with more-preferred rewards, and overrepresented patterns shifted toward opposite arm after the locations of more-preferred and less-preferred rewards were reversed. However, spatial representations of place cells in the dorsal hippocampus were rarely affected by such manipulation. And, during the acquisition of the place-preference task, the ensemble network state in the iHP changed faster than that in the dHP.

Taken together, our results suggest that there are functional segregations between the dorsal and intermediate subregions of the hippocampus. That is, the dorsal hippocampus is specialized in representing the animal's precise locations in the environment, whereas the intermediate hippocampus takes part in the integration of spatial information and its motivational values. These findings imply that the intermediate hippocampus is a functionally significant hippocampal subregion through which critical action-related information (i.e., spatial information from the dorsal hippocampus and emotional/motivational information from the amygdala) is integrated and communicated to the rest of the brain via the medial prefrontal cortex.

Keywords: dorsal hippocampus, intermediate hippocampus, value representation, place cell, remapping

Student number: 2014-21337

TABLE OF CONTENTS

LIST OF FIGURES

LIST OF TABLES

BACKGROUND AND HYPOTHESIS

1.1 BACKGROUND

1.1.1 Episodic memory and hippocampus

The hippocampus is one of the medial temporal lobe structures that is present across all mammalian with its long, curved shape and runs along the dorsoventral (traditionally known as *septotemporal*) axis in rodents, which is corresponding to the posteroanterior axis in primates hippocampus (Grasse, 1955; Insausti, 1993; Stephan and Andy, 1970). Ramón y Cajal (1852-1934) especially took an interest in anatomical drawings of the hippocampus because of its highly organized circuitry (Cajal, 1909). The first milestone of understanding the functions of the hippocampus was revealed by the patient H.M. whose bilateral medial temporal lobes, including the hippocampus, were resected to alleviate the seizure symptom (Scoville and Milner, 1957). After surgery, the H.M. failed to form new episodic memory, which shed light on the functions of the hippocampus in memory encoding. Follow-up researches in human patients whose hippocampus was lesioned produced plentiful evidence of hippocampal functions in encoding and retrieving of certain types of memories (Manns et al., 2003; Squire, 2009; Squire et al., 2010; Wixted et al., 2018). Interestingly, in everyday life, we memorized the episodes if those were associated with certain types of emotions aroused by certain events, such as pleasure or fear (Adolphs et al., 2005; LaBar and Cabeza, 2006; LaBar and Phelps, 1998). This cast doubt on the roles of the hippocampus in processing valence information, presumably from the amygdala (Bermudez and Schultz, 2010; Namburi et al., 2015; Petrovich et al., 2001; Tobler et al., 2005). However, to my knowledge, little is revealed about the neural mechanisms of how the hippocampus associates the episode with its valence information.

1.1.2 Introduction of the rodent hippocampal researches

From the finding of place cells in O'Keefe and Dostrovsky (1971), it has been widely known that the rodent hippocampus is the core system for processing locational information. Subsequently, Okeefe and Nadel (1978) developed *cognitive map theory*, which was first suggested by Tolman (1948). In terms of cognitive map theory, the hippocampus is specialized in the locale system, which takes part in not only recognizing the current location with respect to the allocentric spatial framework but also navigating in space using the highly organized spatial framework (Okeefe and Nadel, 1978). And lots of subsequent studies have found that

spatially tuned cells were found in the hippocampus and parahippocampal, including head direction cells (Taube et al., 1990), boundary cells (Lever et al., 2009), and grid cells (Hafting et al., 2005) (Figure 1-1). Moreover, through radial arm maze (Olton and Werz, 1978) and Morris water maze (Morris et al., 1982), rats whose hippocampus was inactivated or lesioned failed to perform spatial memory tasks, which suggested that the hippocampus is indeed essential for spatial learning and navigation (D'Hooge and De Deyn, 2001; Gilbert et al., 1998; Moser et al., 1993; Moser et al., 1995; Olton, 1987; Packard and McGaugh, 1996; Poucet and Buhot, 1994; Steffenach et al., 2005; Vago and Kesner, 2008; Warburton et al., 2001).

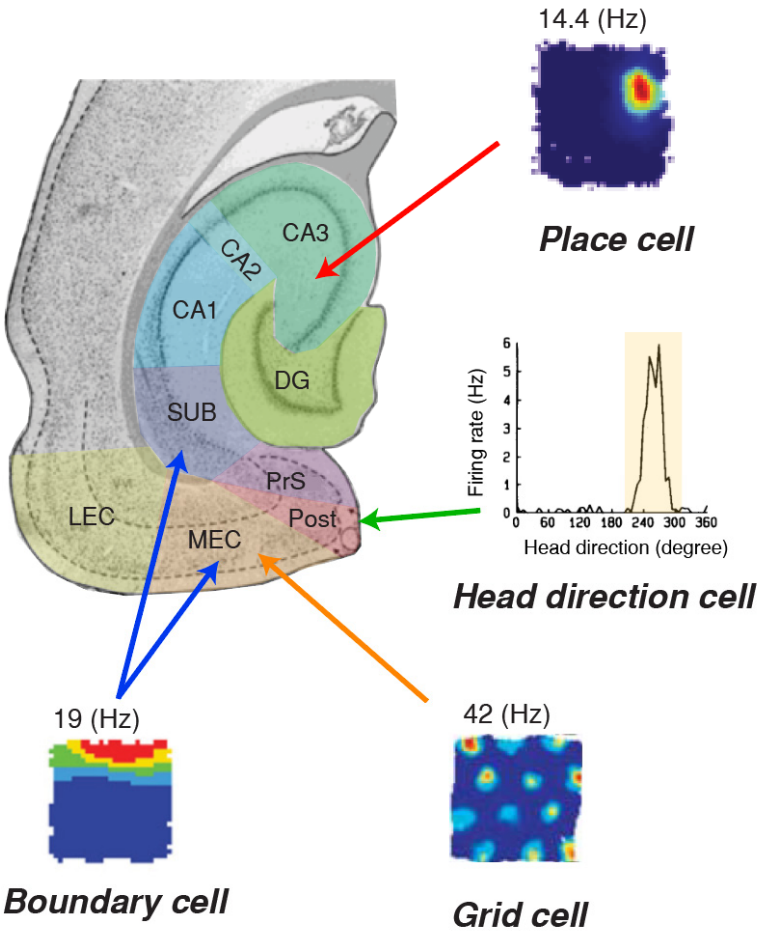

Figure 1-1. Spatially firing cells observed in the hippocampal formation

Abbreviations: DG, dentate gyrus; CA1-3, subfields of Ammon's horn; SUB, subiculum; PrS, presubiculum; Post, postsubiculum; MEC, medial entorhinal cortex; LEC, lateral entorhinal cortex. Head direction cell example is adapted from Taube et al., 1990. Grid cell example is adapted from Hafting et al., 2005. Boundary cell example is adapted from Lever et al., 2009.

1.1.3 Single-cell recording from the rodent hippocampus

In the 1930s, Hodgkin and Huxley, for the first time, directly recorded the action potential from the giant axon of squids by lowering microelectrode inside fiber (Hodgkin and Huxley, 1939). Since then, lots of electrophysiological studies have been conducted and revealed the functions of the brain areas, including findings of receptive fields in the cat's striate cortex (Hubel and Wiesel, 1959). Only relatively recently was it possible to reliably recording of pyramidal neurons of the hippocampus in vivo experiment. This is because hippocampal pyramidal neurons were closely packed together and fired in a complex spiking fashion where the amplitude of the action potential dramatically decreased as much as 50% in the latter spike within a burst (Ranck, 1973). To overcome this difficulty, stereotrode and tetrode, which are made by twisting two or four electrodes, were developed. They utilized the principle that the amplitude of action potential has an inverse relationship of a distance of the electrode from the cell body (Figure 1-2) (Gray et al., 1995; McNaughton et al., 1983b). After stereotrode and tetrode dramatically improved the yield of single-unit recording by increasing the signal-to-noise ratio, numerous in vivo hippocampal studies were followed to examine the functions of the hippocampus.

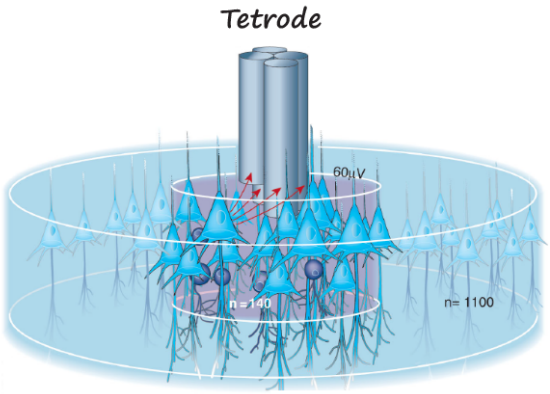

Figure 1-2. Illustration of tetrode recording from the hippocampus

The figure is adapted from Buzsaki (2004).

1.1.3.1 Basic firing properties of place cells

There are well-known fundamental firing characteristics of the place cells. First of all,

the firing rate of place cells is modulated by the speed of an animal's movement during traversing the place field (McNaughton et al., 1983a). Also, when rats passed the same locations on linearized track with opposite directions, place cells fired differentially depending on direction, but this directionality was not observed in the two-dimensional maze (Markus et al., 1995; Muller et al., 1994; O'Keefe and Recce, 1993). In addition, when rats traversed the preferred firing locations, place cells gradually increase their firing rate until reaching the maximal rate position; after then the firing rate was sharply decreased. So, the shape of firing rate by position showed asymmetry (n*egative skewness*) (Mehta et al., 2000). Finally, place cell activities are strongly correlated with theta rhythmic wave (7~12Hz) in that firing consistently began at a certain theta phase as rats entered receptive fields. And then, the spiking phase moved progressively forward on each theta cycle (*phase precession)* (O'Keefe and Recce, 1993; Skaggs et al., 1996).

1.1.3.2 Spatial representation of place cells

Animals, including humans, can recognize their current position both by using allocentric and egocentric information, the former involves the information about the external world, such as a landmark, scene, object, and the latter includes the information generated by self-movement (e.g., vestibular inputs, optic flow, proprioception). Indeed, activities of place cells in the hippocampus were affected by both. For example, when rats randomly foraged inside the cylinder attached with one white cue covering one-fourth of the walls, cells in the hippocampus fired in specific locations. When the cue card was rotated by 90º clockwise, an equal amount of rotations were observed in the place cells, which suggested that the preferred firing location of place cells was determined by relative angular position from the cue cards (Muller and Kubie, 1987). When the color or shape of the recording chamber was changed (i.e., from white to black wall or from square to circular shape) within the same room, place cells were changing their firing rate while remaining in their firing location (*rate remapping*). However, the geometrically same chamber with the same color was tested in two distinctive rooms, preferred firing locations of place cells were completely different from the two rooms (*global remapping*) (Leutgeb et al., 2005). Moreover, place cells can maintain their firing fields even in a totally dark environment (Quirk et al., 1990). Place cells can discriminate two visually identical chambers if rats voluntarily cross over the two chambers (Fuhs et al., 2005; Grieves

et al., 2016; Skaggs and McNaughton, 1998; Tanila, 1999). These results collectively suggest that place cells in the hippocampus maintained their spatial representations using both allocentric information from the external environment and idiothetic information generated inside the animals.

1.1.3.3 Non-spatial representation of place cells

As predicted by Okeefe and Nadel (1978), hippocampal place cells do not merely represent the animal's locations. Instead, they encoded non-spatial features of the environment and cognitive factors within spatial frameworks. Specifically, place cells could fire in certain types of odors or sound frequency when rats were located in the receptive locations of place cells (Aronov et al., 2017; Eichenbaum et al., 1987). Also, neural activities of place cells showed event-related firing patterns, such as approaching the reward port or sniffing the odor (Wiener et al., 1989). Similarly, when rats performed delayed non-match to sample task, place cells selectively fired during the sampling period or choice period (Otto and Eichenbaum, 1992).

The memory of previous traveling path or plan of upcoming choice could also influence place cell activities. For example, when rats traverse the common stem area of T-maze, place cells whose fields fired in differential rates depending on upcoming choice (i.e., left-turn or right-turn; *prospective coding*) (Ferbinteanu and Shapiro, 2003; Wood et al., 2000). Similarly, when place cells were active in rewards zones, firing rates of these cells were modulated by previous traveling path (i.e., start from the north arm or south arm; *retrospective coding*) (Ferbinteanu and Shapiro, 2003).

1.1.3.4 Value representation in the hippocampus

With respect to reward/value representation in the hippocampus, it is still controversial whether the hippocampus is involved in processing value and motivational significance information. In prior literature, place fields can shift their firing locations toward fixed reward locations or displaced reward locations (Breese et al., 1989; Gauthier and Tank, 2018; Lee et al., 2006). In addition, place fields were accumulated near motivationally significant areas (e.g., reward zone or escape platform) (Dupret et al., 2010; Hollup et al., 2001; Mamad et al., 2017). Moreover, it was reported that CA1 represented the action value and outcome value and was critical for

incremental value learning (Jeong et al., 2018; Lee et al., 2012). Overall, these results suggested that the hippocampus is somehow engaged in the process of motivational value information.

However, there are counterstudies arguing that reward value is not represented in the hippocampal place cells. For instance, place cells maintained their original firing fields although the reward location was changed to the opposite arm in a T-maze (Speakman and O'Keefe, 1990). Moreover, place cells could stably maintain their preferred firing locations even after the amount of reward associated with a place was changed (Duvelle et al., 2019; Tabuchi et al., 2003). These results have doubt on whether the hippocampus is indeed involved in the reward and value process.

To my knowledge, until now, most previous studies have focused on the dorsal one-third of the hippocampus [i.e., *dorsal hippocampus* (dHP)], whereas the function of the other ventral two-third of the hippocampus [i.e., *intermediate* (iHP) and *ventral hippocampus* (vHP)] was rarely revealed. Anatomically, the amygdala sends direct axonal projection to both iHP and vHP, but not dHP, and it plays a central role in valence information processing. When considering amygdala-to-iHP/vHP connectivities, it is more feasible that motivational value signals were represented in iHP and vHP than dHP. But, it is largely known how the place cells in iHP and vHP represent motivational values.

1.1.4 Difference in anatomical connectivities along the dorsoventral axis

As abovementioned, the hippocampus has long been known to be divided into three subregions (dorsal, intermediate, ventral) with respect to cortical/subcortical connectivities (Amaral and Witter, 1989; Cenquizca and Swanson, 2007; Gasbarri et al., 1994; Groenewegen et al., 1987; Hoover and Vertes, 2007; Petrovich et al., 2001; Pikkarainen et al., 1999; Risold and Swanson, 1996; Swanson and Cowan, 1977). In dHP, its major cortical inputs originated from the most lateral entorhinal cortex (LEC) and caudomedial parts of the medial entorhinal cortex (MEC) (Dolorfo and Amaral, 1998). And, retrosplenial cortex (RSC) and anterior cingulate cortex (ACC) are major cortical output from the dHP (Cenquizca and Swanson, 2007; Kobayashi and Amaral, 2007; Parvizi et al., 2006; Risold et al., 1997; Roberts et al., 2007; Van Groen and Wyss, 2003; Vogt and Miller, 1983; Wyass and Van Groen, 1992). Also, presubiculum and postsubiculum receive substantial inputs from dHP (Amaral et al., 1991; Swanson and Cowan, 1977; van Groen and Wyss, 1990a; Witter and Groenewegen, 1990). Caudal and mediodorsal-

rostral lateral septum (LS) is also known to be innervated by dHP (Risold and Swanson, 1996, 1997). Lastly, major hippocampal output reaches in rostrolateral nucleus accumbens (NAc) (i.e., NAc core) (Groenewegen et al., 1996; Naber and Witter, 1998), medial and lateral mamillary body (MB), and anterior nucleus of thalamic (ANT) (Ishizuka, 2001; Kishi et al., 2000; Swanson and Cowan, 1975) (Figure 1-3).

Next, although anatomical connections of iHP are relatively unknown compared to dHP and vHP, it has quite different anatomical connections with cortical/subcortical area compared to dHP. Major cortical inputs of iHP originate from relatively medial parts of LEC and more rostral parts of MEC (Dolorfo and Amaral, 1998). Also, iHP receives axonal projections from the amygdala (Petrovich et al., 2001; Pikkarainen et al., 1999). And, its major projections reach in mPFC (denser inputs in the infralimbic cortex) and the intermediate band of LEC and MEC (Cenquizca and Swanson, 2007; Hoover and Vertes, 2007). However, iHP does not project to RSC and ACC as dHP does (Figure 1-3).

Finally, in vHP, it has unique anatomical connectivities with areas that are involved in emotional regulations. The most medial parts of LEC and most rostral parts of MEC send direct inputs to vHP (Dolorfo and Amaral, 1998). And vHP has monosynaptic inputs to mPFC (Chiba, 2000; Hoover and Vertes, 2007; Roberts et al., 2007; Thierry et al., 2000) and olfactory bulb (OB) (Cenquizca and Swanson, 2007; Roberts et al., 2007). In addition, vHP sends axonal projection to subcortical areas, including caudomedial NAc (i.e., NAc shell) (Groenewegen et al., 1996; Naber and Witter, 1998; van Groen and Wyss, 1990b), ventral parts of LS and anteromedial bed nucleus of the stria terminal (BNST) (Canteras and Swanson, 1992; Dong et al., 2001; Risold and Swanson, 1996, 1997), and hypothalamus (Cenquizca and Swanson, 2007; Kishi et al., 2000; Watts et al., 1987) (Figure 1-3).

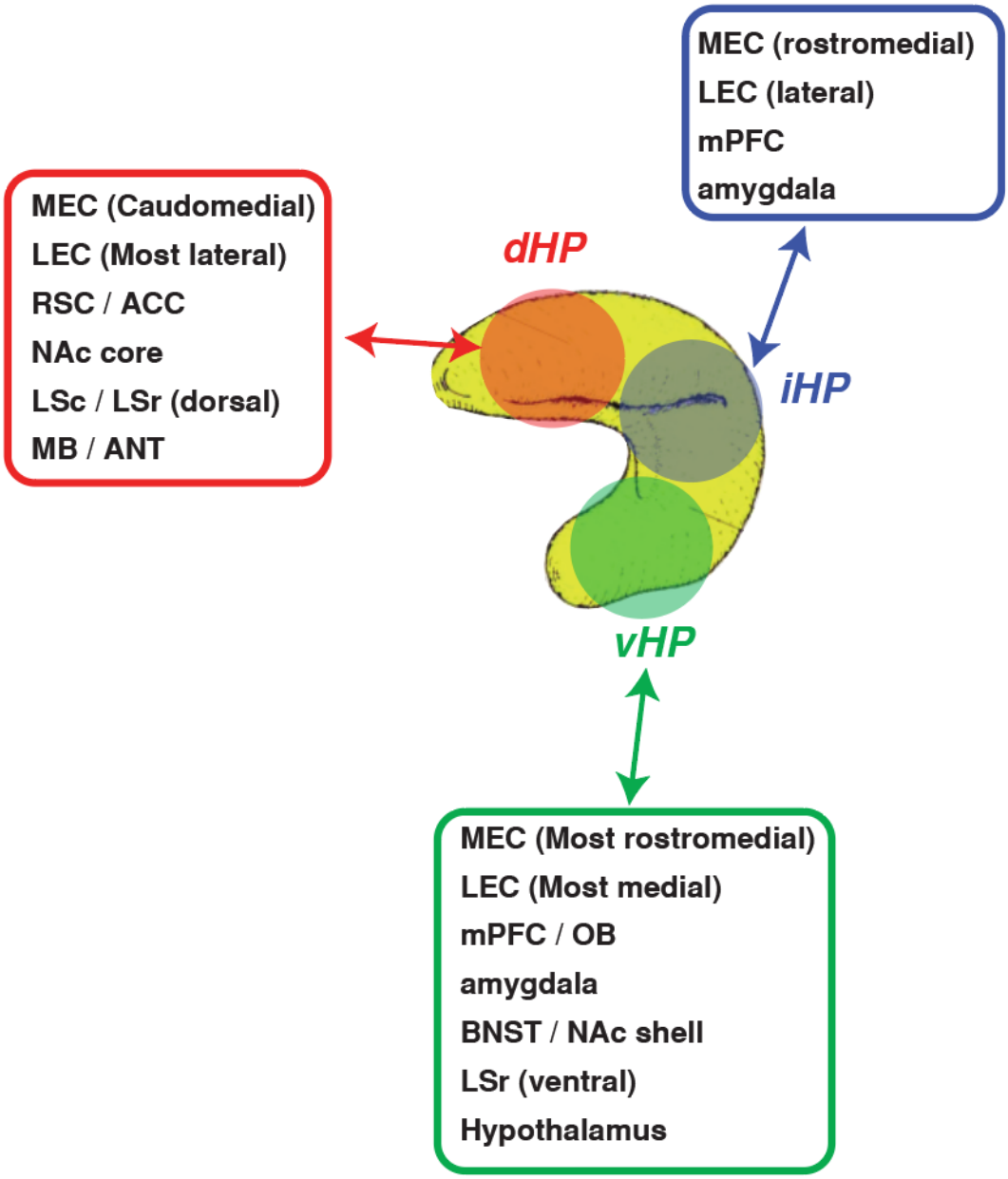

Figure 1-3. Summary of cortical/subcortical connectivities along the dorsoventral axis of the hippocampus

Abbreviations: dHP, dorsal hippocampus; iHP, intermediate hippocampus; vHP, ventral hippocampus; mPFC, medial prefrontal cortex; RSC, retrosplenial cortex; ACC, anterior cingulate cortex; NAc, nucleus accumbens; LSc, lateral septum caudal; LSr, lateral septum rostral; MB, mamillary body; ANT, anterior nucleus of thalamus; BNST, bed nucleus of the stria terminal; MEC, medial entorhinal cortex; LEC, lateral entorhinal cortex.

1.1.5 Difference in functions along the dorsoventral axis

Considering the aforementioned differences in cortical/subcortical connectivity between hippocampal subregions, one may draw a conclusion that there may be fundamental differences in functions along the dorsoventral axis (Moser and Moser, 1998). Indeed, numerous studies have reported that there were significant differences between dHP and vHP. Most importantly, dHP is involved in spatial learning and navigation, whereas vHP is important for the expression of innate anxiety and emotional regulation. For example, when dHP was lesioned or inactivated, rats have difficulty in finding the escape platform in the Morris water maze or arms associated rewards in radial arm maze, whereas lesioning vHP elicit anxiolytic effects with intact spatial memory. That is, vHP-lesioned rats increased tendency to approach the open arm in elevated plus-maze in which normal rats were hesitant to enter (Bannerman et al., 2003; Bannerman et al., 1999; Bannerman et al., 2004; Kjelstrup et al., 2002; Moser et al., 1993; Moser et al., 1995; Richmond et al., 1999). In addition, dHP is engaged in learning the conditional freezing only when an electric shock is associated with the context but not the simple auditory stimuli. In contrast, vHP is important for both context-cued and auditory-cued fear conditioning (Bast et al., 2001; Maren, 1999; Maren and Holt, 2004; Phillips and LeDoux, 1992). Moreover, it has been reported that pyramidal neurons in dHP and vHP have differential firing characteristics in in-vitro and in-vivo experiments. For instance, the whole-cell patch clamping experiment revealed that cells in vHP were intrinsically more excitable than those in dHP (Dougherty, 2020; Dougherty et al., 2012). And, in freely-moving animal experiments, the place field size recorded from vHP was larger than that from dHP (Jung et al., 1994; Kjelstrup et al., 2008). Taken together, there are functional segregations between dHP and vHP on the basis of behavioral and electrophysiological studies.

Recently, the functions of iHP were investigated in terms of its roles in value update of spatial locations or rapid translation of place learning into behavioral performance. Specifically, De Saint Blanquat et al. (2013) performed the place preference task on the cylinder where rats could receive a reward if they successfully navigated towards the goal zone (10cm in diameter). After rats acquired the place preference task, in some days, strobe light was suddenly provided instead of rewards. Normal rats showed inhibition to enter the goal zone in the next trials, not to experience strobe light again. In contrast, iHP-lesioned rats repeatedly enter the goal zone. These results suggest that iHP takes part in updating the value of a place (e.g., from rewarding zone to aversive zone). In another study, Bast et al. (2009) conducted a

spatial learning task in the Morris water maze where rats were required to learn a new hidden platform location daily. They found that iHP should be intact for rats to rapidly (within two trials) learn the spatial memory task among hippocampal subregions (i.e., dHP, iHP, vHP). These results suggested that iHP is essential to translate acquired place information into adaptive behavior rapidly.

1.2 HYPOTHESIS

In light of knowledge from previous literature aforementioned in the background, it is largely unknown how reward and motivational value information are represented outside the dorsal hippocampus, that is, intermediate and ventral hippocampus. It is quite surprising because the intermediate and ventral hippocampus has long been known to be innervated with the amygdala, which takes part in processing the valence information. Thus, in our study, we hypothesized that the intermediate hippocampus integrates spatial and motivational value information based on its unique anatomical connectivities (i.e., spatial information from the dorsal hippocampus and motivational value signals from the amygdala) (Figure 1-4). To test this hypothesis, rats were run in tasks in which various rewards with different degrees of palatability were associated with the locations. Two types of non-mnemonic and mnemonic tasks were performed while single units were extensively recorded along the dorsoventral axis of the hippocampus within one animal.

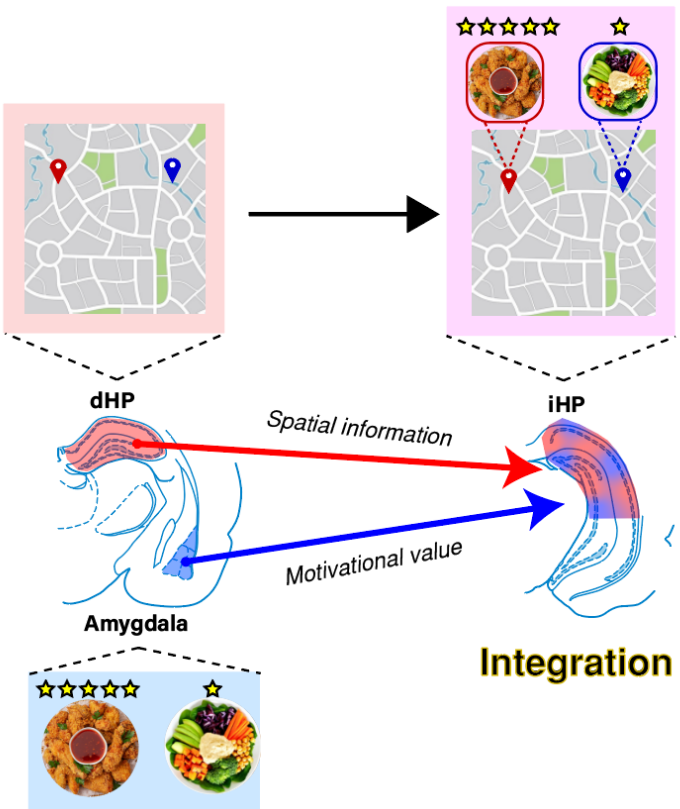

Figure 1-4. Graphical illustration of hypothesis in which iHP would integrate place and its value information

CHAPTER 1

2.1 Introduction

Traditionally, complex-spiking neurons (*place cells*) in the hippocampus were investigated while rats foraged in the square or circular platform to find the scattered small reward (e.g., chocolate sprinkles). Much place cell properties were revealed through an open field platform. In terms of place field size along the dorsoventral axis, it was reported that place cells in vHP had larger place fields than those in dHP (Jung et al., 1994). In Chapter 2, I intended to replicate previous results to verify our experimental setup and recording system, expecting that there might be a spatial gradient from dHP to vHP. Interestingly, we found that spatially selective firings were hardly observed in certain vertical depths from the cortical surface. Thus, we decided to use that depth as the boundary between iHP and vHP when analyzing the experimental data throughout Chapter 1 to Chapter 3.

2.2 Methods

2.2.1 Subjects

Six male Long-Evans rats weighing 300–400g were used for the main experiment. Food was restricted to keep body weight at approximately 85% of free-feeding weight, and water was available ad libitum. Animals were housed in individual cages under a 12-hour light/dark cycle. All protocols and procedures conformed to the guidelines of the Institutional Animal Care and Use Committee (IACUC) of Seoul National University.

2.2.2 Maze familiarization and pre-training

After rats were familiarized with the maze environment for a few days (30 min/d), they were trained to alternate between two adjacent arms of the radial arm maze to get a reward. Rats were trained until they perform a specific criterion (i.e., completing 240 trials in 1 hour), which took about four days (mean, 3.8 days; SD, 1.1 days). At the end of the training, rats were trained to finish 120 trials in 30 minutes, with only two types of rewards: Froot Loops and Cheerios. This procedure was conducted to pre-screen for rats that might not perform enough trials when less-desired rewards were provided.

2.2.3 Surgical implantation of the hyperdrive

A hyperdrive containing 24 tetrodes was implanted for recording single units and local field potentials (LFPs) from the hippocampus. Tetrodes were produced using platinum wires (17.8 μm in diameter). An automatic goal plating device (Nano-Z; Neuralynx) was used to set the final impedance of each tetrode to 130 kΩ (measured in gold solution at 1 kHz). The hyperdrive consisted of two separate bundles, one carrying 18 tetrodes to target iHP and vHP (coordinates for implantation: 5 mm posterior to bregma, 6 mm lateral from midline), and the other containing six tetrodes to target dHP (coordinates for implantation: 3.2 mm posterior to bregma, 3 mm lateral from midline). The bundles were implanted obliquely (5 degrees from the vertical axis) into the hyperdrive frame so that the tetrodes could reach the pyramidal layers as much as possible.

2.2.4 Electrophysiological recording procedures

After one week of the recovery period, rats were placed on a custom-built pedestal outside the experimental room and were habituated to rest during tetrode adjustment. Tetrodes were individually lowered toward the target areas over ~2 weeks. Neural activity was amplified (1,000–10,000 times) and digitized (sampling frequency, 32 kHz; filtered at 600–6,000 Hz for spiking data and 0.1–1,000 Hz for LFP) using a Digital Lynx system (Neuralynx). The rat's head position and head direction were measured using an array of red and green LEDs attached to a custom headstage complex coupled to a preamplifier (HS-36; Neuralynx). A ceiling camera recorded LED lights and fed the signal to a frame grabber (sampling frequency, 30 Hz).

2.2.5 Histological verification of tetrode tracks

After the main recording was ended, tetrode-tip locations were marked by passing a weak electrical current through each tetrode (one of four channels, 10 μA for 10 s). On the next day, the rat was sacrificed using an overdose of carbon dioxide (CO2) and then was perfused transcardially, first with phosphate-buffered saline (PBS) and then with a 4% (v/v) formaldehyde solution. Thereafter, the brain was removed and kept in a 4% v/v formaldehyde-30% sucrose solution at 4°C until it sank. The brain was sectioned in the coronal plane at 40-μm thickness using a sliding microtome (HM 430; Thermo-Fisher Scientific), mounted on a slide glass, and then stained with thionin. Photomicrographs were taken using a digital camera attached to a microscope (Eclipse 80i; Nikon). Tetrode tracks were reconstructed using photomicrographs of a series of sections, taking into account the presurgical configuration of the tetrode-array bundle and electrolytic lesion marks. Dorsoventral (DV) recording position of place cells was quantitatively measured by calculating the vertical distance from the brain surface to electrode tip locations. DV positions of dHP units were within 1.5–2.5 mm, whereas those of iHP and vHP units were distributed from 2.5 to 6.5 mm.

2.2.6 Unit isolation

Single units were isolated using a Windows-based, custom-written program (WinClust) from overall spiking activities from each tetrode. Several parameters (peak, valley, energy, spike width), calculated from waveforms recorded from the four channels of a tetrode, were used for

unit isolation. Unit-isolation quality was evaluated during cluster cutting procedures, with each cluster defined as isolation quality 1 (poorly isolated) to 5 (well isolated) based on how well the cluster was separated from neighboring clusters and background noise. Units with an isolation rating of 1 were excluded from further analysis. Inter-spike interval (ISI) histograms were also used to determine how much a single unit indeed came from a single cell by using the proportion of spikes within the refractory period. Units showing a mean firing rate > 10 Hz (either in the square box or in the radial maze) with a spike width < 300 μs were classified as putative inhibitory interneurons and were excluded from further analysis.

2.2.7 Basic firing properties

To construct a rate map, we first scaled down the 720 × 480-pixel space to 72 × 48-pixel space (1 pixel = 2 × 2 cm). The firing rate associated with a given pixel was calculated by dividing the number of occupancy by the number of spikes fired in each pixel. The raw rate map was then smoothed using an adaptive binning method. The amount of spatial information contained in a single spike was measured by calculating spatial information based on the firing rate map according to the following equation(Skaggs, 1993):

$$\text{Spatial information} = \sum p_i \frac{\lambda_i}{\lambda} log_2 \frac{\lambda_i}{\lambda} \left(\frac{bit}{spike}\right),$$

where i denotes bin, p_i is the occupancy rate in the ith bin, λ_i is the mean firing rate in the ith bin, and λ is the overall mean firing rate. Stability within the square box test was measured by comparing the firing rate maps between the first half and the second half of the session using Pearson's correlation.

2.2.8 Definition of place fields

A place field was defined by using the following steps: First, the spatial firing rate map of a single unit was calculated based on the session, and find the pixel with the maximal firing rate. Then, the firing rates of all other pixels were compared against the maximal firing rate, and only those pixels whose firing rate exceeded 20% of the peak firing rate were retained for

further analysis. Among the remaining pixels, one or more sets of continuous pixels (>40 cm2 in size with a peak firing rate > 1 Hz) were defined as place fields. In cases where multiple place fields were identified during the procedure, the field size was calculated by summing all subfields. The relative field size was calculated by dividing the number of active pixels that satisfied place-field criteria by the total number of pixels in the occupancy map covering the entire behavioral space. Spiking data were included only if instantaneous speeds were greater than 5 cm/s at the time of the spike; spikes in the reward zones were excluded from the analysis. A proximity sensor was installed inside the food well to obtain an exact timestamp for when the rat obtained the reward, and timestamps were fed to Neuralynx. A cell was operationally defined as a 'place cell' if its spatial information was higher than 0.25 bits/spike with a statistical significance of $p < 0.01$ (Lee et al., 2004; Skaggs, 1993) and its mean firing rate was greater than 0.25 Hz. Among place cells whose mean firing rate was between 0.25 and 0.5 Hz were units showing place fields with peak firing rates greater than 1 Hz and high spatial information (Figure 2-4A). Thus, 0.25 Hz was set as a threshold.

2.2.9 Theta-modulation index and burst index

Autocorrelograms for spiking data were constructed by summing the number of spikes in individual time bins (bin size, 5 ms) in a fixed time window (±500 ms; bin size, 5 ms) examining before and after a given spike's timing (time 0 = reference spike's time bin). The aforementioned procedures were repeated for all spikes recorded for a single unit in a recording session, and the resulting autocorrelogram provided information on the overall rhythmicity of the spiking patterns of the neuron. The degree to which the temporal modulation of spiking occurred in the theta range (i.e., 7–10 Hz) was measured [theta-modulation index (TMI)] by computing the normalized difference between the peak (found in 100-140 ms bins) and trough (found in 50-70 ms bins) of the autocorrelogram. The bigger the TMI score, the larger the spikes of cells showed theta rhythmic activities. The burst index was calculated as total areas of the autocorrelograms over 1-6ms generated by the abovementioned methods divided by those over 1-50ms. The bigger the burst index, the more cells fired in a bursty fashion.

2.3 Results

2.3.1 Anatomical boundary between dorsal, intermediate and ventral hippocampus

We simultaneously recorded single units from dHP, iHP, and vHP of six rats using a 24-tetrode hyperdrive (Figure 2-1A and 2-1B). The areas that ranged from 2mm to 4mm posterior to bregma were defined as dHP, alternatively known as the septal hippocampus (de Hoz et al., 2003). vHP started to appear in proximately 4.3mm posterior to bregma (AP -4.3), and at that point, the CA1 subregion of dHP innervated to the medial prefrontal cortex (mPFC) (Hoover and Vertes, 2007) (Figure 2-1A). Based on anatomical connectivities, we set AP -4.3 as the border of discriminating dHP and iHP in our study. This division is similar to previous studies used to define dHP in that dorsal one-third of the hippocampus was considered as dHP (Moser et al., 1993; Patel et al., 2012). To quantitatively measure how cells are located ventrally, the vertical distance from the cortical surface to the tip of the tetrode was calculated (Figure 2-1C). We operationally set the border between iHP and vHP as 5.5mm ventral from the cortex (DV -5.5) based on the fact that associational projections stemmed from the dorsal CA3 extended near this border (Swanson et al., 1978) (Figure 2-1D). Additionally, we found that the proportion of place cells suddenly dropped in the vicinity of DV -5.5.

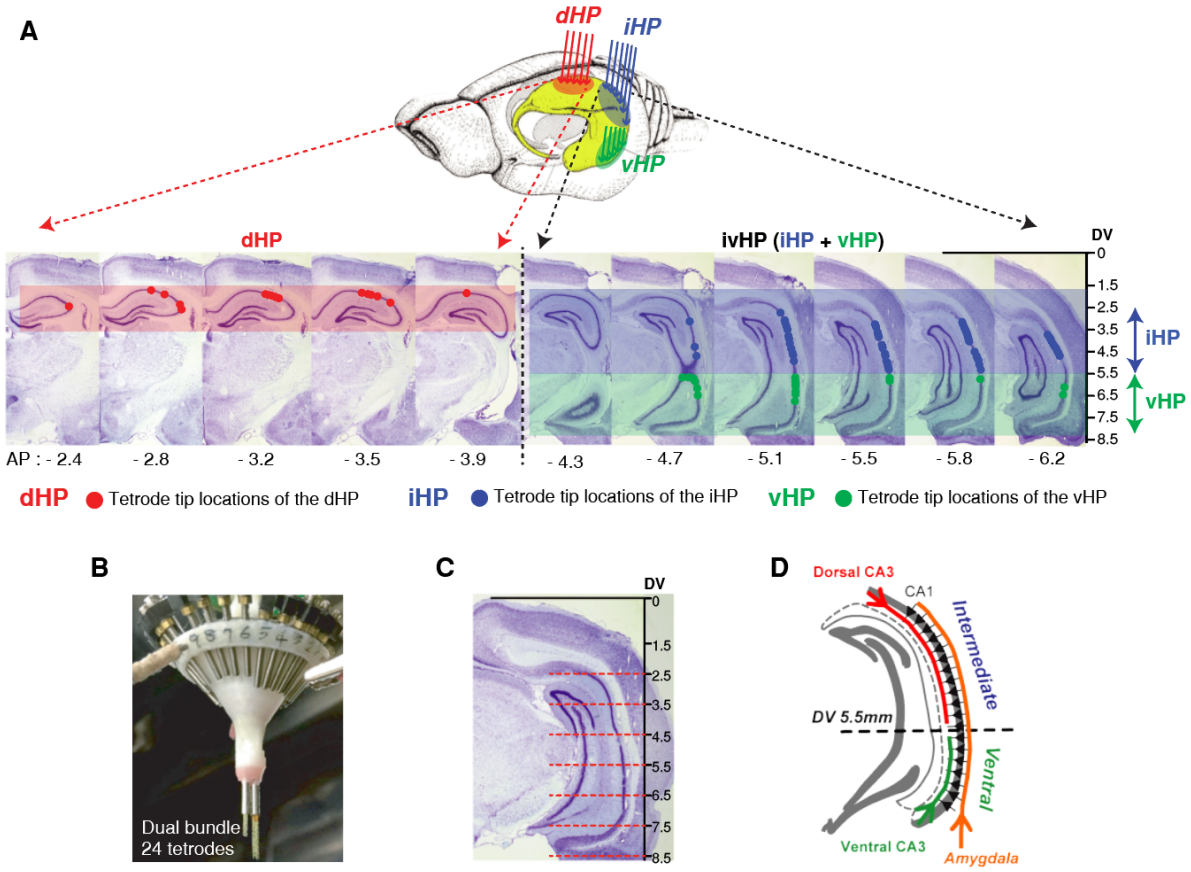

Figure 2-1. Verification of simultaneous recording from dHP, iHP, and vHP

(A) Tetrode tip locations showing recording the single units from dHP, iHP, and vHP. Histological verification of tetrode tip locations in the hippocampal subregions. (B) Bottom view of hyperdrive used in the current study containing two separate bundles. (C) Measuring protocol how much tetrode tips of iHP and vHP located ventrally from the cortical surface. (D) Schematic diagram showing brief anatomical connectivities of iHP and vHP.

2.3.2 Comparison of basic firing properties between hippocampal subregions

Both spike width and mean firing rates for each cell were used to discriminate the putative complex spike (CS) cells and interneurons (Figure 2-2A), and we used only cells that showed clear boundary between clusters and background noises during unit-isolation procedures. With our surgical coordinates, most singles cells came from the CA1, and a minor portion of cells were recorded in CA2 and CA3 (Figure 2-2B and Table 2-1). Also, we only included stable units that fired reliably during pre- and post-sleep recording (Figure 2-2C and 2D). We recorded most cells from dHP and iHP, relatively few cells from vHP due to its poor

unit isolation and geometrical structure that it is hard for tetrode to reach vHP (dHP, n = 1606; iHP, n = 2501; vHP, n = 294).

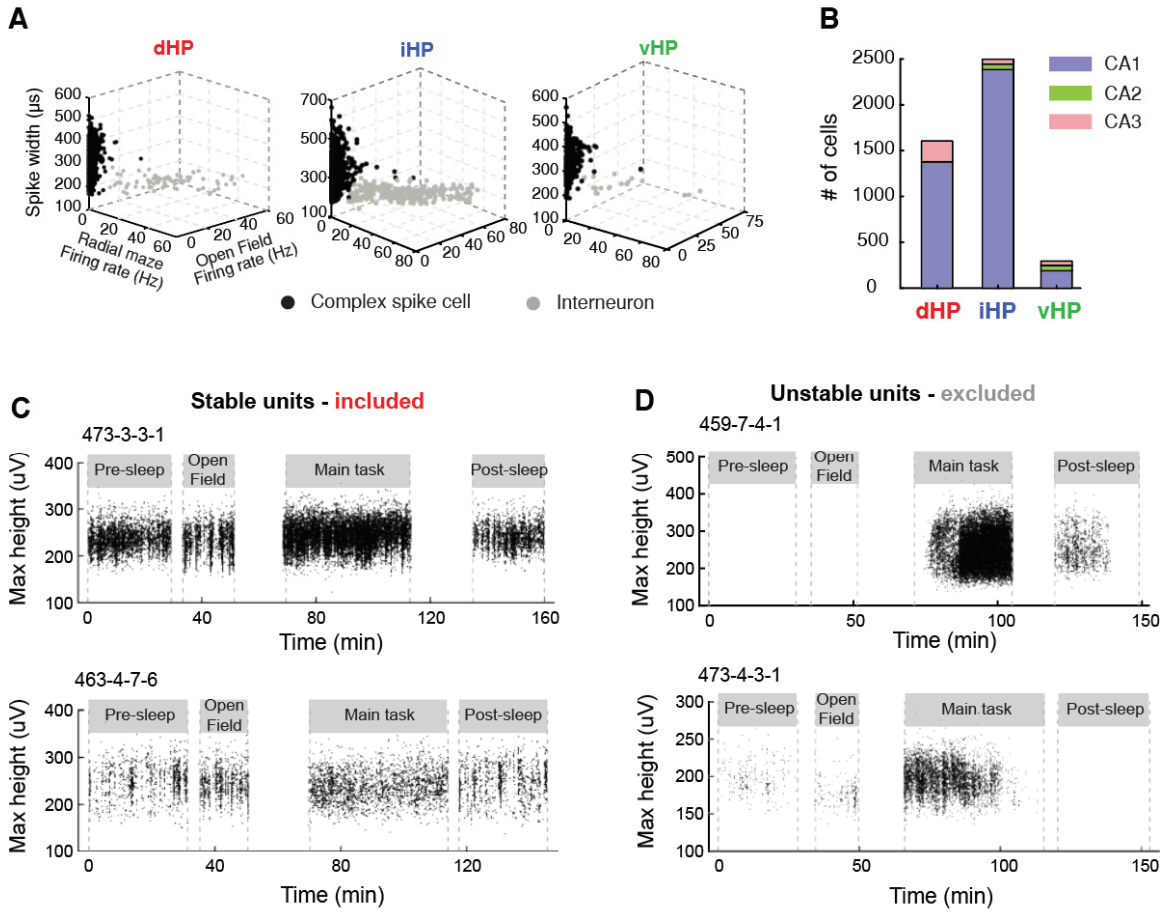

Figure 2-2. Classification of cell types and confirmation of cell's stability

(A) Classification of the complex spike cell (i.e., pyramidal neuron) and interneuron on the basis of the mean firing rate during the radial arm maze and open field and its spike width. (B) The number of cells recorded in the CA1, CA2, and CA3 from each subregion, respectively. (C) Examples of stable units maintaining their firing before and after the main task. (D) Examples of unstable units that we discarded from our main analysis.

		dHP							iHP							vHP						
Day	Session type	r448	r459	r463	r473	r488	r509	Total	r448	r459	r463	r473	r488	r509	Total	r448	r459	r463	r473	r488	r509	Total
1	SS/SS	9	44	45	9	0	21	128	6	24	34	40	4	95	203	8	3	7	0	4	0	22
2	SS/CR	7	40	52	9	0	24	132	26	24	34	42	7	51	184	2	0	8	0	5	0	15
3	SS/CR	4	45	59	11	0	24	143	26	24	46	77	9	55	237	0	4	10	0	5	0	19
4	FL/CR	0	47	61	13	0	26	147	27	29	51	54	7	55	223	3	7	15	0	2	0	27
5	FL/CR	0	51	57	13	0	31	152	37	24	53	52	2	50	218	4	6	16	0	3	0	29
6	SS/FL	0	42	56	9	0	34	141	35	23	58	106	4	52	278	8	11	15	0	1	0	35
7	SS/FL	3	51	43	6	0	23	126	21	25	48	103	0	68	265	7	12	18	0	6	0	43
8	SS/CR (T-maze)	16	52	60	13	0	10	151	20	17	42	97	1	32	209	11	4	9	0	7	0	31
9	SS/CR (T-maze)	10	51	60	17	0	12	150	16	18	36	130	0	40	240	5	3	8	0	4	0	20
10	Quantity (T-maze)	17	52	61	20	0	17	167	25	17	45	124	0	18	229	3	2	15	0	4	0	24
11	Quantity (T-maze)	12	60	54	18	0	25	169	26	15	42	109	0	23	215	8	2	10	0	9	0	29
	Total	78	535	608	138	0	247	1606	265	240	489	934	34	539	2501	59	54	131	0	50	0	294

Table 2-1. Number of single units per session

Previous literature reported that the basic firing characteristics were differed between dHP and iHP-vHP (Dougherty et al., 2012; Jung et al., 1994; Royer et al., 2010). Our findings confirmed to such differences in basic firing properties. To be specific, CS cells in dHP and iHP were more active (i.e., mean firing rate > 0.25Hz) in the radial maze than in the open field (dHP, $\chi^2_{(1)} = 165.78$, $p < 0.0001$; iHP, $\chi^2_{(1)} = 267.66$, $p < 0.0001$), whereas those in vHP fired at similar excitable level in both environments in the ($\chi^2_{(1)} = 1.51$, $p > 0.1$; Chi-square test) (Figure 2-3A). In addition, we found higher firing rates of CS cells in iHP and vHP than those in dHP and firing rates was also higher during behavioral tests than during sleep regardless of subregion (region, $F_{(2,4398)} = 56.7$, $p < 0.0001$; behavioral state, $F_{(1,4398)} = 61.2$, $p < 0.0001$; interaction effect, $F_{(2,4398)} = 3.8$, $p < 0.05$; Two-way mixed ANOVA) (Figure 2-3B). Multiple comparisons with Bonferroni corrections revealed that the firing rates were higher in vHP than in iHP during sleep, whereas those were not significantly different from each other during behavior tasks (sleep, $t_{(2793)} = 2.6$, $p = 0.01$; behavior, $t_{(2793)} = 1.1$, $p > 0.1$). In addition, the degree of spiking activities modulated by theta rhythm (*theta-modulation index*) (Cacucci et al., 2004) gradually decreased along the dorsoventral axis of the hippocampus ($F_{(2,4398)} = 433$, $p < 0.0001$; one-way ANOVA followed by multiple comparision with Tukey-Kramer for all pairwise comparisons among dHP, iHP, and vHP: p-values < 0.0001) (Figure 2-3C). Cells in dHP fired more bursty fashion than those in iHP and vHP, but significant difference was not observed between iHP and vHP ($F_{(2,4398)} = 106$, $p < 0.0001$, one-way ANOVA; dHP vs. iHP and dHP vs. vHP, p-values < 0.0001; iHP vs. vHP, $p > 0.1$; multiple comparisons with Tukey-Kramer) (Figure 2-3D).

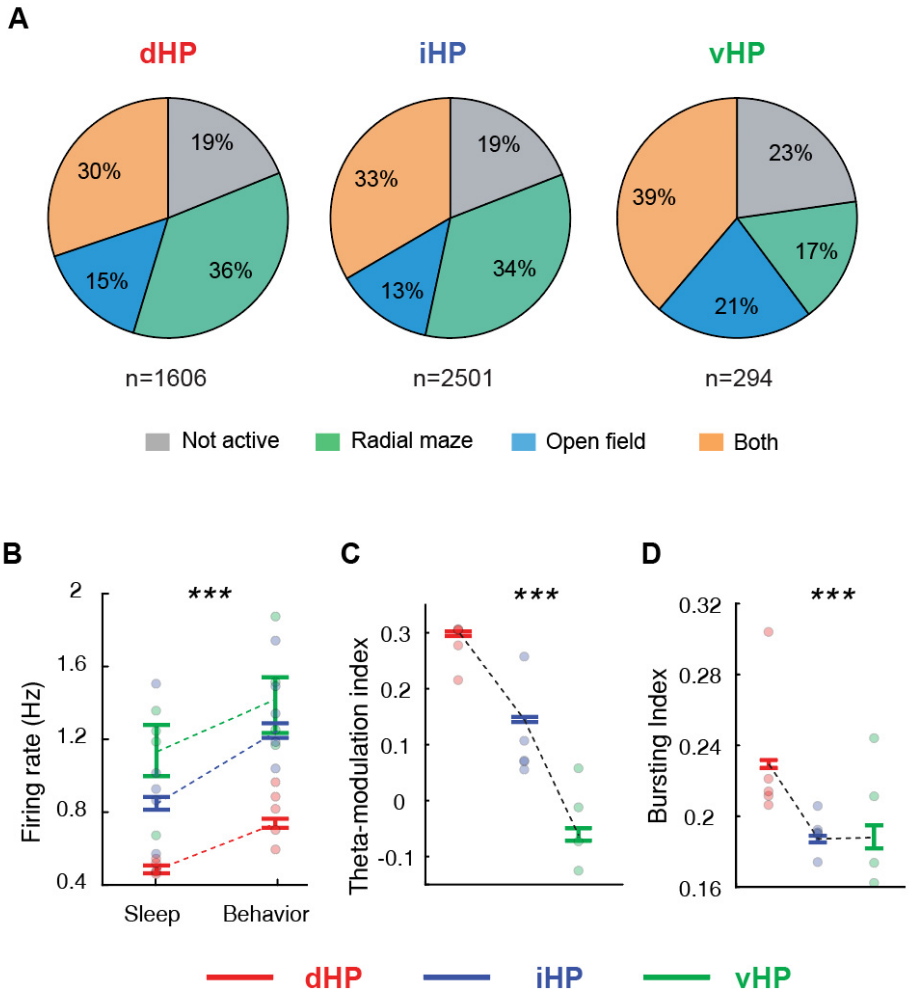

Figure 2-3. Basic firing properties of dHP, iHP, and vHP

(A) Pie charts comparing the proportion of cells that became active during the behavior tasks. The number of overall single cells is denoted below the pie chart. (B-D) Comparison of mean firing rate (B), theta-modulation index (C), and bursting index (D) between dHP, iHP, and vHP. Data are represented as mean ± SEM. Asterisks indicate statistical significance (***$p < 0.001$).

2.3.3 Degree of spatially selective firing patterns sharply decreased at the border between dHP and iHP

Among active neurons, a place cell was identified by using spatial information score (Skaggs, 1993), the mean firing rate, and field size as criteria (Figure 2-4A). Spatial firing patterns observed in dHP, iHP were almost similar compared to previous studies, whereas those in vHP were different compared to prior literature (Jung et al., 1994; Keinath et al., 2014;

Kjelstrup et al., 2008; Komorowski et al., 2013; Royer et al., 2010). Specifically, cells in dHP fired precise locations within the square box or V-shaped radial maze (Figure 2-4B). In contrast, cells recorded from iHP have broader place fields as place cells were recorded at a more ventral position (Figure 2-4C). And, spatial firing patterns that looked like place fields were hardly found vHP (Figure 2-4D).

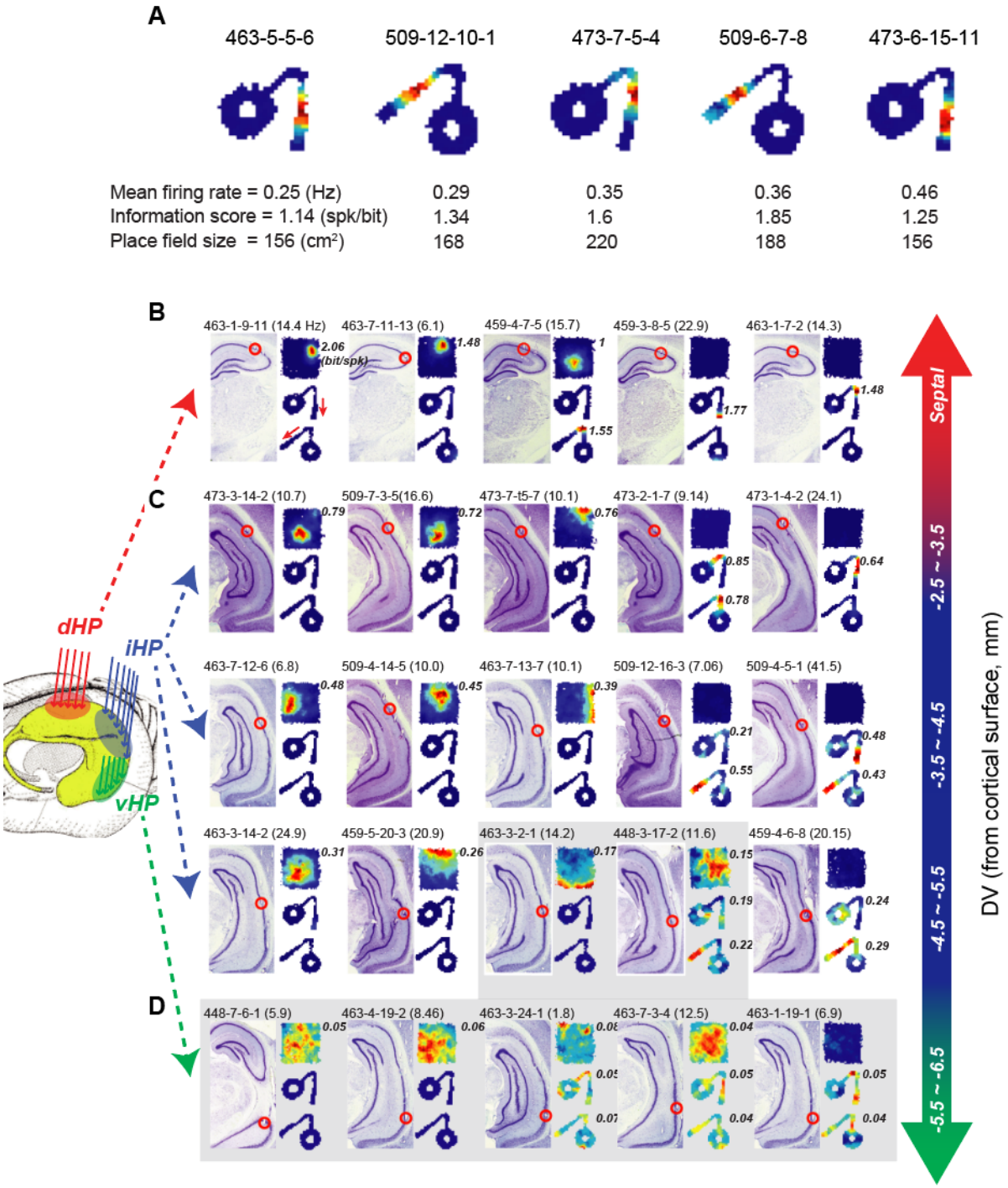

Figure 2-4. Spatial firing pattern changes along the dorsoventral axis of the hippocampus

(A) Examples that were successfully defined as place cells based on our place cell criteria. If the mean firing rate and peak firing rate are greater than 0.25 and 1, respectively, they have a distinct place field. (B-D) Spatial rate maps are sequentially arranged based on the depth of the tetrode. Histological verification of the tip locations of final recording day (red circle) and the rate maps associated with the open field and the spatial alternation task. The number affixed on top of the rate map denotes the cell

identity and peak firing rate, respectively. The number on the right side of the rate map indicates the spatial information score. Cells that did not exceed our place-cell criterion are shaded by grey.

The strength of spatially selective firing carried by a single spike during the open field test was measured to verify the difference in spatial firing patterns between dHP, iHP, and vHP. First of all, we separately investigated the spatial information scores and proportion of place cells depending on recording depth (septal, DV -2.5 ~ 3.5, -3.5 ~ -4.5, -4.5 ~ -5.5, -5.5 ~ -6.5). Spatial information scores decreased abruptly at the border between dHP and iHP and dropped gradually thereafter (Figure 2-5A, orange line). And the percentage of place cells quite linearly decreased along the dorsoventral axis of the hippocampus (Figure 2-5B, black line). Next, we pulled together three categories of iHP (i.e., DV -2.5 ~ 3.5 -3.5 ~ -4.5, -4.5 ~ -5.5) and examined the subregional differences. As previously found, the spatial information score decreased significantly from dHP to iHP and from iHP to vHP ($F_{(2,2391)} = 760$, $p < 0.0001$, one-way ANOVA; p-values < 0.0001 for all pairwise comparisons among dHP, iHP, and vHP, multiple comparisons with Tukey-Kramer method) (Figure 2-5C). Also, the proportion of place cells dropped almost linearly along the dorsoventral axis of the hippocampus ($\chi^2_{(2)} = 124.5$, $p < 0.0001$, Chi-square test; p-values < 0.0001 for all pairwise comparisons among dHP, iHP, and vHP with Bonferroni corrections) (Figure 2-5D).

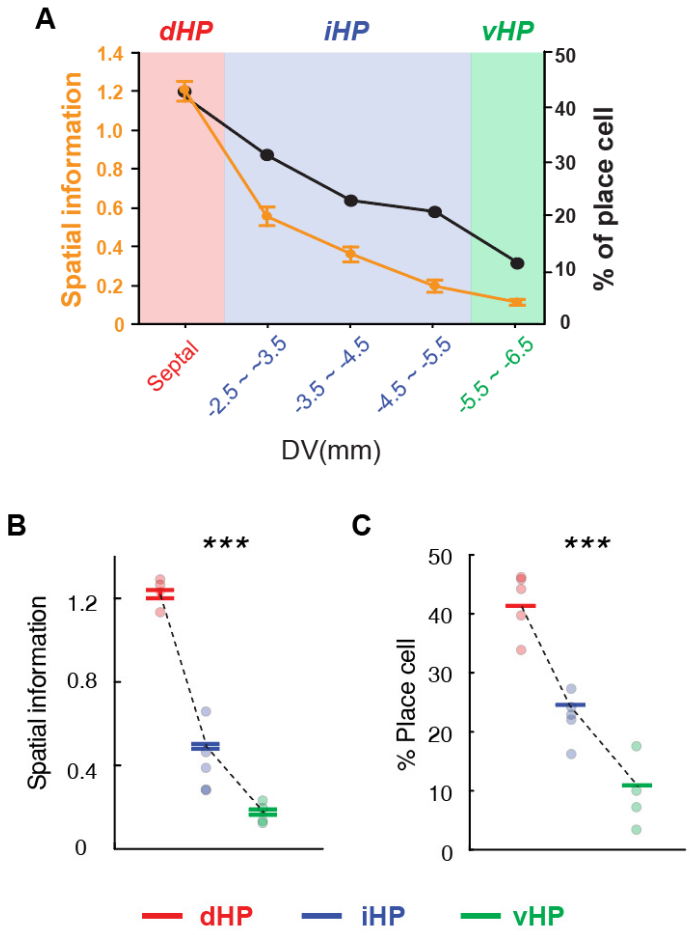

Figure 2-5. Quantitative analysis of the degree of spatially selective firing patterns along the dorsoventral axis

(A) The mean spatial information of population during the open field is plotted in relation to the recording depth of five levels. The proportion of place cells is also overlayed. (B-C) Same analysis as in (A), but DV -2.5 ~ 5.5 was combined as iHP group. Data are represented as mean ± SEM. Asterisks indicate statistical significance (***p < 0.001).

In our study, relatively few cells were obtained from vHP, which made it difficult to analyze the neural response of vHP. This is mainly because of technical difficulties in recording and isolating single unit activities from the deep brain area (Figure 2-1A). We recorded only 25 place cells during the spatial alternation task (Figure 3-10A), which made it hard to perform any quantitative analysis on place cells in vHP. Thus, place-field-based spatial analysis was performed based on the place cells in dHP and iHP.

2.4 Discussion

In previous literature, it has been reported that spatial coding was maintained from dorsal to ventral hippocampus, although the spatial resolution was poorer in vHP than in dHP (Jung et al., 1994; Kjelstrup et al., 2008) (Royer et al., 2010). However, in our study, well-defined place cells were rarely found in vHP. To reconcile such discrepancy, one may need to compare the experimental conditions between ours and the previous one in detail.

Jung et al. (1994), the most famous study of recording the vHP place cells, found that the place cells in vHP have bigger place fields than those in dHP. However, in this paper, they recorded place cells from iHP but not vHP (by our study's standard). Thus, when comparing our iHP data with the vHP results of this experiment, the findings are consistent. Another ventral hippocampal study, Kjelstrup et al. (2008), insisted that spatial gradients were found along with the entire hippocampus. However, this result was basically based on the linear track environment where rewards were always provided at the end of the track. Thus, it may be possible that large spatial fields in vHP are basically the reward-related responses associated with rewards provided at both ends. Moreover, they reported that these place cells in linear track actually did not fire spatially in an open field foraging environment. These results collectively suggest that the discrepancies between ours and previous studies may come from the differences in recording sites and recording environments (i.e., linear track vs. open field). Importantly, Ciocchi et al. (2015) recorded cells from vHP (by our study's criteria) while rats foraged in the open field, and they reported that only 14% of entire cells could be defined as place cells. This proportion of place cells is similar to our results (11%), which suggested that cells in the very ventral hippocampus are rarely involved in spatial information processing.

Anatomically, vHP has limited intrinsic connections inside vHP via recurrent collaterals and association projections but did not project to and receive from dHP-iHP (Amaral et al., 1991; Cenquizca and Swanson, 2007; Dolorfo and Amaral, 1998; Ishizuka, 2001; Kishi et al., 2006; Pikkarainen et al., 1999; Risold and Swanson, 1996; Swanson and Cowan, 1975, 1977; Van Groen and Wyss, 2003). Moreover, vHP is innervated with areas in which control the emotional information or endocrine response, such as the amygdala, hypothalamic periventricular, anterior and ventromedial hypothalamus zone, and preoptic nucleus. Thus, vHP may not anatomically suitable area for processing spatial information. Still, the ventral

subregion of the medial entorhinal cortex (MEC) that has large-scaled grid cells may deliver locational signals to vHP (Brun et al., 2008), although it is still controversial whether the primary origin of spatial signals in the hippocampus stems from the MEC. (Hales et al., 2014; Miao et al., 2015; Navawongse and Eichenbaum, 2013; Ormond and McNaughton, 2015; Robinson et al., 2017; Schlesiger et al., 2018; Van Cauter et al., 2008).

CHAPTER 2

3.1 Introduction

In our study, as previous literature has shown, the place cells in iHP exhibited less accurate spatial representation compared to dHP. In other words, there should be stronger non-spatial information. Considering the fact that the amygdala, ventral tegmental area (VTA) is heavily innervated with iHP (Gasbarri et al., 1994; Petrovich et al., 2001; Pikkarainen et al., 1999), it may represent motivational significance associated with locations (Bannerman et al., 2003; Kjelstrup et al., 2002; Royer et al., 2010; Schumacher et al., 2016).

To test this possibility, we have attempted a variety of pilot experiments to control the motivational values of locations. First of all, during pilot experiments, we tested negative stimulus to make rats avoid certain space. Specifically, we tried 1) spouting a strong air puff in front of the rat's face, 2) vibrating the radial arm maze, 3) laying the tissues coated with peppermint oil that has a rat-repelling odor, and 4) playing the owl crying sound. However, all tries failed because rats quickly habituated those stimuli. They no longer showed reluctance to approach the arm associated with those stimuli after rats were exposed to them 1~2 times. Thus, it is impossible to obtain enough sampling trials to analyze the electrophysiological data. To overcome the problem mentioned above, we decide to manipulate the level of the reward value by using various types of foods with different palatabilities. Among candidate foods (e.g., nuts, dried fruits, grain, Cereal), we used sunflower seeds, Froot Loops and Cheerios as rewards in which rats showed a distinct food preference.

To examine whether the motivational values were represented in iHP, we conducted the spatial alternation task in which rats experienced changes in reward type in the middle of sessions while shuttling between two fixed arms. Above all, in this task, we developed the simplest version of behavior tasks because lots of task-relevant factors could affect the place cells activities, such as upcoming and previous trajectories, item-location paired associations, task demand, motivational state (i.e., hunger or thirst) and goal location (Eschenko and Mizumori, 2007; Ferbinteanu and Shapiro, 2003; Lenck-Santini et al., 2001; Spiers et al., 2018; Wood et al., 1999; Wood et al., 2000). In our shuttling paradigm, we directly compared the neural activities of dHP and iHP in response to changes in the motivational significance of place while controlling the aforementioned cognitive factors.

3.2 Methods

3.2.1 Behavior paradigm

3.2.1.1 Food preference test

A rectangular chamber (45 × 30 × 30 cm) made by transparent red acrylic material was used to test the food preference among sunflower seeds, Froot Loops, and Cheerios. A door was installed in the middle to divide the chamber into two sections. An acrylic wall was built to create a 9-cm wide passage in the center, and rats were required to use the central passage to traverse to another section. A food tray (4 × 2 × 1 cm) that allowed rats to sample the rewards equally was located at the end of the passage. Two of the three food types were paired to test which food type rats preferred more, and three different pairs of food types were performed (i.e., sunflower seeds vs. Cheerios, sunflower seeds vs. Froot Loops, Froot Loops vs. Cheerios). The food preference test was conducted just before the spatial alternation task, and the reward pair to be used in the spatial alternation task was tested to check the animal's food preference. That is, the rat's food preferences for the pairs of sunflower seeds vs. Cheerios, Froot Loops vs. Cheerios, and sunflower seeds vs. Froot Loops were separately tested in Day 2-3, Day 4-5, and Day 6-7 of the spatial alternation task, respectively.

A food tray contained two types of foods side by side, and rats were given a single opportunity to choose a reward. Immediately thereafter, the food tray was pulled out by the experimenter in preparation for the next trial, and the reward location was pseudo-randomly assigned (Figure 3-1A). Preference tests consisted of 20 trials. The experiment consisted of the following steps: Step 1 – The rat waited for the start door to open. Step 2 – After the door opened, the rat ran along the central passage to arrive in the food tray, where it selected one of the two food options. Step 3 – As soon as the rat chose the food, the food tray was pulled back so that the rat could no longer access the food. Step 4 – The rat, now on the opposite side of the previous trial, waited for the next trial to begin (Figure 3-1A). Food preferences for sunflower seeds vs. Cheerios and Froot Loops vs. Cheerios pairs were tested for thirteen rats (n = 6 for the main experiments and n = 7 for the pilot experiments), and those for sunflower seeds vs. Froot Loops pair were conducted for nine rats (n = 6 for the main experiments and n = 3 for the pilot experiments). Among thirteen rats, eleven rats strongly preferred sunflower seeds or Froot Loops to Cheerios. Because two rats did not significantly prefer sunflower seeds or Froot Loops over Cheerios, they were excluded from the main experiment. In the case of

sunflower seeds vs. Froot Loops pairs, all rats equally preferred both rewards (Figure 3-1B and 3-1C).

3.2.1.2 Spatial alternation task

An 8-arm maze (central platform size, approximately 2cm in diameter; arm size, 8 × 45 cm; height, 70 cm from the floor) was used in the spatial alternation task. Two adjacent arms were used in the task. An L-shaped transparent acrylic panel (50 × 30 cm) was placed in the center platform to restrict the rat's navigation within the two arms. A food well (2 cm in diameter and 8 mm in depth) was installed at the end of each arm, with a proximity sensor attached underneath the well to record the displacement of a small disc (2.5 cm in diameter) that covered the food well. Two different types of latencies were calculated. The first, which assessed the motivational drive to get a reward, corresponding to the time taken to cover a distance of 10 cm from the food well to get a reward (Figure 3-2D). This latency was designed to capture the rat's behavior as they usually ran rapidly until reaching a point near the food well and then paused briefly before displacing the food-well disc covering the Cheerios. The second latency, which gauged fatigue level, was the time elapsed from entry to reaching the food well (Figure 3-2B) by using signals of infrared sensor installed at each arm entry. Transistor-transistor logic (TTL) sensor signals were fed to a data-acquisition system (Digital Lynx SX; Neuralynx). An LED light illuminating the experimental room and digital cameras monitoring animals' positions were installed on the ceiling. The maze was surrounded by black curtains, and numerous visual cues were attached to them. Unwanted noise generated outside the experimental room during the recording session was masked by turning on white noise (80 dB).

3.2.2 Post-surgical training and main recording

After one week from surgery, rats were retrained in the spatial alternation task. Retraining of rats reaching the pre-surgical criterion required 10 ± 3 days (mean ± SD). During the post-training, tetrodes were lowered into the target regions in the hippocampus while the rat was fully rested in a custom-made booth. Once most tetrodes reached pyramidal cell layers both in the dorsal and intermediate-ventral hippocampus, the main recordings started according to the following schedule: (i) Spatial alternation task – Day 1: Only sunflower seeds were provided

as a reward for 3 blocks (60 trials/block); Day 2–3: sunflower seeds were provided as a reward in blocks 1 and 3, and Cheerios were baited in Block 2; Day 4–5: Froot Loops were used as a reward in blocks 1 and 3, and Cheerios were baited in Block 2; Day 6-7: sunflower seeds were provided as a reward in blocks 1 and 3, and Froot Loops were used in Block 2 (Figure 3-2A).

3.2.3 Constructing the population rate map

Population rate maps for spatial alternation tasks were constructed by stacking the linearized spatial rate maps (bin size = 2 cm). All trials of each block were used to create a spatial rate map, and the population rate map was independently made per each block. In a linearized rate map, the firing rate in each bin was calculated by dividing the number of spikes by the number of occupancies by the rat within that bin. In the curved parts near the choice point, a fan-shaped boundary with 22.5-degree internal angles was defined as a bin. Linearized firing rate maps then were smoothed using a Gaussian window (window size, 22 cm; full width at half maximum [FWHM], 10 cm).

3.2.4 Categorization of place field responses

We categorized place field firing patterns in responses to a change in reward as 'ON-cell,' 'OFF-cell,' and 'Maintain' by using the in-field firing rate, which was calculated by dividing the total number of spikes within the place field boundary by the total occupied time within it. First, the in-field firing rate for the entire session was calculated and multiplied by 0.1; that value was used as a threshold to determine whether the place cell was active or not in a given block. Then, we calculated the in-field firing rate for each block and compared it to the threshold. If it was larger than the threshold, that place cell was identified as active in the block. By doing so, single units were categorized into the three classes according to whether or not the units were active in adjacent two-blocks: (1) 'Maintain' – cells active in both blocks; (2) 'ON-cell' – cells that started to fire in the second block; and (3) 'OFF-cell'' – cells that were inactive in the second block.

3.2.5 Reward-type coding analysis

To define the unit that encoding the identity of reward, we used the following criterion: the rate modulation index (RMI) between different reward blocks should be greater than 0.25 and the RMI between the same reward blocks was lower than 0.25, which was the same criterion in the rate-remapping analysis. Also, the RMI_{diff} should be within 1% of the shuffled RMI_{diff} distribution generated by 10000 permutations. Since the running speed of rats could affect the firing rate of the place cell (McNaughton et al., 1983), the units with a strong correlation between firing rate and running speed were excluded (Figure 3-6B and 3-6C).

3.2.6 Speed-correlated cells

In previous literature, place cell's firing rate is positively correlated with the animal's running speed (McNaughton et al., 1983a). To investigate whether speed-correlated cells would affect our main results, we calculated in-field firing rate and in-field speed, the latter of which is the size of the place field in a linearized rate map divided by the time required to pass the boundary. Robust linear regression was applied to examine positive correlations between in-field firing rate and speed. If the correlation coefficient was > 0.4, and the p-value of the linear regression was < 0.01, place cells were defined as *speed-correlated cells* (Figure 7F). About 15% of overall place cells in dHP and iHP were classified as speed-correlated cells (Figures 7G and 7H). In contrast, few speed-correlated cells (~4%) among place cells in vHP were found, although there was no significant difference in the proportion between regions (Figure 7I). Because the inclusion of these cells has no impact on our main findings, these cells were included throughout the study.

3.3 Results

3.3.1 Rat's food preference for sunflower seeds and Froot Loops over Cheerios

Right before rats performed the spatial alternation task, we tested the food preference reward pair that was going to use in the spatial alternation task (e.g., sunflower seeds vs. Cheerios on day 2-3) among three types of foods [sunflower seeds (SS), Froot Loops (FL), and Cheerios (CR)] (Figure 3-1A). Rats preferred sunflower seeds over Cheerios and Froot Loops over Cheerios, but they do not show food preference between sunflower seeds and Froot Loops ($\chi^2_{(2)} = 20.27$, $p < 0.0001$; Kruskal-Wallis test) (SS-CR vs. FL-CR, $p > 0.1$; SS-CR vs. SS-FL, p =

0.0014; FL-CR vs. SS-FL, $p < 0.001$; Wilcoxon signed-rank test with Tukey-Kramer corrections) (Figure 3-1B). In our pilot experiments, two out of thirteen rats did not show strong food preference for sunflower seeds or Froot Loops over Cheerios, and we excluded those rats from our main experiment. (Figure 3-1C)

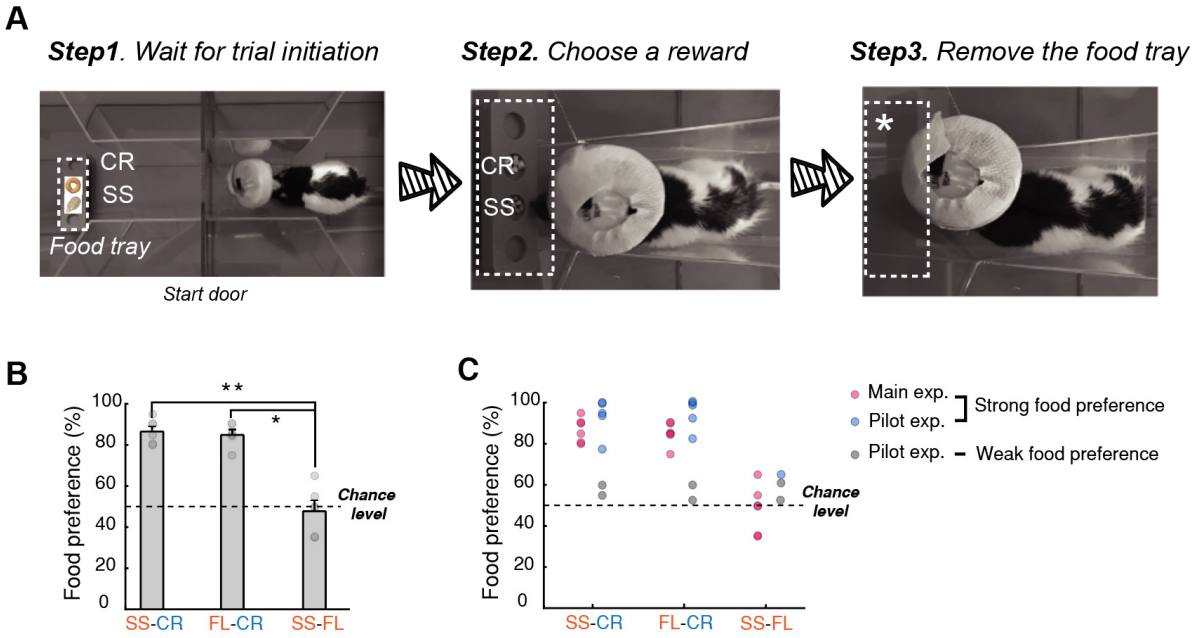

Figure 3-1. Behavior paradigms for food-preferene task and behavioral results

(A) A series of pictures showing how the procedure of the food-preference task. Sunflower seeds and Froot Loops were baited side by side in pseudorandom order on the food tray (Step 1). After the rat select one of two food rewards (Step 2), experiments removed the food tray (Step 3). The asterisk denotes the absence of the food tray. (B) Food preference results showing rats preferred sunflower seeds and Froot Loops over Cheerios. Only data of the main experimental group were presented. (C) Overall data including main and pilot experiment groups. The preference level of each animal is plotted by a circle. Two rats were excluded from the main analysis due to weak food preference for sunflower seeds and Froot Loops. Data are represented as mean ± SEM. Asterisks indicate statistical significance (*$p < 0.05$; **$p < 0.01$).

3.3.2 Place cells in iHP, but not dHP, encode changes in motivational values of place via global remapping

Next, rats were required to shuttle between two arms of radial arm maze during the spatial alternation task for 7 days (Figure 3-2A; see more details in method). All rats were

trained using sunflower seeds at first and then went through Cheerios and Froot Loops as new reward types. Based on our pilot experiments, counterbalancing the training sequence by training with less-preferred type (i.e., Cheerios) was not feasible. This is because rats were required to be more food deprivation to run the task using Cheerios than using sunflower seeds. However, we found that robust food preference disappeared when rats were too hungry compared to when hunger level was optimally controlled. One block consisted of 60 trials, and rats were required to finish 3 blocks in one session. After one block was finished, reward type was changed without any cues. The food well was located at the end of arms and a small acrylic disc (2.5cm in diameter) cover it to prevent rats from using reward odor as cues indicating reward changes. We omitted the reward in 10% of trials to examine whether odor might guide the rat's choice. There is no difference in latency between rewarded trials and omitted trials, suggesting that rats might not solve the task using odor cues ($t_{(41)} = -0.82$, $p > 0.1$; paired t-test) (Figure 3-2B). And, the time taken from disc displacement to receipt of reward was 0.46 ± 0.08 s (mean ± SD). We excluded the trials whose latencies exceeded two standard deviations from mean from main analysis (Figure 3-2C). After rats noticed that the type of rewards was changed from sunflower seeds (or Froot Loops) to Cheerios on trial 61, the latency increase significantly compared to previous one ($\chi^2_{(2)} = 14.76$, $p < 0.001$, Friedman test) [pre-Cheerios (sunflower seeds) vs. post-Cheerios, $p = 0.0039$; pre-Cheerios (Froot Loops) vs. post-Cheerios, $p = 0.0024$; pre-Froot Loops (sunflower seeds) vs. post-Froot Loops, $p = 0.06$; Wilcoxon signed-rank test with Bonferroni corrections] (Figure 3-2D). These results showed that the rat's motivational level in spatial alternation tasks decreased after changes in reward type from more-preferred to less-preferred option. In addition, there was no significant decrease in latency when reward type was changed to Froot Loops from sunflower seeds, suggesting that the decrease in latency with the introduction of Cheerios may not stem from fatigue or satiety.

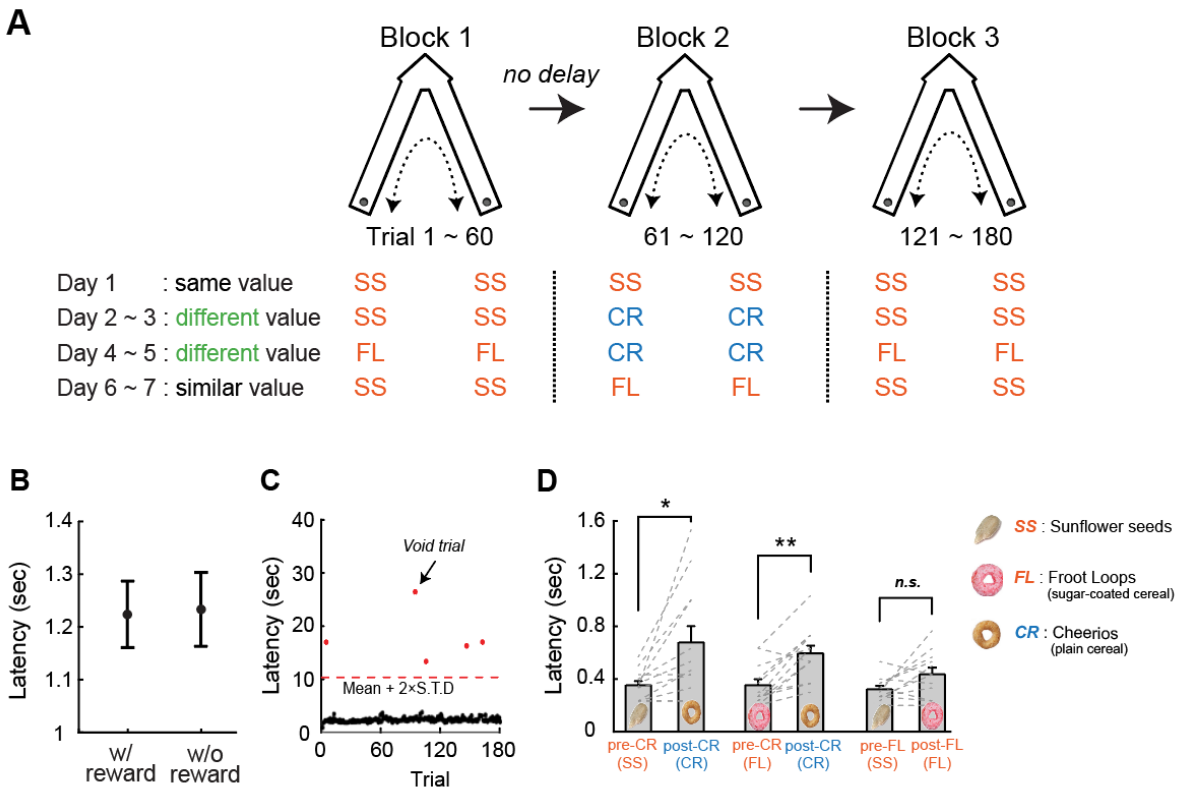

Figure 3-2. Behavior paradigms for spatial alternation task and behavioral results

(A) Experimental procedures of spatial alternation task for electrophysiological recordings. Both food wells contained the same type of rewards [e.g., sunflower seeds (SS) or Froot Loops (FL) or Cheerios (CR)]. Except for Day 1, the type of reward was going to be changed in Block 2. (B) Comparing the latencies taken from arm entry to reaching the reward site between rewarded trials and reward-omitted trials. (C) Latency data of one session are plotted. If the latency was exceeded the threshold (red dotted line), those trials were excluded from the analysis. (D) Comparing the latencies trials before (pre) and after (post) reward was changed. After the reward was changed to Cheerios from sunflower seeds or Froot Loops. Data are represented as mean ± SEM. Asterisks indicate statistical significance (*$p < 0.05$; **$p < 0.01$).

Next, we investigated how place cells in dHP and iHP responded to changes in reward types. On Day 1, only sunflower seeds were given throughout the session, and place cells in dHP and iHP maintained spatial representations from Block 1 to Block 3 (Figure 3-3A). These results implied that hidden variables, such as satiety and fatigue, might not have an influence on the spatial firing patterns of place cells in spatial alternation tasks. However, when rats

experienced Cheerios as rewards in Block 2 on Day 2-5 (Figure 3-3B and 3-3C), place cells in dHP and iHP showed different remapping patterns. In dHP, place fields maintained their firing locations as they did on Day 1. However, those in iHP globally remapped, either newly activated or shifted their place fields (red shaded in Figure 3-3B and 3-3C). In Block 3, place cells in iHP did not go back to original firing patterns as they did in Block 1. It is interesting because those remapping patterns in iHP differed from results in dHP in previous literature (Leutgeb et al., 2005; Leutgeb et al., 2004; Muller and Kubie, 1987). The remapping observed in iHP cannot be explained by the elapse of time as recording proceeded because such global remapping was not sufficiently observed when reward was switched to Froot Loops from sunflower seeds on Day 6-7 as it did on Day 2-5 (Figure 3-3D). These results implied that global remapping of place cells in iHP on Day 2-5 was mainly attributable to changes in motivational values rather than to changes in reward identity or other general factors.

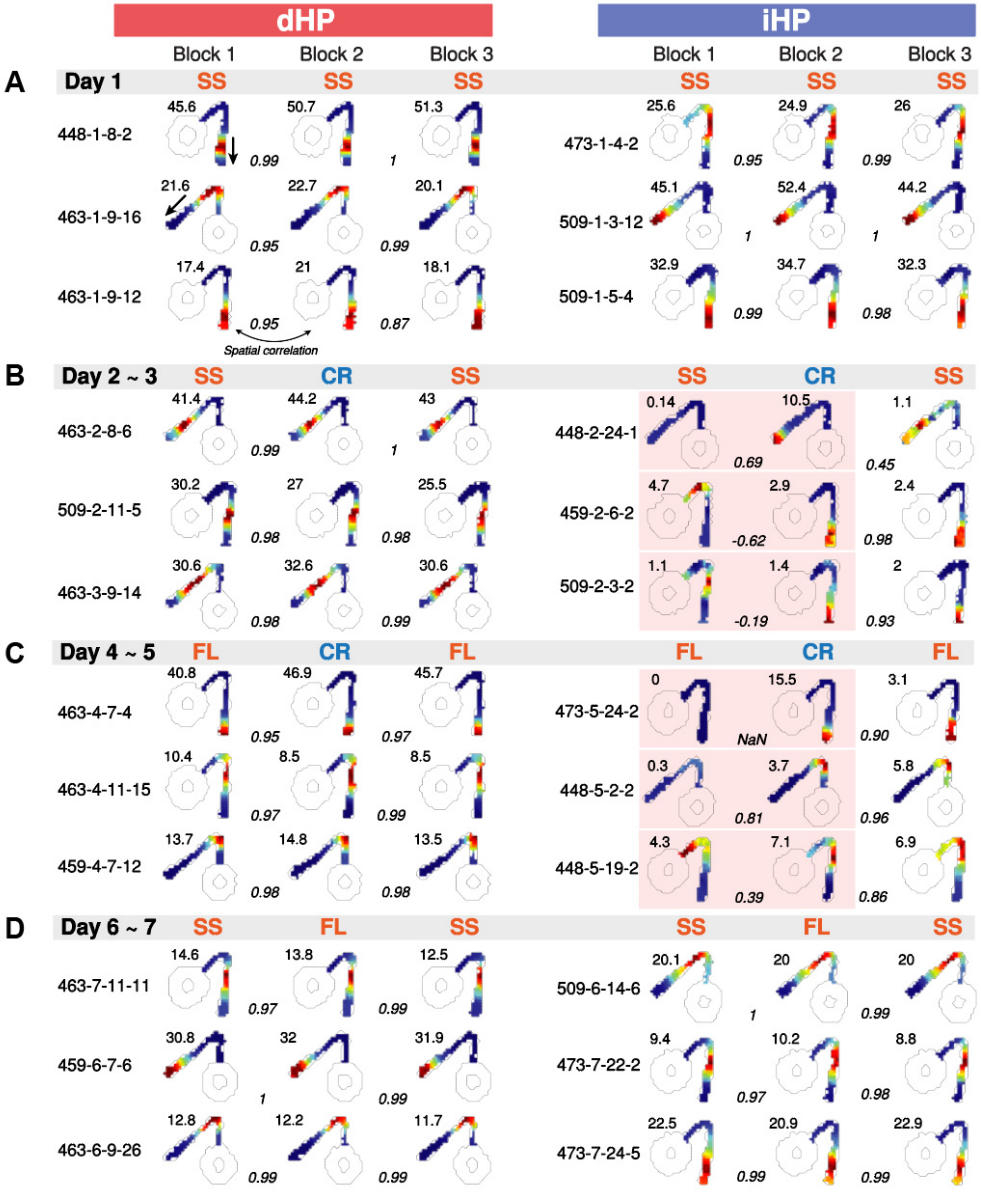

Figure 3-3. Place cell examples recorded from dHP and iHP during the spatial alternation task

(A-D) Representative spatial rate map examples in response to reward changes. Place cells in dHP maintained their preferred firing locations for all conditions, whereas global remapping (marked by red shaded boxes) was found in iHP. The black circular contour in the rate maps at the end of the arm indicates the outline of rat's position trajectory where rats ate the rewards and turned around to initiate the next trial. This area was excluded from the rate map analysis. The number affixed on the left side of spatial rate maps denotes cell identity. Peak firing rate of rate maps and spatial correlation coefficients between adjacent rate maps were given on top of the rate map and between the rate maps, respectively.

When comparing the spatial rate maps between Block 1 and 2, we used the rate maps associated with a trajectory in which rats underwent the reward changes for the first time (Route 1, Figure 3-4). This is because place cells in iHP showing global remapping in response to changes in reward value were more frequently found on Route 1 compared to the opposite trajectory (Route 2) (Figure 3-4). All the results reported hereafter are based on the neural activities in association with Route 1.

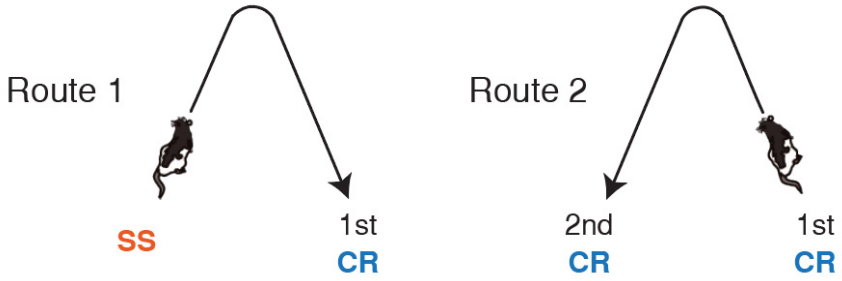

Figure 3-4. Schematic illustration of the spatial alternation task

The trajectory where rats exposed to the reward change to Cheerios (from sunflower seeds in this example) for the first time is labeled as Route 1, and the opposite path as Route 2.

As previously presented in Figure 3-3, place cells in iHP differentially responded to the events that Cheerios was first introduced in Block 2 compared to those in dHP did. To be specific, in dHP, the proportions of place cells exhibited global remapping, rate remapping, and no remapping were not significantly different between (i) no reward change (only sunflower seeds), (ii) reward identity changes with minimal value difference (sunflower seeds-to-Froot Loops), and (iii) changes in both reward identity and its value (sunflower seeds or Froot loop-to-Cheerios) ($\chi^2_{(4)} = 1.2$, $p > 0.1$; Chi-square test) (Figure 3-5A). Importantly, 19% of place cells in dHP globally remapped even in the absence of any reward change (SS-SS condition in Figure 3-5A). This baseline level of global remapping was kept across the following reward-changing conditions (i.e., Cheerios from sunflower seeds or Froot Loops, and Froot Loops from sunflower seeds) ($\chi^2_{(2)} = 0.5$, $p > 0.1$ for sunflower seeds-only vs. sunflower seeds-to-Froot Loops condition; $\chi^2_{(2)} = 0.7$, $p > 0.1$ sunflower seeds-only vs. sunflower seeds/Froot Loops condition; $\chi^2_{(2)} = 0.2$, $p > 0.1$ for sunflower seeds-to-Froot Loops vs. sunflower seeds/Froot

Loops condition). A similar proportion of rate remapping was observed across all experimental conditions (Figure 3-5A).

In contrast, in iHP, the proportion of place cells underwent global remapping was significantly increased in a value-dependent manner ($\chi^2_{(4)} = 14.7$, $p < 0.01$) (Figure 3-5B). Specifically, under the condition in which sunflower seeds were provided throughout the session, only 4% of place cells in iHP underwent global remapping in Block 2. However, the proportion of globally remapped cells increased by 10% when the reward type was changed to Froot Loops from sunflower seeds in Block 2 (SS-FL condition in Figure 3-5B), although there was no significant difference compared to the sunflower seeds-only condition ($\chi^2_{(2)} = 4$, $p > 0.1$). Moreover, the proportion of remapping cells significantly increased by another 10% as reward was changed to less-preferred rewards (i.e., Cheerios) in Block 2. ($\chi^2_{(2)} = 11.3$, $p < 0.01$ when compared with sunflower seeds-only condition; $\chi^2_{(2)} = 6$, $p < 0.05$ in comparison with sunflower seeds-to-Froot Loops condition) (Figure 3-5B and Table 3-1).

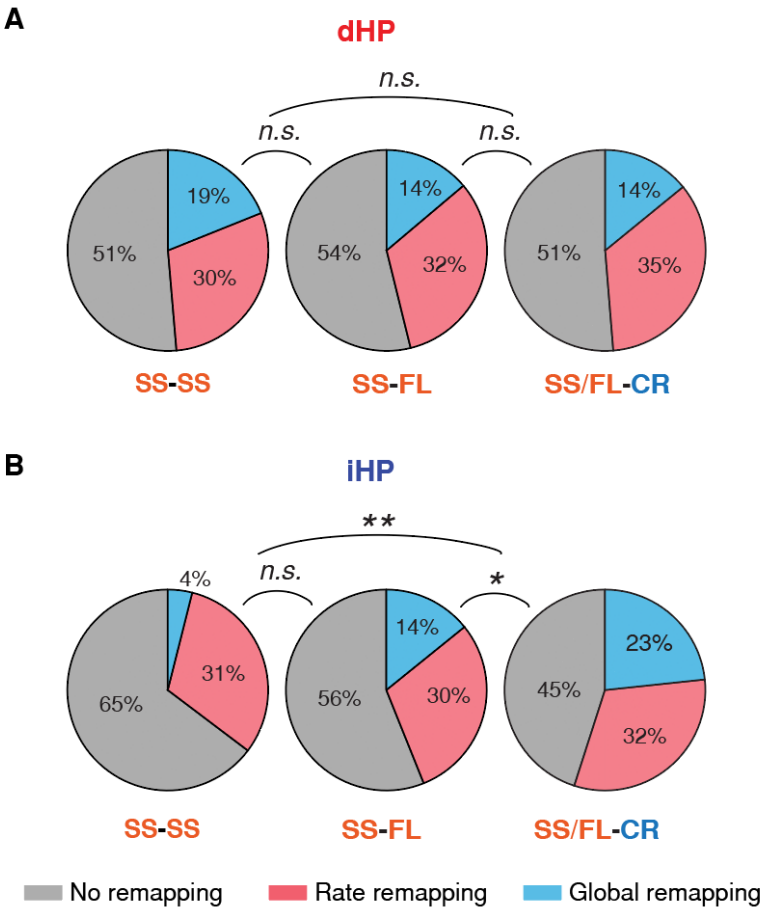

Figure 3-5. Proportion of place cells in response to reward changes

(A-B) Comparing the proportion of place cells exhibiting global and rate remapping in sunflower seeds-only, sunflower seeds-to-Froot Loops, and sunflower seeds/Froot Loops-to-Cheerios conditions in dHP (A) and iHP (B). Asterisks indicate statistical significance (*$p < 0.05$; **$p < 0.01$).

		dHP			iHP		
		No remapping	Rate remapping	Global remapping	No remapping	Rate remapping	Global remapping
value neutral	SS-SS	19	11	7	33	16	2
	SS-FL	35	21	9	83	44	21
value decrease	SS-CR	40	23	14	67	44	31
	FL-CR	40	34	7	47	36	27
Total		134	101	38	230	140	81

Table 3-1. The number of cells according to the region, remapping type and experimental conditions.

Differential degrees of global remapping between dHP and iHP across reward-changing conditions were also confirmed by spatial correlation coefficients of each cell between Block 1 and 2 (Figure 3-6A). That is, when the reward was switched to Cheerios, there was no significant decrease in correlation coefficients at the population level in dHP ($\chi^2_{(2)}$ = 1.7, $p > 0.1$) (Figure 3-6A), but that was not the case in iHP ($\chi^2_{(2)}$ = 10.2, $p < 0.01$; Kruskal-Wallis test; $p < 0.01$ for sunflower seeds only vs. sunflower seeds/Froot Loops-to-Cheerios, and $p = 0.098$ for sunflower seeds only vs. sunflower seeds-to-Froot Loops; Wilcoxon rank-sum test with Tukey-Kramer corrections) (Figure 3-6A). When the value-decrease conditions were divided into two separate groups (sunflower seeds-to-Cheerios and Froot Loops-to-Cheerios), there was no difference in correlation coefficients between sunflower seeds-to-Cheerios and Froot Loops-to-Cheerios conditions. (dHP, $\chi^2_{(3)} = 1.8$, $p > 0.1$; iHP, $\chi^2_{(3)} = 10.7$, $p = 0.014$; Kruskal-Wallis test) (iHP, $p < 0.05$ for sunflower seeds only vs. sunflower seeds-to-Cheerios; $p < 0.01$ for sunflower seeds only vs. Froot Loops-to-Cheerios; $p > 0.1$ for sunflower seeds only vs. sunflower seeds-to-Froot Loops; $p > 0.1$ for sunflower seeds-to-Cheerios vs. Froot Loops-to-Cheerios; Wilcoxon rank-sum test with Tukey-Kramer corrections) (Figure 3-6A). These results were preserved when the same analysis was applied without the cells whose firing rates were positively correlated with the animal's speed (Figure 3-6B and 3-6C, see more details in Method) (McNaughton et al., 1983a). Overall, these findings strongly suggest that global remapping found in iHP is correlated with changes in reward value, whereas same

phenomenon in dHP may be owing to other factors.

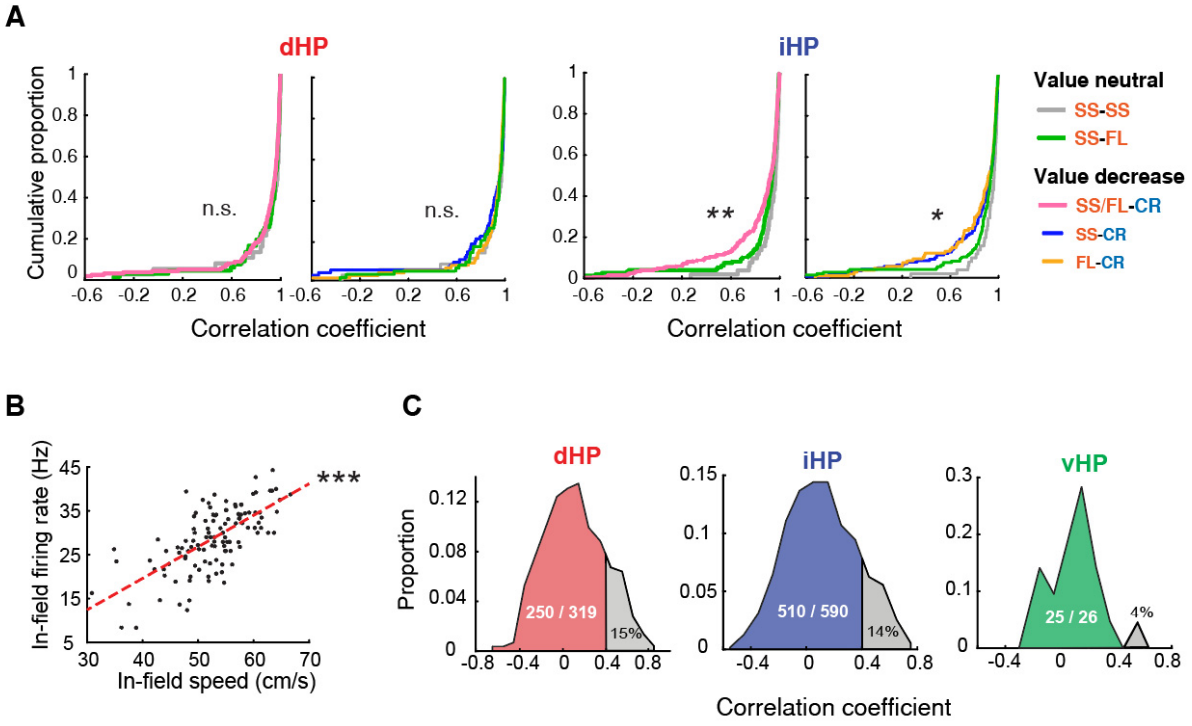

Figure 3-6. Changes in reward value induced global remapping in iHP, but not dHP

(A) For each cell, spatial correlation coefficients were calculated by comparing Block 1 and 2 in dHP and iHP and plotted using cumulative density functions. (B) An example of a place cell whose firing rate is positively correlated to movement speed (i.e., speed-correlated cell). In-field speed was measured by dividing the field width by the time it took to pass through the place field. $r = 0.81$, $p < 0.001$ by robust linear regression. (C) The proportion of speed-correlated cells during spatial alternation task by dHP, iHP, and vHP, respectively. Asterisks indicate statistical significance (*$p < 0.05$; **$p < 0.01$; ***$p < 0.001$).

To characterize the aforementioned global remapping at the population level, a population rate map was constructed by ordering and stacking the linearized rate maps. On Day 1, spatial correlations between the population rate map for Block 1 and 2 were comparatively high in both dHP and iHP when there were no reward changes (Figure 3-7A and 3-7B). The spatial correlation was higher in dHP than in iHP probably because place cells in dHP fired more spatially selective manner than those in iHP. On Day 2-3, when reward type was changed to Cheerios from sunflower seeds in Block 2, the spatial correlation dropped in both dHP and

iHP in comparison with Day 1 (purple shaded box in Figure 3-7B and 3-7C). Although the spatial correlation in both dHP and iHP decreased on Day 2-3, it is important to note that spatial correlation in dHP decreased only on Day 2 (R = 0.81) and recovered on Day 3 (R = 0.9), which is a similar level of results on Day 1 (R = 0.92). In contrast, coefficient values in iHP remained at the low level both on Day 2 and 3 (R = 0.82) (data not shown). These results suggest that a decrease in population rate map correlations in dHP on Day 2 may be attributable to novelty of events (i.e., the first experience of reward change) (Valenti et al., 2018), not necessarily related to motivational value changes as in iHP. On Day 4-5, population rate map similarity remained at lower levels in iHP when rewards were changed to Cheerios from Froot Lops, but it is not case of dHP (Figure 3-7C). Lastly, on Day 6-7, when rewards types of similar preference (i.e., sunflower seeds and Froot Loops) were used, the degree of population rate map similarity between Block 1 and 2 in iHP rebounded to a level similar to that of Day 1 (Figure 3-7C). Interestingly, a decrease in rate map similarity of place cells was observed specifically on the route (Route 1), where rats discovered a reward that was different from what they had expected for the first time (Figure 3-7C, solid lines). It is unlikely that that route-dependent differences could be explained by the differences in basic firing properties between the two routes. This is because the mean firing rate and spatial information scores were not significantly different between Route 1 and 2 (spatial information: dHP, $t_{(499)} = 0.55$, $p > 0.1$, and iHP, $t_{(825)}=1.38$, $p > 0.1$; mean firing rate: dHP, $t_{(1680)} = 1.28$, $p = 0.038$, and iHP, $t_{(2808)} = 1.78$, $p > 0.1$; independent t-test with Bonferroni corrections) (Figure 3-7D).

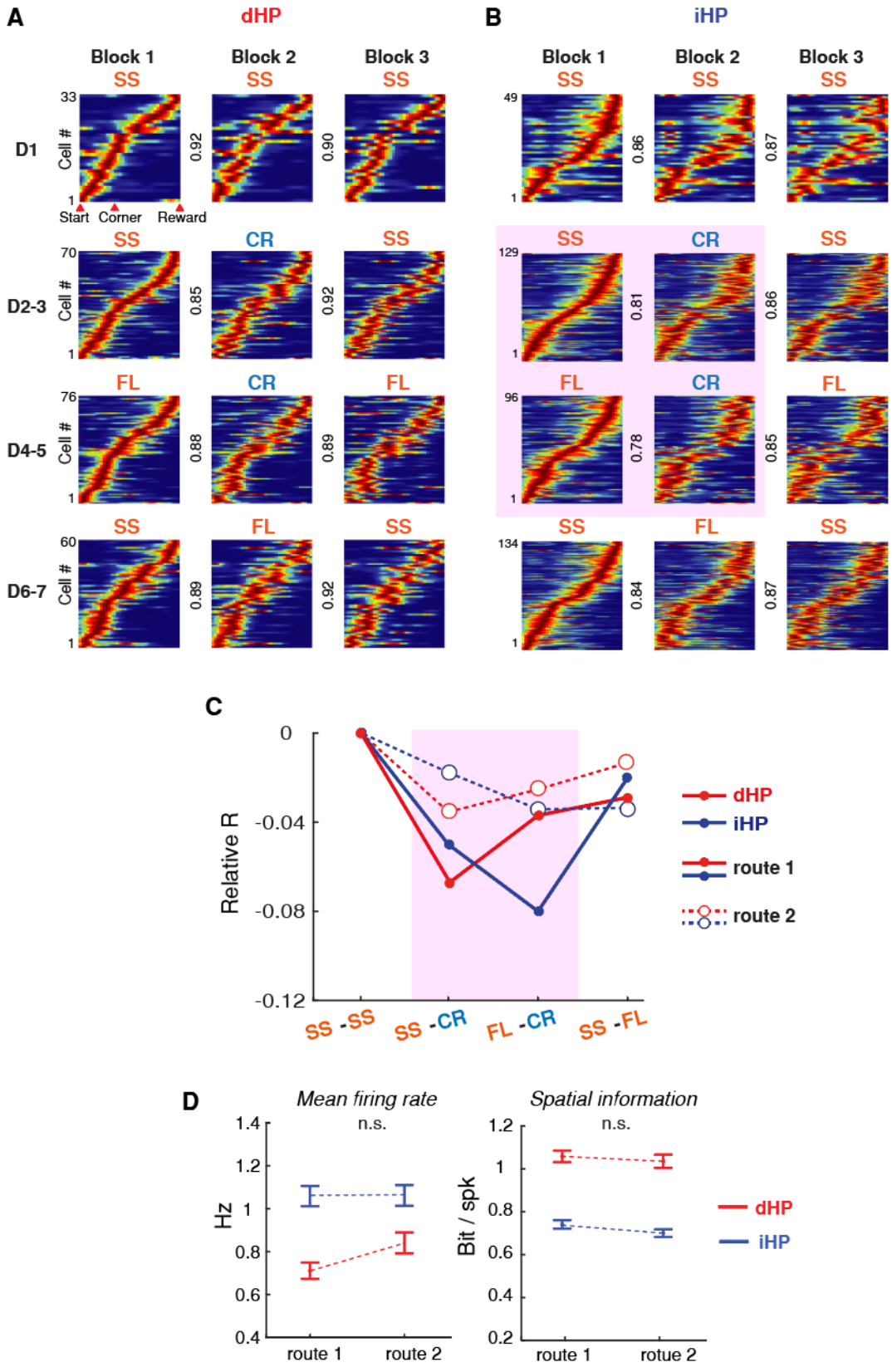

Figure 3-7. Decrease in reward value induced global remapping in iHP, but not dHP

(A-B) Population rate maps for all reward-changing conditions of dHP (A) and iHP (B). The spatial

correlation between two adjacent population rate maps is provided between them. The x-axis of the population rate map denotes the position along the linearized track. (C) Spatial correlation coefficients between adjacent blocks were calculated for all conditions. Relative R was measured by subtracting each R of sunflower seeds-only, sunflower sees-to-Cheerios, Froot Loops-to-Cheerios condition from the R of sunflower seeds-only condition. R-values obtained from Route 1 and 2 were plotted by using solid and dashed lines, respectively. The blue box denotes the value-decrease conditions. (D) Comparing the mean firing rate and spatial correlation coefficient between Route 1 and Route 2. Data are represented as mean ± SEM.

Furthermore, we investigated whether the decrease in spatial correlation of place cells in iHP was indeed correlated to the decrease in motivational significance. To examine this possibility, we cross-correlated the difference in latency between pre-Cheerios and post-Cheerios trials with mean correlation coefficient of session ensemble between Block 1 and 2 (Figure 3-8). The mean spatial correlation decreased as the latency increased after the demotivating reward (Cheerios) was introduced, which was only observed in iHP, but not in dHP (Figure 3-8) [dHP, $r^2 = 0.018$, $p > 0.1$; iHP, $r^2 = 0.31$, $p = 0.002$ (robust linear regression)]. These results suggested that the degree of demotivation in motivational significance in response to reward changes may underlie the global remapping found only in iHP.

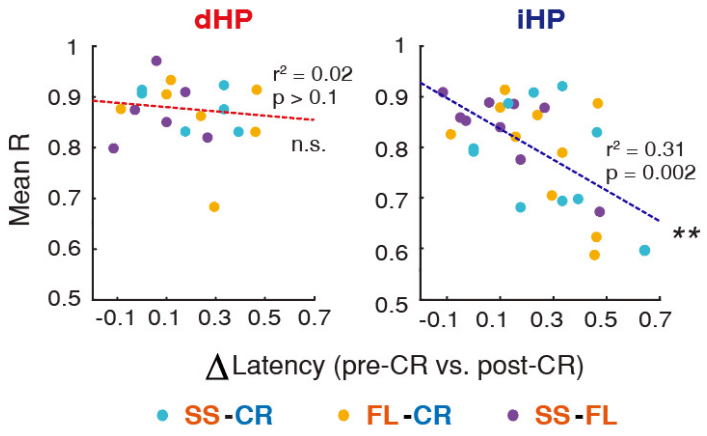

Figure 3-8. Subjective value difference reflected on the amount of global remapping in iHP, but not dHP

Cross-correlation between latency difference (across rewards change) and rate map similarity (measured by mean of R) between Block 1 and 2 for all place cells. Types of reward changes are

provided in different colors for data points. Robust linear regression was applied to test the significance of linear relationship. Asterisks indicate statistical significance (**p < 0.01).

3.3.3 Identity of reward type is coded in the iHP by rate remapping, but not in the dHP

Although it is known that place cells represent nonspatial variables through rate remapping (Eichenbaum et al., 1987; Hampson et al., 1999), place cells in both dHP and iHP did not seem to encode changes in motivational significance through rate remapping in the spatial alternation task (dHP: $\chi^2_{(3)} = 2.1$, $p > 0.1$; iHP: $\chi^2_{(3)} = 3.2$, $p > 0.1$; Kruskal-Wallis test; Figure 3-9A). However, we found that the firing rates of some cells in the iHP were associated with the identity of the reward type. That is, some cells fired consistently more when CR was provided as a reward (cell 509-2-23-1 and 448-5-24-1 in Figure 3-9B). Other cells fired more when SS (cell 463-3-14-2 and 473-6-24-7 in Figure 3-9B) or when FL was used as a reward (cell 473-6-1-2 and 473-4-15-8 in Figure 3-9B). These cell types were more frequently observed in the iHP than in the dHP ($\chi^2_{(1)} = 8.7$, $p < 0.01$, Chi-square test; Figure 3-9C). And there no proportional difference between reward-changing conditions in the dHP and iHP (dHP: $\chi^2_{(2)} = 0.02$, $p > 0.1$, iHP: $\chi^2_{(2)} = 1.6$, $p > 0.1$; Chi-square test; Figure 3-9D and 3-9E).

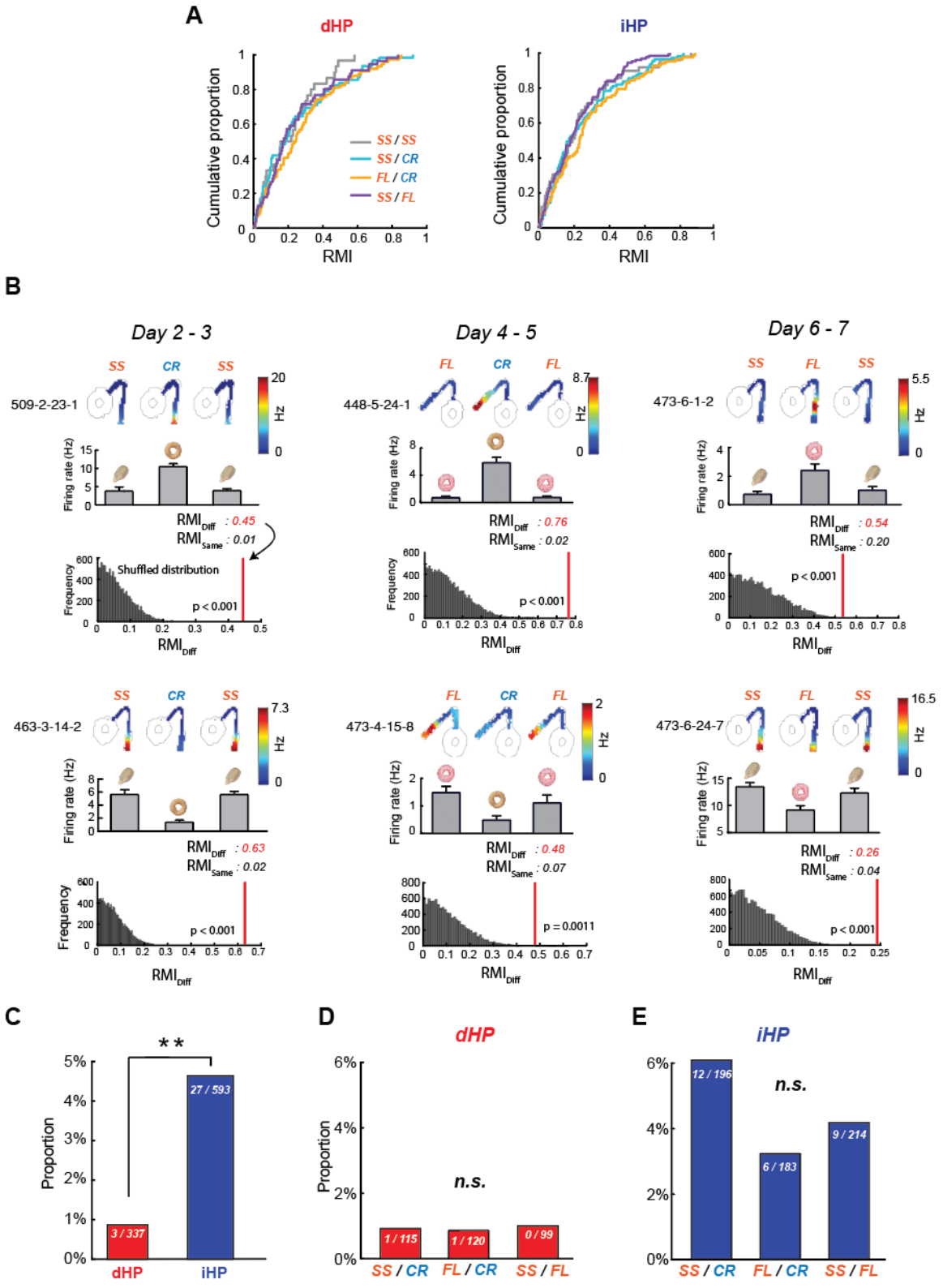

Figure 3-9. Encoding of reward type by rate remapping in the iHP, but not in the dHP

(A) For each cell, rate modulation index was calculated between Block 1 and 2 in dHP and iHP and plotted using cumulative density functions. (B) Representative examples are showing that place cells

encoded the type of rewards by modulating their firing rates in reward-changing conditions. The boundaries of rat's occupancy map are indicated by black contours in the rate maps. The mean of in-field firing rates for each block was plotted. The RMI between different reward blocks and the reward blocks was calculated and test its statistical significance by using shuffled distribution. Cell ID numbers were provided near the rate maps. (C to E) The proportion of cells encoding the reward types by region and reward-changing conditions. Asterisks indicate statistical significance (*$p < 0.05$; **$p < 0.01$).

3.3.4 Neural activity of single cells recorded from vHP in response to motivational value changes

Next, non-place cells (n = 40) obtained from vHP were analyzed to investigate if motivational values might have altered the neural activities of those neurons (Figure 3-10B). Specifically, the degree of rate-map similarity (Figure 3-10C), the difference in the amount of spatial information carried by a single spike (Figure 3-10D), and the strength of rate modulation (Figure 3-10E) in vHP between Block 1 and 2. Spatial correlation coefficients were relatively high in the sunflower seeds-only condition (Figure 3-10C). Those coefficients were significantly different among reward-changing conditions ($\chi^2_{(3)} = 8.7$, $p < 0.05$; Kruskal-Wallis test), and this primarily came from the condition where the reward was changed to Cheerios from Froot Loops ($p > 0.1$ for sunflower seeds only vs. sunflower seeds-to-Cheerios, $p < 0.05$ for sunflower seeds only vs. Froot Loops-to-Cheerios, $p = 0.11$ for sunflower seeds only vs. sunflower seeds-to-Froot Loops; Wilcoxon rank-sum test with Tukey-Kramer corrections) (Figure 3-10C). Moreover, changes in spatial information score and firing rate from Block 1 to Block 2 were not significantly different between recording conditions (spatial information, $\chi^2_{(3)} = 4.2$, $p > 0.1$; rate remapping index, $\chi^2_{(3)} = 1.3$, $p > 0.1$; Kruskal-Wallis test) (Figure 3-10D and 3-10E). These results imply that the motivational significance might not be represented in vHP as robustly as iHP, although this might be owing to our small sample size for vHP.

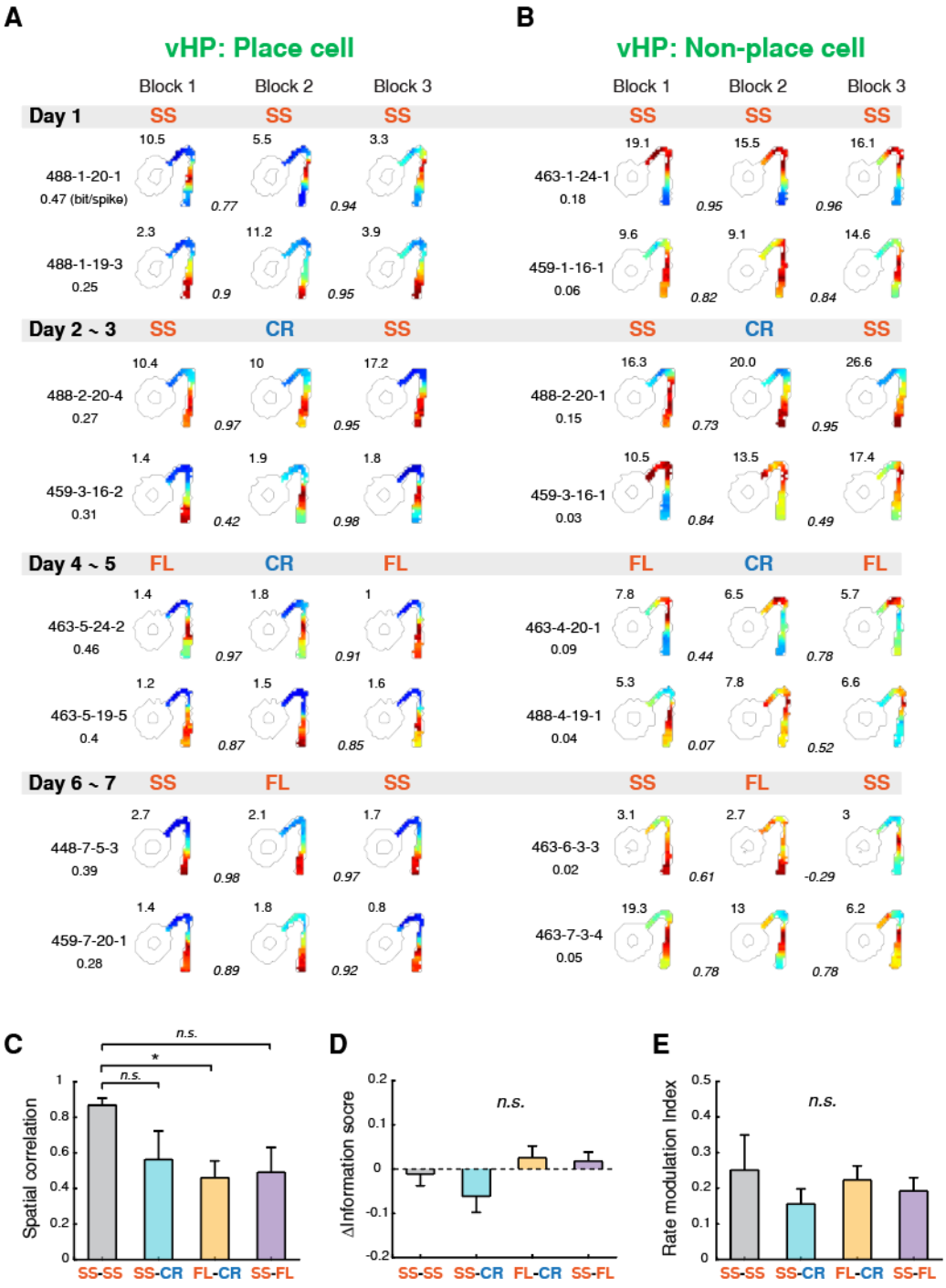

Figure 3-10. Examples of single cell recorded from vHP

(A-B) Examples of place cells (A) and non-place cells (B) that were recorded from vHP during the spatial alternation task (cell ID numbers provided). The rat's positional boundaries are indicated by the black contours in the rate maps. The maximal firing rate of each rate map and the spatial correlation coefficient between the adjacent rate maps are provided on top of the rate map and between the rate maps, respectively. Also, spatial information score is provided under the cell ID number. (C-E) Among

non-place cells in vHP, spatial correlation coefficients (C), changes in spatial information score (D), and the amount of rate remapping (E) were calculated in response to reward-changing to Block 2 from Block 1. Data are represented as mean ± SEM. Asterisks indicate statistical significance (*$p < 0.05$).

3.4.5 Immediate coding of the changes in motivational values in iHP, but not in dHP

The changes in neural activities described so far were investigated mostly based on the place cells whose firing fields were maintained across reward-changing events. Importantly, after the rats displace the food-covered disc and find the new type of rewards (e.g., Cheerios) for the first time, some place cells that previously kept silent started to fire (hereafter, *ON cells*) (Figure 3-11A-i and 3-11A-i). Specifically, among 389 place cells, 34 place cells were ON cells in dHP (8.6% ON cells in value-neutral conditions, and 8.8% ON cells in value-decrease conditions), and in iHP, 61 out of 626 cells were ON cells (8.2% ON cells in value-neutral conditions and 10.8% ON cells in value-decrease conditions). Some ON cells were almost instantly (i.e., within the 4th trial) activated (i.e., > 20% of peak firing rate) and we termed them as *immediate ON* cells. Such cells were more significantly found in iHP [13/61 (21%); n = 2/13 in value-neutral conditions and n = 11/13 in value-decrease conditions] than in dHP [2/34 (5.8%); n = 1 in both conditions] ($\chi^2_{(1)} = 3.9$, $p < 0.05$; Chi-square test) (Figure 3-11A-ii and 3-11B-ii). The remaining ON cells turned on in a delayed manner, termed *delayed* ON cells [dHP : 32/34 (94.2%); n = 12/32 in value-neutral conditions and n = 20/32 in value-decrease conditions] [iHP : 48/61 (21%); n = 20/48 in value-neutral conditions and n = 28/48 in value-decrease conditions] (Figure 3-11C-i and 3-11C-ii and Table 3-2).

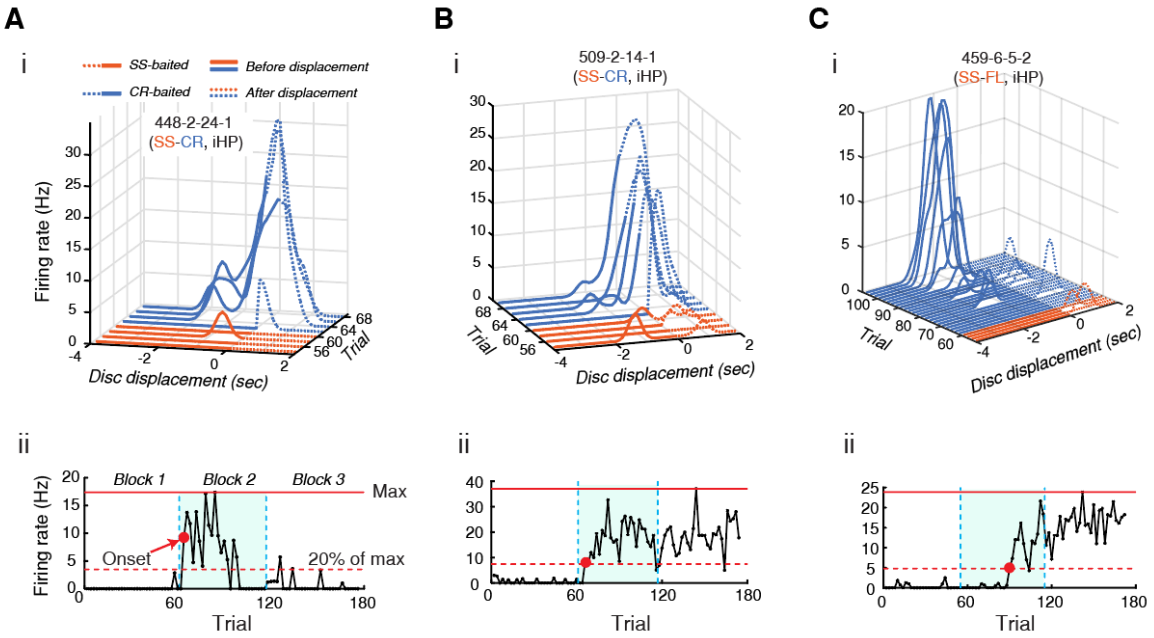

Figure 3-11. Examples of immediately activated place cells in response to the decreased in reward value

(A-i and B-i) Examples of immediate ON cells and their trial-by-trial firing rate changes near reward-changing trials. The trial in which cells were activated was indicated by red dot. Place cells that were silent in Block 1 suddenly were activated within two trials in response to reward changes to Cheerios. The firing rates are aligned to the moment (0 on the x-axis) when rats displaced the disc covering the food well. (A-ii and B-ii) In-field firing rate was plotted in trial by trial to confirm that place cells maintained silent until Block 1 but abruptly started to fire in Block 2. Some cells fired maximally in Block 2, followed by a diminishing their firing rate (A-ii). Others maintained their initial firing rate until the session ended (C-i and C-ii). Examples of delayed ON-cells. Place cells did not immediately turn on in response to reward change between similar value rewards.

		dHP		iHP	
		Immediate	Delayed	Immediate	Delayed
value neutral	Transient	0	1	0	2
	Sustained	1	11	2	18
value decrease	Transient	0	2	4	5
	Sustained	1	18	7	23
Total		2	32	13	48

Table 3-2. Number of ON-cells classified by immediate response types

Interstingly, when the reward was changed to less-preferred to more-preferred one (i.e., value-decrease condition), significantly large number of immediate ON cells was observed only in iHP ($\chi^2_{(1)} = 6.7$, $p < 0.05$; Chi-square test) (for value-decrease vs. value-neutral conditions in iHP, $\chi^2_{(1)} = 3.1$, $p = 0.08$; for dHP vs. iHP in value-decrease conditions, $\chi^2_{(1)} = 4.7$, $p = 0.03$; Chi-square test with Bonferroni corrections) (Figure 3-12A). Although there is very sparse distribution of immediate ON cells in iHP, it is important to note that such class of cells wre robustly observed in iHP across all animals in value-decrease conditions [rat 448 (n = 3, 1.7%), rat 459 (n = 1, 0.6%), rat 463 (n = 1, 0.3%), rat 473 (n = 4, 0.8%), rat 488 (n = 1, 3%), rat 509 (n = 1, 0.3%)], whereas the same cell type was observed in iHP in only two rats during value-neutral conditions [rat 463 (n = 1, 0.3%), rat 509 (n = 1, 0.3%)] or in dHP in only two rats during both conditions [rat 459 (n = 1, 0.3%), rat 463 (n = 1, 0.3%)]. Aforementioned ON cells may not be attributable to general novelty because the same phenomenon was als foun on the second day of same value-decrease condition (Figure 3-12B).

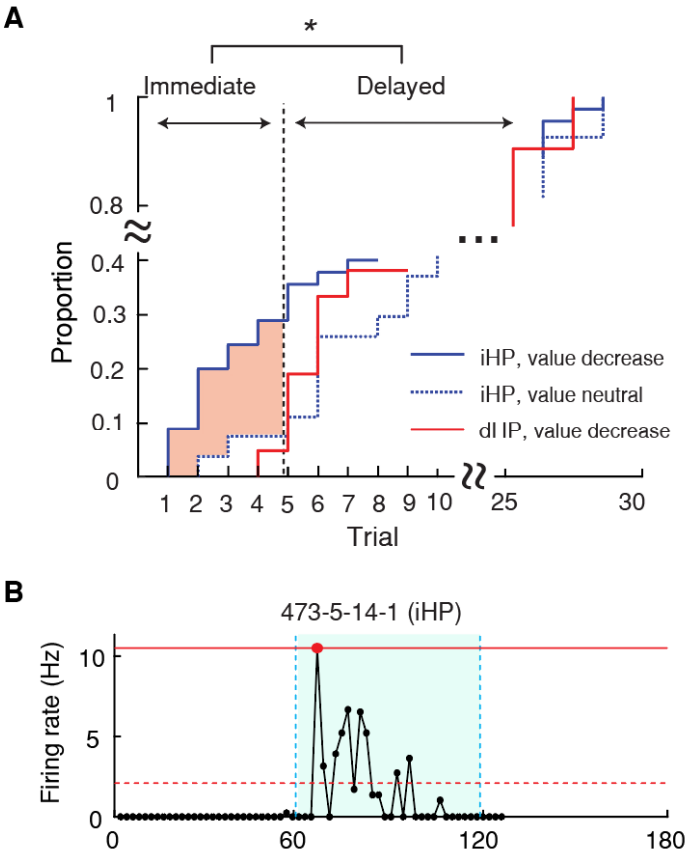

Figure 3-12. More immediate ON cells in iHP than dHP

(A) The cumulative density function of the proportion of ON cells [immediate ON cells (<= trial 4) and delayed ON cells (> trial 4)] across reward-changing conditions in dHP and vHP. The asterisk denotes that there was a significant proportional difference between immediate and delayed ON cells among the three groups. (B) Example of immediate ON cell that was observed in the second day of same reward schedules. Asterisks indicate statistical significance (*p < 0.05).

After place cells were turned on, most ON cells maintained their firing rates until the end of the session (*sustained ON cells*) (n = 31/34 for dHP and n = 50/61 for iHP) (Figure 3-11B), whereas 10% to 20% of ON cells (n = 3/34 for dHP and n = 11/61 for iHP) maximally fired in Block 2 and became silent during or after Block 2 (*transient ON cells*) (Figure 3-11A). These transient activity patterns cannot be accounted for by recording instability because cells exhibiting stable firing during both pre- and post-sleep sessions were only used for analysis (Figure 2-2C and 2-2D, Figure 3-13). There is no proportional difference of transient ON cells between dHP and iHP ($\chi^2_{(1)}$ = 1.5, p > 0.1; Chi-square test). Most transient ON cells were

observed in iHP in value-decrease conditions across all animals [rat 448 (n = 2, 1.1%), rat 459 (n = 2, 0.9%), rat 463 (n = 1, 0.3%), rat 473 (n = 2, 0.4%), rat 509 (n = 2, 0.5%)], whereas the same types of neurons was observed in iHP in only two rats during value-neutral conditions [rat 459 (n = 1, 0.6%), rat 463 (n = 1, 0.3%)] or in dHP in only two rats during both conditions [rat 459 (n = 2, 0.6%), rat 463 (n = 1, 0.3%)]. We conducted only qualitative descriptions here because the number of cells exhibiting immediate activation in value-decrease conditions was overall small. Furthure researches are needed to find whether the resutls reflect the sparesly distributed nature of this functional class of cells or it is sampling bias in recording session (i.e., failing to record such cells in value-neutral conditions because of very sparsely distributed properties).

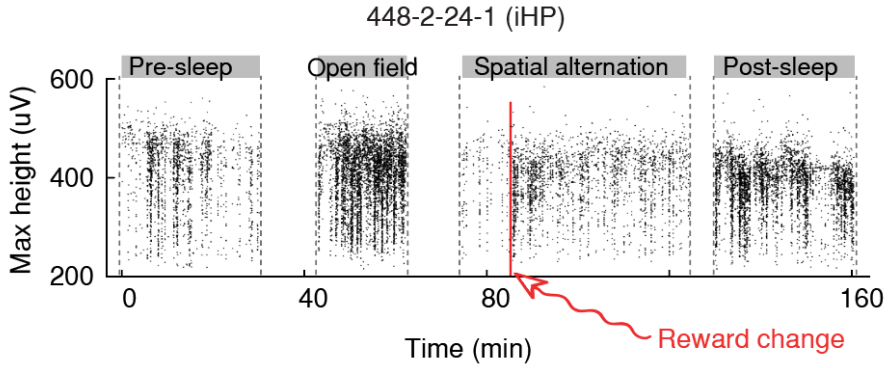

Figure 3-13. Verification of cell's stability by pre- and post-sleep session

The peak height of individual spikes is plotted as the function of time to confirm the stability of an ON-cell (448-2-24-1, Figure 3-11A). During the pre- and post-sleep recording sessions, the spike heights were maintained consistently.

Interestingly, most transient ON cells (n = 9/11) in iHP were activated in the earlier phase of Block 2 (< trial 9) (Figure 3-14A). And transient ON cells maintained for 12 ± 9 trials (mean ± SD) similarly between value-neutral (17 ± 4 trials) and value-decrease (11 ± 10 trials) conditions ($t_{(9)} = 0.96$, $p > 0.1$; independent t-test). Overall It is important to note that ON cells defined as both immediate and transient were only observed in iHP as well as only under value-decrease condition (Figure 3-14B). To summarize, most ON cells in dHP exhibited delayed and sustained neural activities in both value conditions, whereas, in iHP, the proportion of immediate ON cells increased ~3-fold in value-decrease conditions compared to value-neutral

conditions. Moreover, immediate and transient ON cells were only found in value-decrease, but not value-neutral, conditions in iHP (Figure 3-14B).

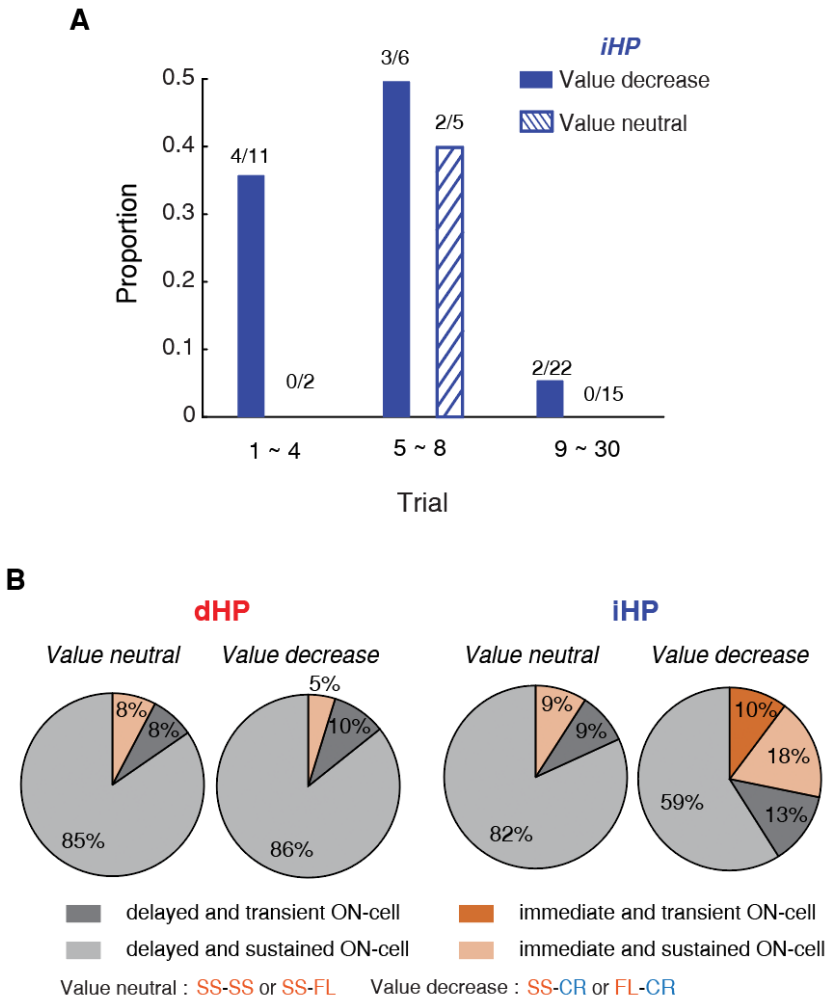

Figure 3-14. Proportion of immediate and transient ON cells in response to reward value-changing conditions

(A) The proportion of transient ON cells in value-decrease and value-neutral conditions was shown depending on their onset trials (i.e., place cells were activated within trial 1 ~ 4, trial 5 ~ 8, and trial 9 ~ 30). The number above each bar denotes the percentage of the number of transient ON cells divided by the number of overall ON cells that activated in certain trial epochs (i.e., trial 1 ~ 4, trial 5 ~ 8, and trial 9 ~ 30). (B) Pie chart summarizing the proportion of ON-cell types across all conditions in dHP and iHP. The types of ON cells were classified as a 2-by-2 matrix by (1) immediate or delayed and (2) transient and sustained.

In addition to the aforementioned neural firing properties in HP, some place cells in iHP immediately shifted their place fields [measured by the center of mass (COM) of the field] after Cheerios was introduced in value-decrease conditions. Two place cells examples showed the neural activity patterns of exhibiting immediate place-field shift both in value conditions (from sunflower seeds to Cheerios and from Froot Loops to Cheerios) (Figure 3-15A). We found that some fields moved toward reward locations (Forward, positive ΔCOM, n = 7 both in sunflower seeds-to-Cheerios and Froot Loops-to-Cheerios conditions), and others shifted in the opposite direction (backward, negative ΔCOM, n = 11 in sunflower seeds-to-Cheerios conditions, and n = 6 in Froot Loops-to-Cheerios conditions). ΔCOM in sunflower seeds-to-Cheerios conditions tended to move abruptly in both forward and backward directions after the reward type was changes (Figure 3-15B). Interestingly, ΔCOM in Froot Loops-to-Cheerios conditions shifted right before the type of reward changed (Figure 3-15C). These remapping patterns may be attributable to the expectation of reward changes because rats already underwent the same reward-changing schedules for 2 days before Froot Loops-to-Cheerios conditions. Taken together, these results suggest that some place cells in iHP immediately changed their neural activities in response to changes in motivational significance vai global remapping (either by creating or shifting the place fields), whereas such class of neurons is rarely found in iHP.

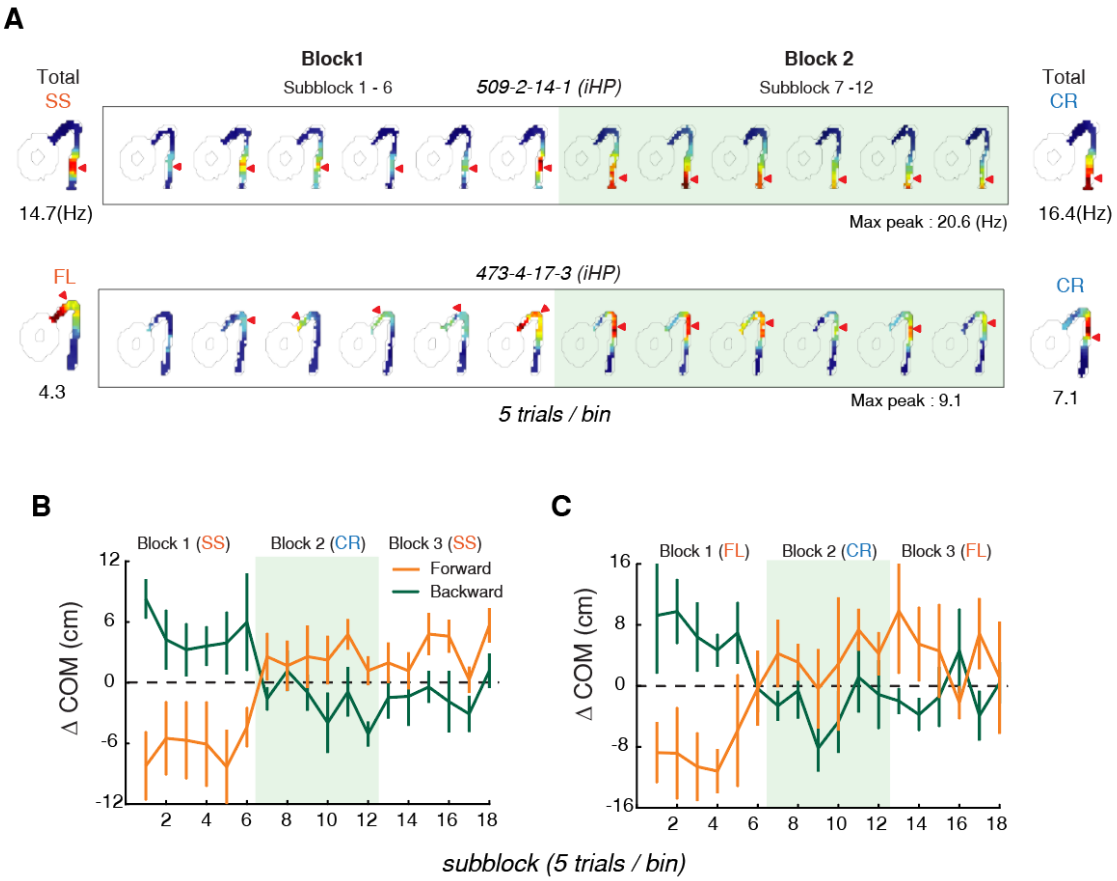

Figure 3-15. Immediate place field shifts in response to the decreased in reward value

(A) Place cell examples exhibiting their place field shifted immediately in Block 2. Tracking the place fields changes by constructing the rate maps for consecutive 5 trials (black-outlined box) and calculating the center of mass (COM, red arrowhead) of place fields. The average place field calculated by using overall trials for each block was located at the ends of left and right arms, respectively. Immediately after the Cheerios was introduced from sunflower seeds or Froot Loops (green-shaded box), there was an abrupt COM shift in place fields. (B-C) Tracking the relative COM of each subblock from Block 1 to 3 (greed-shaded box during Block 2 compared with COM of place fields based on overall trials during Day 2-3 (B) (from sunflower seeds to Cheerios) and Day 4-5 (C) (from Froot Loops to Cheerios). Data are presented as mean ± S.E.M.

3.4 Discussion

It is widely known that global remapping and rate remapping are the way of place cells to process the environmental changes, the former occurring after some significant changes in the environment and the latter generated by minor changes (Colgin et al., 2008). In our studies,

global remapping of place cells in iHP was observed in response to changes in motivational value, while place cells in dHP mostly maintained their fields. Approximately 15% of place cells in dHP went through global remapping during spatial alternation task, regardless of value-neutral and value-decrease conditions, whereas the number of globally remapped cells nearly doubled in iHP during value-decrease condition compared to value-neutral condition. Global remappings of place cells in iHP might occur due to behavioral changes, such as movement velocity. It is natural that motivationally significant information influences an animal's behavior. For example, when animals find prey in the wild, they run as quickly as possible to catch it. In our task, the rat's velocity was decreased after encountering the Cheerios, and they hesitated to displace the food-well disc covering Cheerios (Figure 3-2D). Although it is difficult to disentangle whether the cause of global remapping was a change in reward value or a change in behavior, I tried to test the possibility that global remapping was affected by rat's movement speed (McNaughton et al., 1983a). I did the same analysis by excluding the cells whose firing rate was positively correlated with velocity (Figure 3-6B and 3-6C). The exclusion of speed-correlate cells did not influence our main findings.

Kennedy and Shapiro (2009) reported that cells in dHP do not show remapping in terms of motivational state by comparing the water-foraging task (i.e., thirsty state) and food-foraging task (i.e., hungry state) during the random raging task. In contrast, motivational state-dependent remapping was observed when rats were required to spatial choice behavior in a trident maze. Direct comparison between Kennedy and Shapiro (2009) and ours is difficult because they did not discriminate cells showing global remapping and rate remapping, and they only recorded dHP, but not iHP. Also, the difference between motivational state (i.e., thirst and hunger) and motivational value (i.e., more-preferred and less-preferred rewards) made it hard to compare the results.

Globally remapped place cells in iHP may depend on amygdala inputs. Tobler et al. (2005) and Bermudez and Schultz (2010) reported that neurons in the non-human primate amygdala could vary their firing rates in response to changes in the amount of reward. Tye and Janak (2007) suggested that amygdala cells in rodents could encode the motivational level. These results implied that amygdala neurons dramatically changed their firing rate after the type of rewards was changed from sunflower seeds to Cheerios in our experiments. Considering the innervations from amygdala to iHP (Petrovich et al., 2001; Pikkarainen et al., 1999), such dramatic changes in amygdala may be directly conveyed to iHP, subsequently

inducing the global remapping of place cells in iHP. Although only a very sparse subset of neurons in iHP immediately turned their activities on in accordance with value-decrease episodes, it is important to report that such types of cells were observed across all animals. Thus, it is feasible that there is a sparsely distributed type of neurons in iHP that encodes sudden motivationally significant changes in the environment.

In the current study, when rats experienced a demotivating event (from sunflower seeds to Cheerios), approximately one-fourth of total neurons in iHP showed global remapping. However, the same amount of global remapping was not observed when the reward was switched from Cheerios to sunflower seeds again (Figure 3-16A). One possibility is that the motivational level for sunflower seeds during block 3 is lower than during block 1. This is because rats already ate 120 pieces of reward until block 2, which takes up the half amount of food they eat in a day. Therefore, rats were less crave sunflower seeds during block 3 than block 1. This probably explains why speed in block 3 became lower than that in block 1, although it is higher than that in block 2 (Figure 3-16B). On a related note, place cells with their fields along Route 1 (the path where rats went through the reward changes for the first time) only exhibited significant remapping, whereas that did not observe in the place fields associated with Route 2. Even though its fundamental mechanisms are unknown, novelty-related modulation may play a role in these neural activity changes associated with Route 1 when rats experienced unexpected reward changes for the first time. If more sophisticated experiments will be conducted, changing the only one of two rewards may be a option to investigate whether place cells were accumulated near high-value arms compared to low-value arms in spatial alternation situations as they did in place-preference task.

In the current experiment, reward value was controlled only by the palatability of food types. However, the value can be manipulated in various ways, such as reward amount (Tobler et al., 2005), reward probability (Lee et al., 2012), and delay length (Masuda et al., 2020). Thus, it needs to be further experiments to examine whether the hippocampus would process generalized value-changing condition or specific types of the condition. In my speculation, changes in reward type and reward amount would elicit similar effects on rat's motivational significance. Therefore, the latency would increase if rats performed spatial alternation tasks in response to decreases in reward amount.

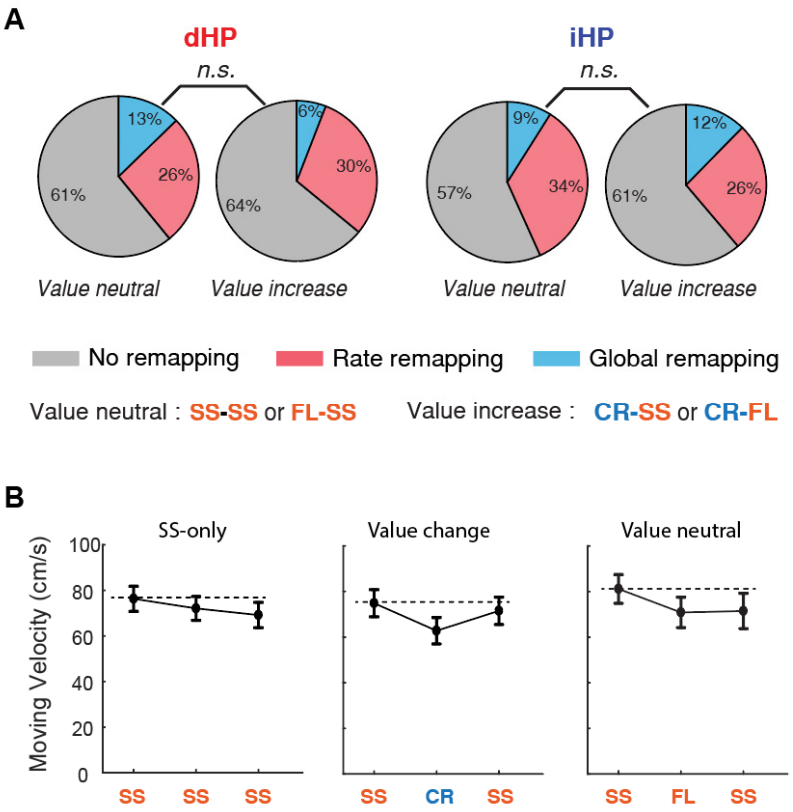

Figure 3-16. Proportion of remapping cells from Block 2 to Block 3

(A) Comparison of the proportion of cells exhibiting global and rate remapping between dHP and iHP after the reward was back to baseline from Block 2 to 3.

Throughout all experimental conditions, approximately 30 to 35% of place cells in both dHP and iHP showed rate remapping. In literature, it has been reported that place cells could encode environmental changes in the way of rate remapping without changing their preferred firing locations. For instance, manipulation of changing the color or shape of the recording chamber or visual context caused firing-rate modulation (Jeffery and Anderson, 2003; Lee and Lee, 2020; Lee et al., 2018; Leutgeb et al., 2005). Because our results showed that the amount of rate remapping was not significantly differed between value-neutral and value-decrease conditions, it would be possible that rate remapping might not be used as neural mechanisms of encoding a motivational value in the hippocampus.

CHAPTER 3

4.1 Introduction

In the spatial alternation task described in chapter 2, rats were required to minimal mnemonic load because they shuttled between two fixed reward zones in the radial arm maze. Thus, we developed hippocampal-dependent memory tasks (i.e., place-preference task) to examine the possibility that the aforementioned difference in motivational significance coding between dHP and iHP would be more manifest during a mnemonic task (Duvelle et al., 2019; Ferbinteanu and Shapiro, 2003). Compared with the spatial alternation task that the rat traversed two reward locations with fixed routes, during the place-preference task, rats were required to choose between two arms differently associated with motivational values. Thus, this task may enable rats to dynamically process the conjunctive coding between the locational information (e.g., visual cues and path integrated information) and motivational values of the reward. Moreover, because the starting locations were reversed in some trials to make conflict between allocentric and egocentric information, rats were required to flexibly use their cognitive map in the place-preference task than the spatial alternation task.

4.2 Methods

The method already introduced in Chapter 2 has been omitted here.

4.2.1 Behavior paradigm

Place-preference task (T-maze): The 8-arm maze abovementioned in chapter 2 was transformed into a T-shape maze by installing a transparent acrylic structure in the center platform. The rat was confined to the start arm by an acrylic blocker. All other experimental conditions were the same as in the spatial alternation task. In the place-preference task, rats were required to select an arm associated with a more preferred type of reward (e.g., sunflower seeds) over a less-preferred reward (e.g., Cheerios cereal). Rats learned the arm in which high-value reward (sunflower seeds) was baited by trial and error in Block 1. When the rat selected the high-value arm for 12 of the final 15 trials in Block 1, the start arm was changed to the arm opposite the start arm used for Block 1, whereas the location of high-value reward in relation to room cues remained the same (Block 2). This manipulation recruited the hippocampus to be involved during performing the task (Packard and McGaugh, 1996). If the rat met the

performance criterion in Block 2, rats were located at the original starting arm in Block 3, but the relationship of reward type and room cues was reversed (Figure 4-1). After the rats had been performed for two successive days with sunflower seeds and Cheerios, they were tested in the same paradigm, but this time sunflower seeds were only provided in the two reward arms but in different amounts (i.e., 4/4 sunflower seeds vs. 1/4 sunflower seeds). The location of sunflower seeds on the first day was pseudo-randomly determined, and all rats departed from the south arm in Block 1.

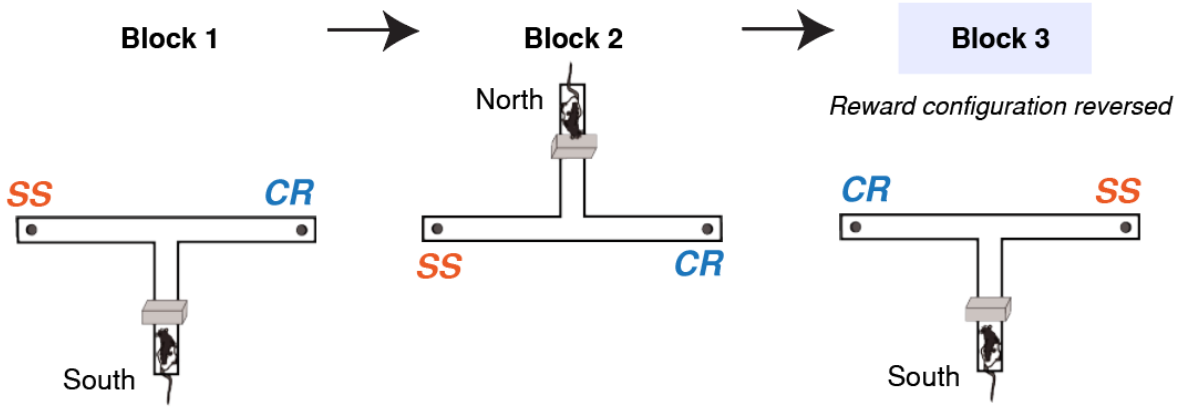

Figure 4-1. Behavioral paradigms of place-preference task

Illustration of the procedures for the place-preference task. Rats were confined at the end of the south arm (Block 1 and 3) or north arm (Block 2) by an acrylic blocker before each trial began. The type of reward and its location were swapped in Block 3 (blue shaded box).

4.2.2 Principal component analysis for neural ensemble state

To examine the neural state changes in response to motivational value changes in Block 3, we applied principal components analysis (PCA). For each trial, we calculated the mean firing rate of the place field for each trial and used it as constructing the population array of firing rate, which has as many columns as the number of ensembles. After applying PCA, a network state was determined by the first N principal components (PC) that captured 80% of the variance, and the first three PCs were utilized to visualize neural state trajectories across trials (Liu et al., 2014). Point consisted of N PCs was defined as the neural state in that trial. The mean neural

state of the post-learning stage was calculated as the average of N PCs. To quantitatively calculate changes in neural states, we measured the Euclidean distance in N principal dimensions between the neural state of each trial and the mean neural state in the post-learning period (Figure 4-7B). When visualizing trajectories and measuring Euclidean distance, PCs smoothed by a Gaussian filter (window size, 7; FWHM, 5) were used. Neural trajectories of rats (n = 6) were overlaid after normalizing trials during the pre-learning stage and post-learning stage, respectively. To ensure there was sufficient dimension for PCA analysis, we included sessions in which the number of ensembles in either dHP or iHP was larger than 9 (Table 5-1). The Euclidean distance lines for each rat were overlapped after normalizing trial 1 to N (acquisition trial) and trial N+1 to trial M (block end) (Figure 4-7I and 4-7J).

# of ensemble in T-maze		r448		r459		r463		r473		r488		r509	
Day	Session type	dHP	iHP	dHP	iHP	dHP	iHP	dHP	iHP	dHP	iHP	dHP	iHP
8	SSCR	3	10	18	10	22	18	2	33	0	5	4	14
9	SSCR	2	11	15	11	16	15	2	40	0	3	4	19
10	Quantity	6	13	17	11	14	10	6	40	0	3	5	6
11	Quantity	4	11	15	7	12	9	4	34	0	4	5	6

Table 4-1. Number of ensembles recorded during the place-preference task

Some sessions failed to identify the acquisition onsets in block 3 when applying the state-space model and were excluded in the ensemble analysis (grey shaded session).

4.2.3 Synchronization of spiking activity

Cross-correlograms were employed similarly as autocorrelograms, but using a different time bin size (1 ms) and time window (±100 ms). Gaussian smoothing (window size, 21 ms; FWHM, 10 ms) was applied to the cross-correlogram, and analyses were performed using smoothed data. All possible pairs were checked, and pairs for which the peak of the correlogram was greater than 6 (number of spikes per bin) were used for analyses to exclude pairs with an insufficient number of coincident firings. Two different spike trains were used, with one neuron assigned as a reference and the other neuron as a target. The zero-point indicates the time of a reference cell discharge. Each spike in a train was randomly and independently jittered at a uniform interval of -30 to +30 ms to generate a surrogate data set. This process was repeated 10,000 times, forming 10,000 surrogate cross-correlograms. Significant cross-correlogram bins

were defined as those that exceeded the predicted 1% spike count band of surrogate data sets (Valenti et al., 2018). Interactions between pairs of cells were accepted as significant if a significant bin was detected. If the peak of the correlogram was within -100 to 0 ms, we inferred that spikes in the iHP led to those in the dHP (i.e., iHP preceding); if the peak of the correlogram was within 0 to 100 ms, spikes of the iHP were considered to lag those of the dHP (i.e., dHP preceding). Spike trains were divided according to behavior status (e.g., sleep, open field, main task), and cross-correlograms were obtained separately. Except for using a different jittering window from -500ms to 500ms of the raw spike data, all other procedures were performed in the same way to obtain the chance level.

4.3 Results

4.3.1 Overrepresentation of the motivationally significant place by the place cells in iHP, but not in dHP

In the first block of the place-preference task, rats learned by trial and error to choose the arm associated with more-preferred rewards (sunflower seed) than that associated with less-preferred rewards (Cheerios) until they reached the behavioral criteria (*acquisition onset*) (Figure 4-1). In Block 2, the spatial relationships between reward locations and allocentric reference frame defined by multiple visual cues surrounding the maze remained the same, but rats were started from the opposite side of the arm compared to Block 1. This required rats to use an allocentric navigation strategy to memorize the arm locations, which is known to recruit the hippocampus to be involved (Packard et al. 1996). In Block 3, the starting point was back to the same arm as in Block 1, but the spatial contingencies between the type of reward and its locations were reversed (Figure 4-1).

To identify the acquisition onset trial where learning took place in each block, a state-space model (Smith et al., 2004) was applied to behavior performance, which has been used in previous literature to estimate the probability of making a correct choice in a trial-by-trial manner (Figure 4-2A and 4-2B) (Jadhav et al., 2012; Park et al., 2021; Sosa et al., 2019). Rats learn to choose the sunflower seeds-baited arm reliably within about ten trials in both Block 1 and 2 (Figure 4-2A), suggesting that rats were able to use the allocentric navigation strategy. But, when the room-referenced spatial contingency for reward locations was swapped in Block

3, it took approximately 3-times as many trials for rats to learn the new sunflower seed-baited arm locations. To verify that the motivational values of places were the key factor in learning the task, we also conducted the same experiments, only using sunflower seeds but in different amounts. That is, rats carried out the same place-preference task on Day 10-11, but this time, a whole piece of sunflower seeds (4/4 sunflower seeds) and a quarter piece of sunflower seeds (1/4 sunflower seeds) were baited in arms, respectively (Figure 4-2B). The number of trials required to reach acquisition onset was not significantly different between Day 8-9 (sunflower seeds vs. Cheerios) and Day 10-11 (4/4 sunflower seeds vs. 1/4 sunflower seeds). ($p > 0.1$ for Blocks 1 and 3, $p = 0.03$ for Block 2, alpha = 0.016; independent t-test with Bonferroni corrections) (Figure 4-2C). And, the delayed learning in Block 3 cannot be attributable to a decrease in motivation because rats run the task with fairly constant latencies to arrive in reward location from starts throughout all blocks (p-values > 0.1 for all block pairs) (Figure 4-2D).

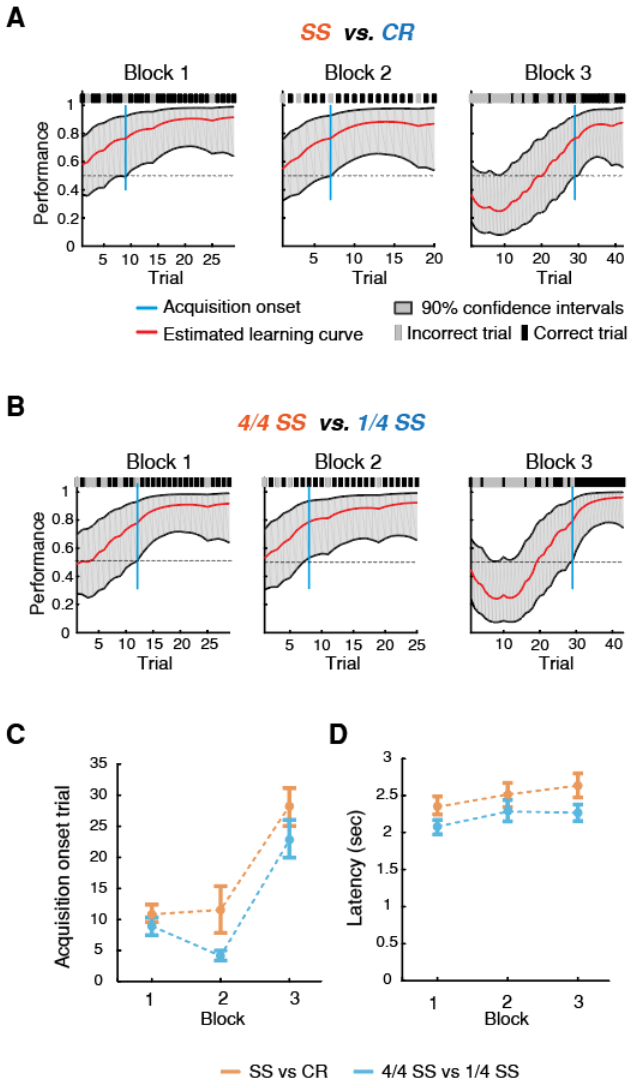

Figure 4-2. Behavior performance for place-preference task

(A-B) The estimated learning curve when sunflower seeds and Cheerios were used as a reward in Day 8-9 (A), or when 4/4 sunflower seeds and 1/4 sunflower seeds were baited in Day 10-11 (B). Correct and incorrect trials are plotted by black and gray lines on top of each graph, respectively. The red line denotes the estimated learning curve, and the light-gray shade indicates the 90% confidence interval of the performance. The estimated trial at which the learning occurred is marked by a blue line. (C) Average of acquisition onset trials for each block. (E) Average latencies for each block. Data are presented as means ± SEM.

In the place-preference task, some place cells seemed to remap when there was a mismatch between allocentric and egocentric information in Block 2, but their firing fields

returned back to original fields when spatial contingency was restored in Block 3 (Figure 4-3A, 463-8-11-4 and 463-10-9-19). Other cells globally remapped in Block 2, seemingly in response to changes in start-arm location, and maintained their remapped fields until the end of the session (Figure 4-3A, 463-8-9-13 and 459-10-11-4). Interestingly, some place cells in dHP have the same place fields across the blocks, which indicated that these cells fired in relation to only allocentric visual cues (Figure 4-3A, 509-9-9-2 and 459-11-10-11).

In contrast, place cells in iHP exhibited more complex remapping patterns in response to changes in motivational value compared with those in dHP. In iHP, a finding cannot be fully explained by allocentric and egocentric frames as in dHP. To be specific, in Block 1 and 2, cells in iHP fired on the arms where high-value rewards (i.e., sunflower seeds and 4/4 sunflower seeds) were provided, seemingly irrespective of the mismatch in allocentric and egocentric situations. More importantly, in Block 3, place cells in iHP tended to remap toward the arm where high-value rewards were baited (Figure 4-3B, 463-9-12-7 and 473-10-4-2). This result suggested that the place cells in iHP represent the place in which the high-value rewards were associated, rather than the place represented by the spatial relationships between allocentric and egocentric information. This was also observed in place cells whose firing fields were larger and represented multiple areas of the maze (Figure 4-3B, 509-9-4-10 and 448-10-23-1). Moreover, some place cells initially silent in Block 1 (and/or Block 2). However, in Block 3, they were suddenly activated or radically remapped to represent the arm newly associated with high-value rewards (Figure 4-3B, 488-8-20-1 and 473-10-22-2).

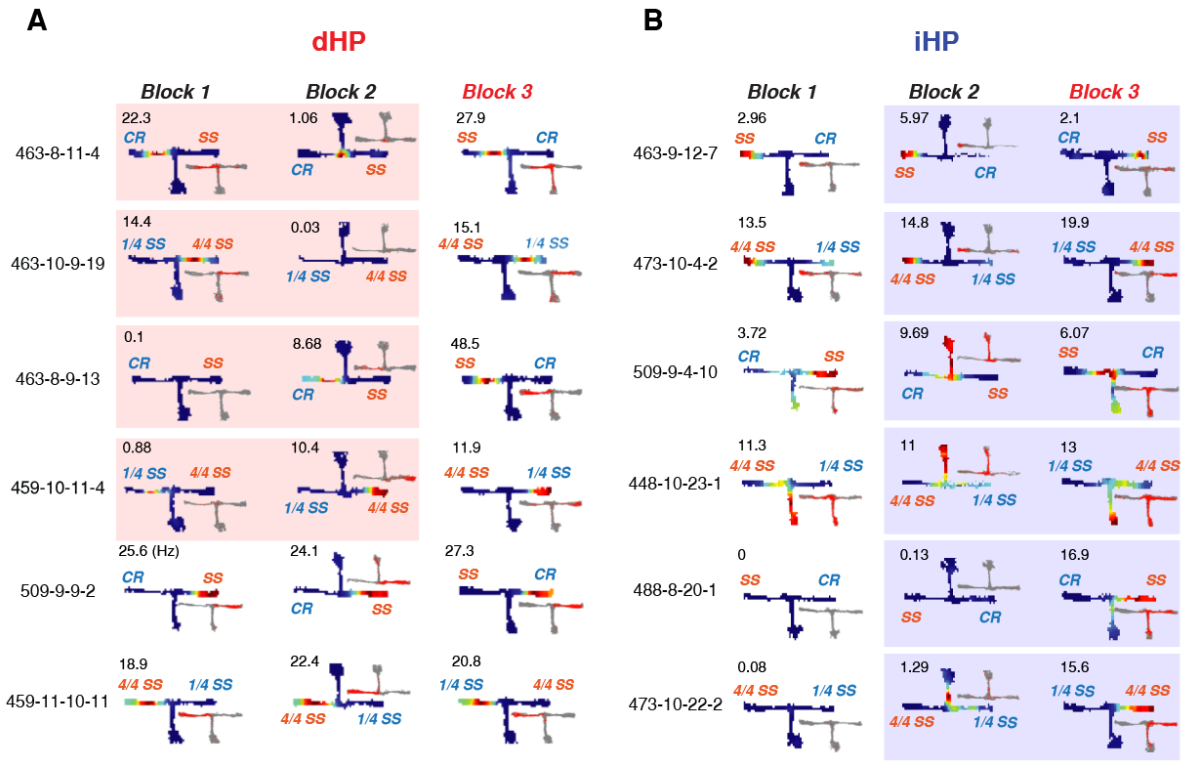

Figure 4-3. Examples of place cells in place-preference task

(A-B) Representative spatial rate maps and corresponding raw spiking maps during the place-preference task. The spatial relationship between reward type and its associated value was swapped in Block 3. The maximum firing rate is provided above the spatial rate map. The spatial rate maps in which global remapping occurred are marked by red- and blue-colored shaded in dHP (A) and iHP (B), respectively.

We quantitively measured the effects of reversing the start-arm location on place cell activities by calculating the spatial correlation between spatial rate maps for Block 1 and 2. When rats started from the opposite side of arms in the sunflower seeds-Cheerios task (Day 8-9) in Block 2, the spatial rate maps became more deformed significantly in dHP than in iHP ($Z = -2.6$, $p = 0.01$; rank-sum test) (Figure 4-4A). Similar results were observed in the sunflower seeds-only task (Day 10-11) ($Z = -3.4$, $p < 0.001$; rank-sum test) (Figure 4-4A). In contrast, opposite neural firing patterns were found in dHP and iHP between Block 1 and 3 when all physical conditions were the same except for the changes in the locations of more-preferred rewards (sunflower seed-Cheerios task: $Z = 2.7$, $p = 0.006$; sunflower seed-only task: $Z = 3.2$, $p = 0.0014$ [rank-sum test]) (Figure 4-4B). These results suggest that dHP is specialized in processing the changes in cognitive rules, whereas iHP takes priority in representing the

motivational values in an environment.

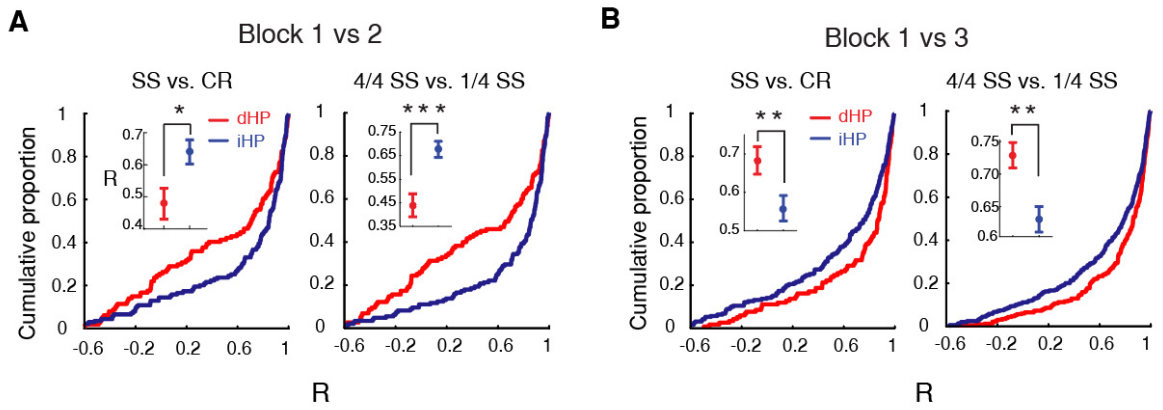

Figure 4-4. Spatial correlation coefficients in response to changes in starting arm or preferred-reward locations

(A-B) Cumulative density functions of the spatial correlation coefficients of spatial rate maps between Block 1 and 2 (A) and Block 1 and 3 (B) for different types of devaluating manipulations. Data are represented as mean ± SEM. Asterisks indicate statistical significance (*p < 0.05; **p < 0.01; ***p < 0.001).

Next, we investigated the degree of representing the motivationally significant places in dHP and iHP (Duvelle et al., 2019; Tabuchi et al., 2003). First, we constructed a population rate map for each choice arm by ordering and stacking the place fields representing one of the choice arms (Figure 4-5A and 4-5B), using only the trials (defined by the state-space model) that rats learned the task. Because the global remapping patterns were similar between Day 8-9 and Day 10-11 (Figure 4-4), place cells obtained from Day 8-9 and Day 10-11 were combined. The population rate maps for Block 1 and 3 were almost similar in dHP, with a somewhat thicker and less linear diagonal line on the population rate map associated with sunflower seeds-baited left arm in Block 1 and right arm in Block 3 (Figure 4-5C). In iHP, place fields were significantly concentrated in the left and right reward zone associated with high-value rewards in Block 1 and 3, respectively (Figure 4-5D). This overrepresentation results in distorting the linearity of a diagonal line of the population rate map, which was weakly observed in dHP.

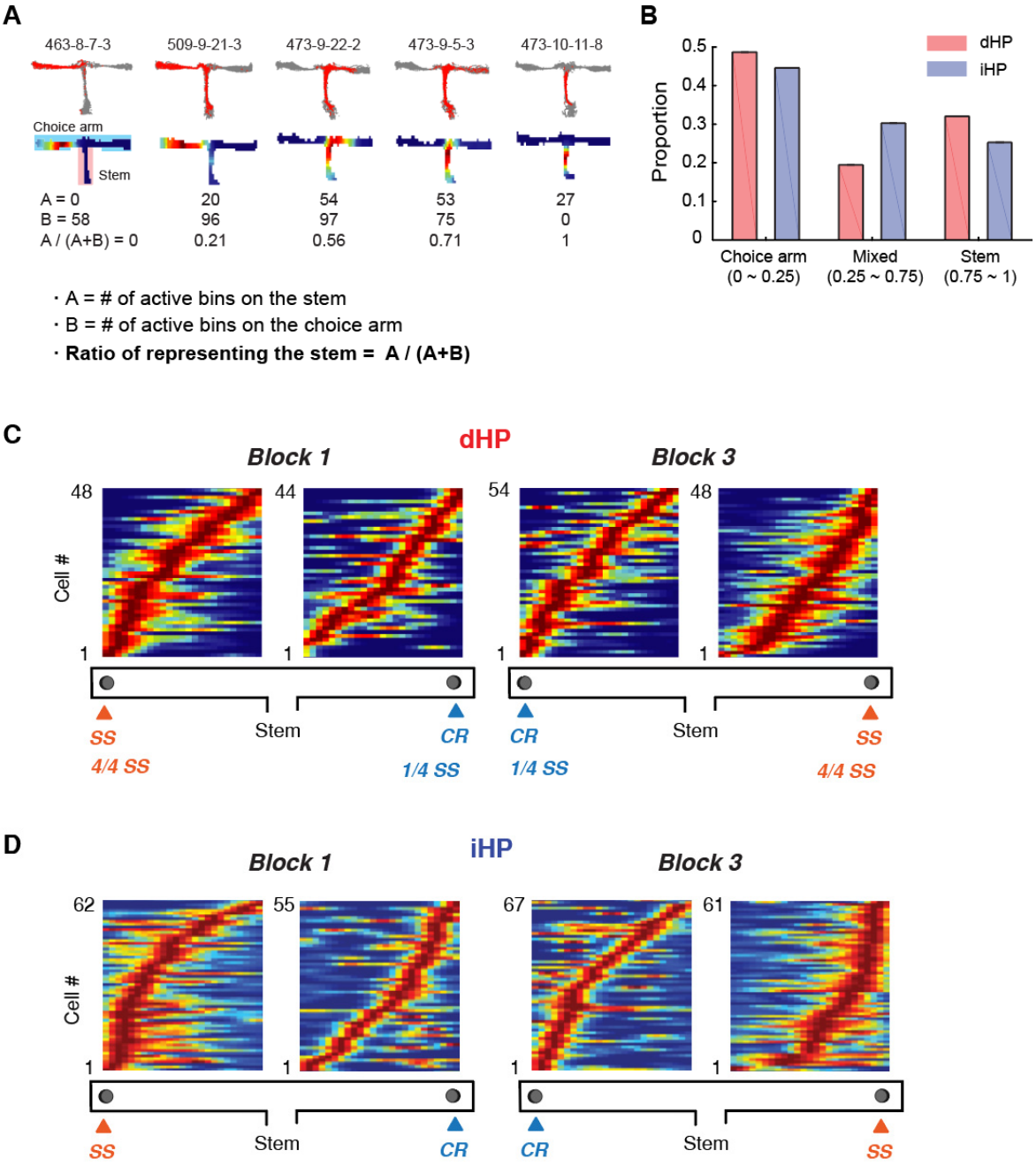

Figure 4-5. Overrepresentations of motivationally significant areas in iHP, not dHP

(A) Five representative examples to show the relationships between the place fields boundary and the ratio of representing the stem. The raw spike maps (top) and spatial rate maps (bottom) are shown together. Cell identity is provided on top of the raw spike maps. The ratio of representing the stem was calculated by dividing the number of active bins on the stem by the sum of the number of active bins both in stem and choice arm. (B) The proportion of place cells representing the choice arm, mixed, and stem. Half of the place cells represented the choice arm. (C-D) Population rate maps in dHP (C) and iHP (D) constructed using linearized rate maps of each arm of the T-maze for individual cells.

To quantify the strength of accumulation of place fields near the high-value reward areas, the distribution of maximum-firing locations of individual place cells was made for Block 1 and 3 and overlapped along the choice arm. The distribution of peak-firing locations was significantly differed between Block 1 and 3 in iHP ($p < 0.1$, Kolmogorov-Smirnov test), but not in dHP ($p > 0.1$), mainly because place cells in iHP fired more vigorously in the reward zones associated with more-preferred reward (Figure 4-6A). The proportion of place cells whose firing fields were located near high-value zones was also significantly higher in dHP than iHP (Figure 4-6B). That is, for dHP, the proportion was similar between high- and low-value arms in both Block 1 and 3, whereas approximately 15% of place cells in iHP were more accumulated in the high-value arm compared with the low-value arm both in Block 1 and 3. Moreover, the width in linearized place fields in which robust firing was found (i.e., > 50% of maximal firing) was significantly larger for place fields located in the high-value arm than those in low-value arm in iHP, but not dHP (dHP, $p > 0.1$, $t_{(99)} = 1.2$; iHP, $p < 0.001$, $t_{(124)} = 3.4$; independent t-test with Bonferroni corrections) (Figure 4-6C). Overall, these results suggest that place cells in iHP overrepresent the motivationally significant area to a greater extent than those in dHP in the place-preference task.

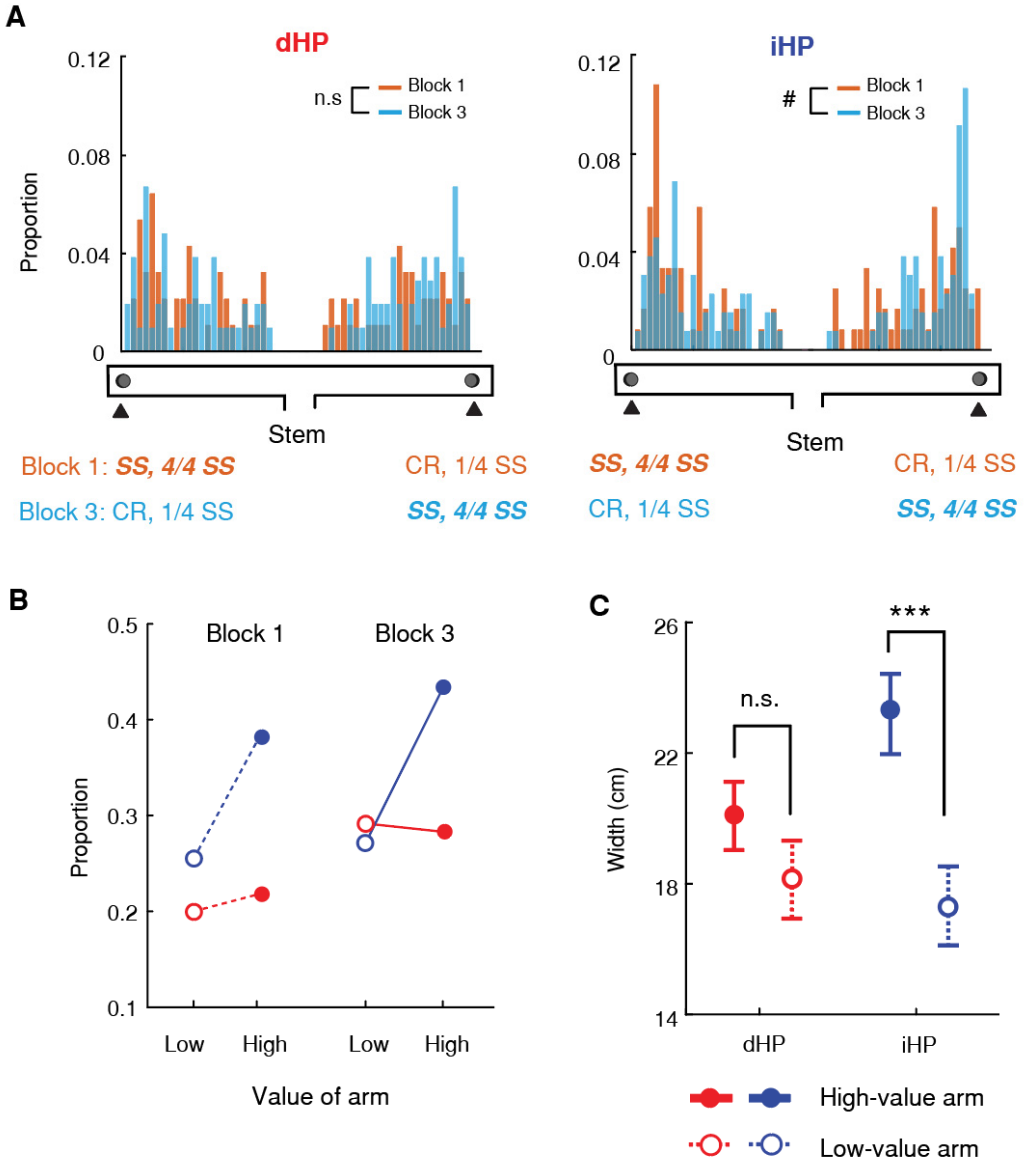

Figure 4-6. Quantitative verification of overrepresentations of place fields near high-value arm in iHP, but not in dHP

(A) Distributions of the peak firing locations of linearized place fields in Block 1 and 3 (overlaid for the matching arms). (B) The percentage of place cells whose maximum firing position was within 10cm of the reward zone. (C) Average widths of the place fields based on linearized rate maps for the high- and low-value arms, respectively. Data are represented as mean ± SEM. Asterisks indicate statistical significance (#$p < 0.1$; ***$p < 0.001$).

4.2.2 Rapid changes of the ensemble network changes in iHP, compared to those in dHP

We further investigated the contribution of neural ensemble activities to the acquisition of the place-preference task by investigating dynamic changes in both dHP and iHP neural networks as rats learned the place-preference task (Bast et al., 2009). To achieve it, we calculated the ensemble network state of Block 3 using a principal component analysis (PCA) (see more details in Method). Because upcoming choice (e.g., left or right arm choice in our case) has an impact on the firing rates of place cells on the stem of T-maze (Ferbinteanu and Shapiro, 2003), we separately analyzed sunflower seeds-chosen trials (Figure 4-7A to 4-7D) and Cheerios-chosen trials (Figure 4-7E to 4-7H).

In the case of sunflower seed-chosen trials, the neural ensemble state of dHP maintained stably during the initial visits to the sunflower seed-baited arm (yellow circles in Figure 4-7B). After approximately the 6th visit, the neural state started to move to reach a state which was near the average neural state of the post-learning phase (red dot in Figure 4-7B). In contrast, the neural state in iHP immediately shifted from the beginning and reached the average post-learning neural state earlier than dHP did (Figure 4-7C). Also, the Euclidean distance measured between each trial state and mean neural state of post-learning stage rapidly decreased in iHP beginning with trial 1, well ahead of acquisition onset of place-preference task, whereas this time course was slower in dHP (Figure 4-7D). These differences between dHP and iHP were significantly distinct during the initial stage of Block 3 (from the second to the fourth time bin) during the pre-learning stage (dHP vs. iHP in the second time bin, $p = 0.0015$; the third time bin, $p = 0.0006$; the fourth time bin, $p = 0.0019$; alpha = 0.005; independent t-test with Bonferroni corrections) (Figure 4-7I). However, when the same analysis was applied to Cheerios-chosen trials, we did not observe such dynamic ensemble state changes as in sunflower seed-chosen trials (Figure 4-7E to 4-7H and Figure 4-7I). Taken together, these results suggest that changes in motivational values in space were more rapidly represented in iHP than dHP.

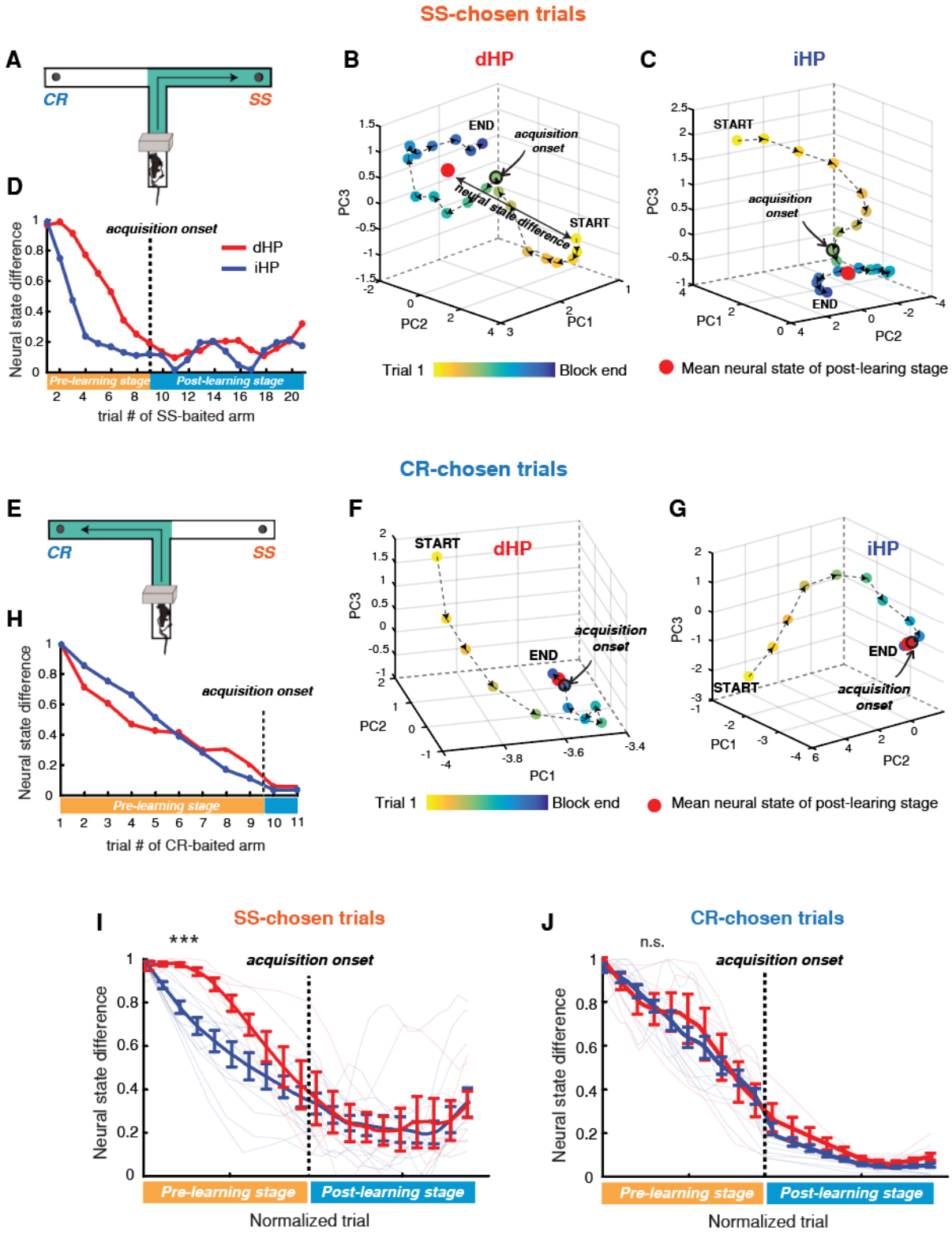

Figure 4-7. Immediate changes of neural ensemble state during the acquisition of spatial memory task in iHP, but not in dHP

(A) Illustration of rat's path of sunflower seed-chosen trials. (B-C) The ensemble network states of the

sunflower seed-chosen trials in Block 3 were plotted three-dimensional way using principal component (PC) 1, 2, 3. The average neural state of the post-learning phase is indicated by a red dot, and the acquisition onset point is marked by a black-outlined circle. The degree of difference in the neural state (*neural state difference*) was defined as the Euclidean distance between each trial's state and the mean neural state of the post-learning phase. (D) Only the trials in which sunflower seeds were chosen in Block 3 were used to plot the changes in the neural state difference. (E to H) The same analysis of Figure 4-7A to 4-7D was applied to Cheerio-chosen trials. (I-J) Average neural-state differences changes of the neuronal ensemble of dHP and iHP from the sunflower seed-chosen trials (I) and Cheerio-chosen trials (J), respectively. Data are represented as mean ± SEM. Asterisks indicate statistical significance (*$p < 0.05$).

4.2.3 Place cells in the dHP and iHP co-fire more strongly during a mnemonic task than non-mnemonic tasks

We next investigated the degree to which coordination of spiking activities in the dHP and iHP differed in a mnemonic task (place-preference task) compared with a non-mnemonic task (e.g., random foraging or shuttling in the linear track). First, a spiking cross-correlogram was constructed using pairs of place cells simultaneously recorded from both the dHP and iHP (Figure 8A). Some examples of pairs of place cells simultaneously recorded in Block 3 in the place-preference task are shown in Figures 8A–8D. In some pairs, spiking activity in the iHP preceded that in the dHP (*iHP-preceding* cell pairs), manifesting as an association of negative time bin with the peak of the cross-correlogram (Figure 8A–8C, pairs #1 to #3), whereas other cell pairs exhibited the opposite temporal relationship (*dHP-preceding* cell pairs; Figure 8D, pairs #4 and #5). In the place-preference task, 48% (n = 72/149) of cell pairs were iHP-preceding and 52% (n = 77/149) were dHP-preceding. There was no significant difference in the proportion of the two types of cell pairs ($z = 0.49$, $p > 0.1$; one-proportion Z test), which implies that the dHP and iHP may exchange information reciprocally to solve a goal-directed mnemonic task.

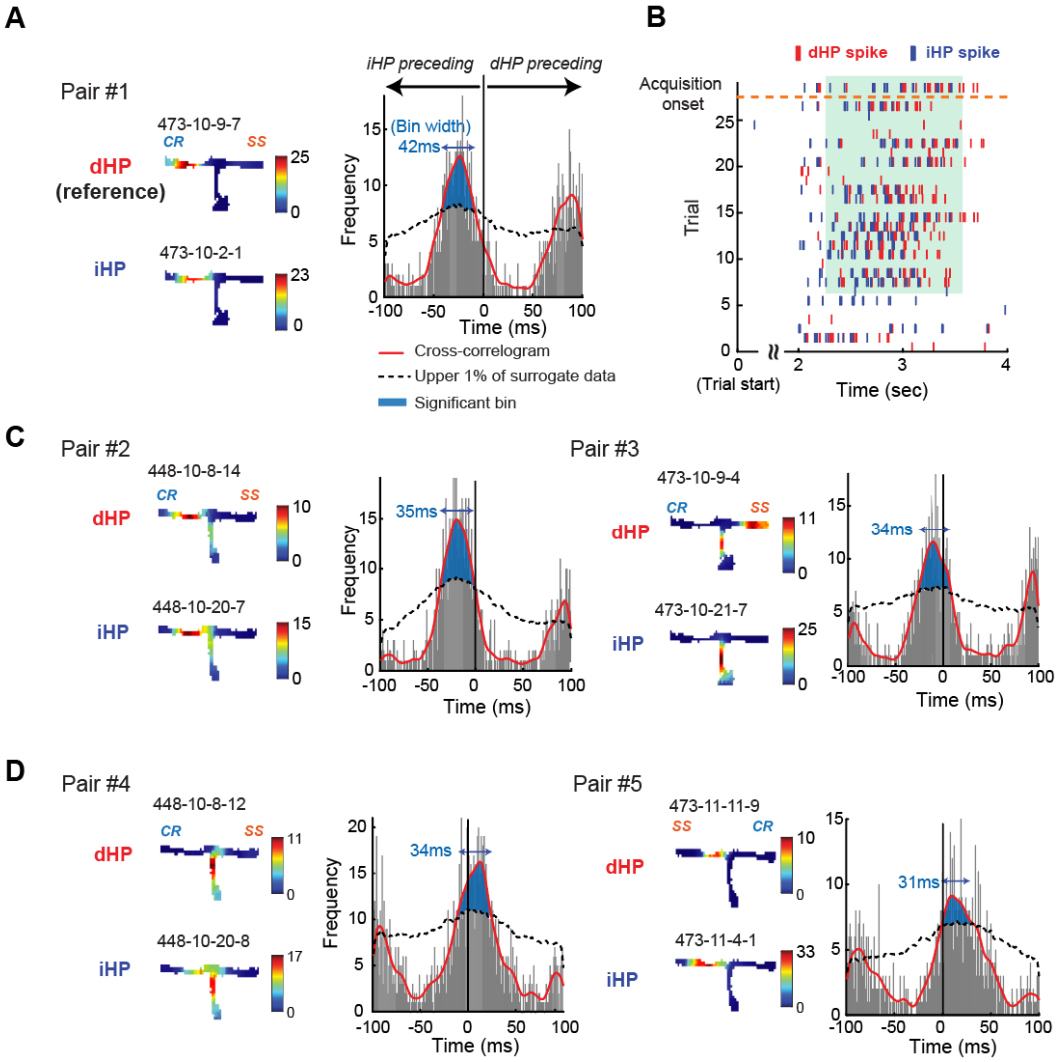

Figure 4-8. Co-firing neural activity between the dHP and iHP increased to a greater extent during a mnemonic task than during non-mnemonic tasks

(A) Examples of the rate maps of simultaneously recorded place cells from the dHP and iHP (iHP-preceding example) during Block 3 of the place-preference task (left). The number on the color bar indicated the maximum firing rate of the rate map. The cross-correlogram was constructed by using the spikes from the dHP as a reference. A raw cross-correlogram was smoothed using a Gaussian filter (red line). A black dotted line indicated the upper 1% of 10,000 surrogate cross-correlograms. Time bins where cross-correlogram was larger than upper 1% of surrogate correlograms were defined as significant bins implying that there were synchronized firings between the dHP and iHP (blue shaded area). (B) Raw spike trains of pair #1 are shown in (A) during the place-preference task. The value of 0 on the x-axis denotes the trial start. The areas where neuronal co-firing was clearly visible were marked with a green-shaded box. Note that the spikes from iHP closely led to the spikes from the dHP in time. The orange dotted line indicated the acquisition onset trial. (C-D) Examples of co-firing neuronal pairs

for showing iHP-preceding (C) and dHP-preceding (D) cases.

We then tested the strength of coincidental firing between place cells by measuring the area of the spiking correlogram that exceeded the upper 1% of the cross-correlogram constructed from surrogate spike trains in the original datasets (Amarasingham et al., 2012; Fujisawa et al., 2008; Louis et al., 2010) (Figure 8A, blue area in the cross-correlogram). At the population level, cell pairs with at least one significant bin within the ±100 ms time window were identified as showing strong co-firing relationships (*co-firing pairs*) (Narayanan and Laubach, 2009). The proportion of co-firing pairs was calculated by dividing the number of co-firing pairs by the number of pairs that exhibited a sufficient degree of coincidental firing (peak > 1). This analysis revealed that a higher proportion of dHP and iHP cell pairs co-fired during the mnemonic task compared with non-mnemonic tasks (Figure 8E). Specifically, in a non-mnemonic context, approximately 7 to 8% of cell pairs showed significant co-firing during random foraging in the open field (n = 532/7250) and also during shuttling between the fixed reward locations in a linear track (n = 127/1511). By contrast, the proportion of co-firing pairs during the place-preference task in the T-maze was approximately 20% (n = 149/786), indicating a sharp increase from the level of co-firing in the non-mnemonic tasks (random foraging vs. place-preference task, $\chi^2_{(1)} = 123$, $p < 0.0001$; shuttling vs. place-preference task, $\chi^2_{(1)} = 54.5$ $p < 0.0001$; Chi-square test with Bonferroni corrections) (Figure 8E). Because chance levels did not significantly differ between the three behavior tasks, the increase in co-firing proportion in the T-maze task was not because the chance level of co-firing was higher in the T-maze task than the random foraging and spatial alternation task ($\chi^2_{(2)} = 3.8$, $p > 0.1$, Chi-square test). The proportion of co-firing pairs was not significantly different between Block 1 and 3 ($\chi^2_{(1)} = 0.03$, $p > 0.1$; Chi-square test).

It is important to note that, as the preferred reward location was switched to the other side of the choice arm in the T-maze between Blocks 1 and 3, the strength of co-firing (measured as the length of time bins that exceeded co-firing strength in the surrogate distribution) between cell pairs in the dHP and iHP increased substantially only in iHP-preceding cell pairs ($t_{(112)} = 1.87$, $p = 0.06$), but not in dHP-preceding pairs ($p > 0.1$, $t_{(112)} = 1.07$; independent t-test with Bonferroni corrections) (Figure 8F). These results suggest that place cells in the iHP that send inputs to place cells in the dHP, but not vice versa, may deliver

signals that convey information on the change in spatial motivational significance when the preferred reward location was shifted to the opposite side in Block 3 in the place-preference task.

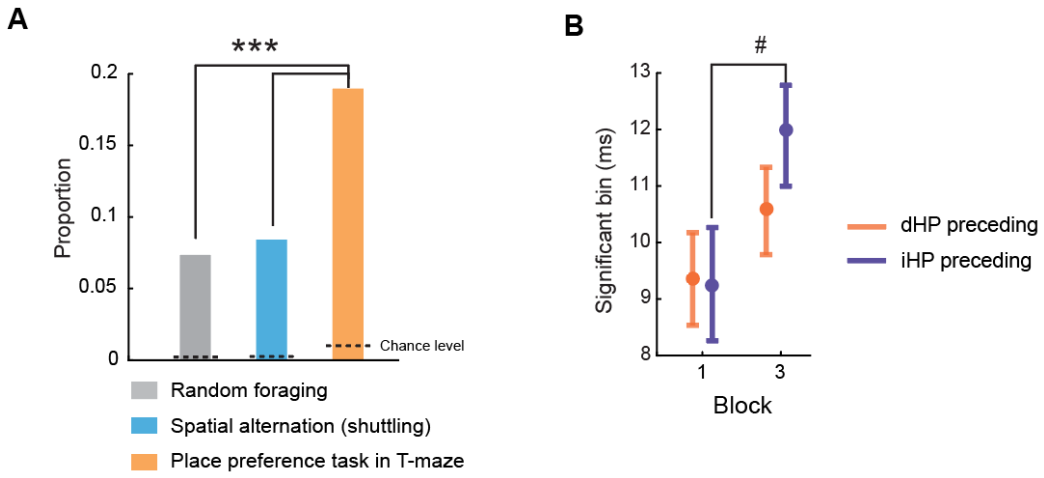

Figure 4-9. Co-firing neural activity between the dHP and iHP increased to a greater extent during a mnemonic task than during non-mnemonic tasks

(A) The proportion of co-firing pairs across different behavior tasks. (B) The average length of a time period that contained the time bins exceeding the upper 1% of the surrogate cross-correlogram in Blocks 1 and 3. Data are represented as mean ± SEM. Asterisks indicate statistical significance (#$p < 0.1$; ***$p < 0.001$).

4.4 Discussion

During the place-preference task, place cells in iHP could dramatically reorganize their place fields to overrepresent the locations associated with high-value rewards. Specifically, the place fields in iHP were accumulated near the left arm associated with the more-preferred reward (sunflower seeds) in Block 1. But, after sunflower seeds were baited in opposite arm in Block 3, the populations of place fields overrepresented the right arm via global remapping.

In spite of previous studies that reward and value signals were observed in dHP (Dupret et al., 2010; Hollup et al., 2001; Lee et al., 2012; Lee et al., 2006), we cannot found robust motivational value signals in dHP in our paradigms. One way to reconcile the discrepancy is to postulate that iHP is more sensitive to encoding the motivational value changes than dHP.

For example, cells in dHP may encode the all-or-none type of motivational changes (e.g., presence vs. absence of reward) (Breese et al., 1989; Dupret et al., 2010; Gauthier and Tank, 2018; Hok et al., 2007; Hollup et al., 2001; Lee et al., 2012; Lee et al., 2006; Mamad et al., 2017). With respect to this hypothesis, dHP may not respond to a change in motivational values if it does not exceed the particular threshold (Duvelle et al., 2019; Tabuchi et al., 2003). Accordingly, changing the reward types from more-preferred to less-preferred one may not strong enough to drive the global remapping in dHP, only driving the place cells in iHP. Another possible explanation is that our recording was biased toward proximal CA1 that received strong spatial signals from the MEC and weak non-spatial signals from the LEC (Steward, 1976; Wyss, 1981). Alternatively, previous studies might have recorded the place cells from iHP (by the standard in the current study) given the surgical coordinates in previous studies.

Although both dHP and iHP represented value information, the iHP received denser value signals from subcortical areas, such as the amygdala and ventral tegmental area. Also, it has been known that intermediate CA3 sends associational projections to dorsal CA3 and CA3 (Swanson et al., 1978). Thus, it is possible that the value signals found in dHP may be derived from the iHP. Our results of cross-correlogram analysis between dHP and iHP may support this idea. While rats learned the preferred reward locations in block 3 during the place-preference task, we found that the strength of co-firing between dHP and iHP increased significantly only in iHP-preceding cell pairs. These results implied that value signals in iHP might be conveyed to dHP when high-value reward locations were reversed in block 3 in the place-preference task.

The results of place-preference tasks seem contradictory when compared to those of spatial alternation tasks. This is because place cells in the iHP only remapped when reward value was only decreased in the spatial alternation task, whereas those in the iHP remapped toward high-value locations in the place-preference task. When designing the tasks, we intended to test different types of value-changing conditions that one is decreasing the value of a place, and the other is changing the locations of preferred reward (Figure 4-10). Therefore, in my speculation, place cells in the iHP could not only remap in response to value-decrease episodes but also overrepresent the location associated with high-value reward.

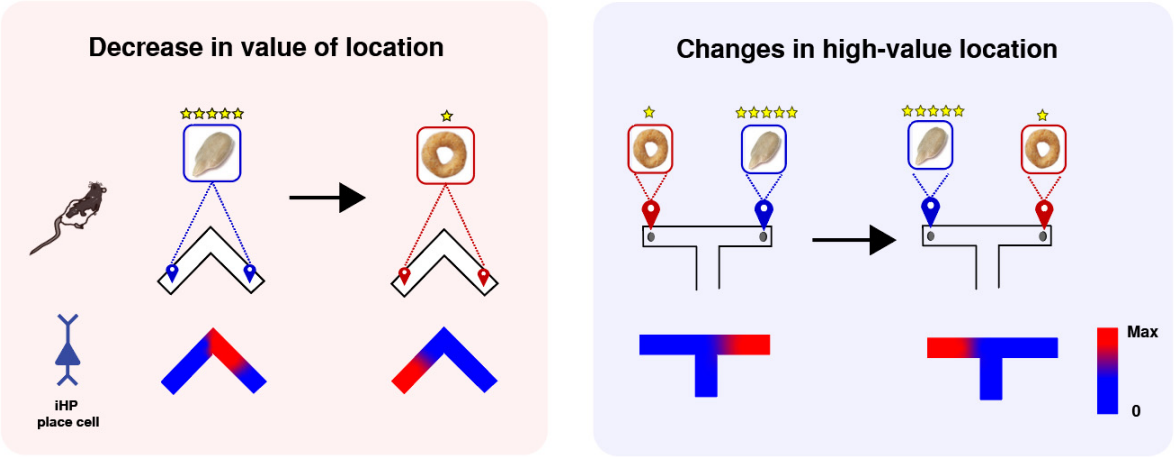

Figure 4-10. Graphical illustration showing the differential task demands between spatial alternation task and place preference task

There was little literature to report whether the place cells in iHP indeed encoded motivationally significant place or goal location. However, it is important to note that there was a study that was recording the single-cell activities from the mPFC while lesioning iHP and vHP. Burton et al. (2009) performed a spatial memory task in which rats were required to wait for few seconds within a goal zone in a circular arena. After rats achieve the mission, small rewards were automatically released from a food dispenser on the ceiling. In control groups, some cells in mPFC maximally fired when rats were waiting for the upcoming rewards within the goal zone. In contrast, the aforementioned neural activities disappeared after iHP and vHP were damaged by the electrolytic lesion. These results may support our findings in terms of the roles of iHP as representing the motivational significance of locations.

Anatomically, iHP simultaneously receives both accurate locational information from dHP and motivational value signals conveyed from the amygdala and VTA and sends monosynaptic axonal projections to the mPFC, especially the infralimbic cortex (Hoover and Vertes, 2007; Petrovich et al., 2001; Swanson et al., 1978). If we posit that two types of information were integrated into iHP, iHP will judge the location's value whether it is valuable enough to visit there next time. Such processes enable rats to change their behavior adaptively (e.g., change from left to right turn in our study) to maximize the value in hippocampal-dependent mnemonic tasks via the iHP-mPFC network.

In our working model, iHP is a critical junction for integrating spatial information with

value information (Figure 4-8). To be specific, motivationally significant signals in iHP stem from the amygdala or VTA (Gasbarri et al., 1994; Petrovich et al., 2001; Pikkarainen et al., 1999) in which is known to mediate reward palatability information (Chen et al., 2020; Fontanini et al., 2009). Also, amygdala neurons send direct projection to layer III of the intermediate band of LEC in which projects to the intermediate CA1 (not shown in Figure 4-8) (Dolorfo and Amaral, 1998; Pikkarainen et al., 1999). These projections may convey multimodal associative sensory signals intermixed with motivational value information. Given these anatomical connections, we posit that place cells in iHP may receive plentiful motivational value information via multiple routes. Along with emotional and motivational information fed by subcortical areas in iHP, Schaffer collaterals and associational fibers of the dorsal CA3 extensively send projection to the intermediate CA1 and CA3, respectively (Swanson et al., 1978). And cells in the CA3 region of iHP also widely project to dHP via Schaffer collaterals and associational fibers in return, possibly carrying some non-spatial information, including value signals to dHP.

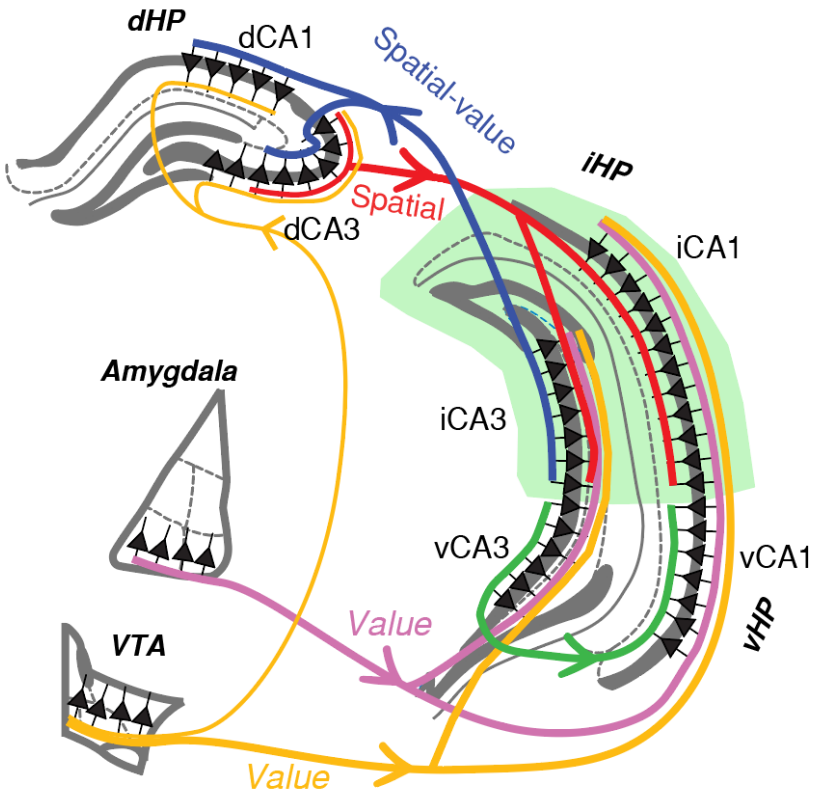

Figure 4-11. Current working model that iHP as integrating the spatial information and

motivational value information

A hypothetical model is proposed based on the intra-hippocampal and subcortical-to-hippocampal connectivities. In this model, iHP was considered as a hub for coding locational information combined with its value. Spatial information is transmitted to iHP via the recurrent collaterals or associational projections from dCA3 (red line). Value information is transmitted to iHP from the subcortical areas, such as the amygdala (purple line) and/or VTA (yellow line). The iCA3 is also innervated by dCA3 and dCA1 (blue line), which may contain mixed information of place with its value. Although vCA3 and vCA1 receive value-related inputs from subcortical areas, vHP does not interact with dHP or iHP. The vCA3 has limited connectivity with only vCA1 (green line).

GENERAL DISCUSSION

5.1 Conclusion

In our studies, single units were simultaneously recorded from the dorsoventral axis of the hippocampus to investigate how the motivationally significant episodes were represented in the hippocampus. We reported three main findings. First, cells in dHP fired more spatially selective fashions than those in iHP, and cells in vHP fired in an almost non-spatial manner. Second, when motivational values associated with places were changed, place fields in dHP maintained their original preferred firing locations. However, those in iHP globally remapped their place field immediately by shifting place fields or turning place fields on in response to the same events. Third, motivationally significant areas were overrepresented by the place cells in iHP but not in dHP. The ensemble level of network state in iHP was shifted rapidly than that in dHP while rats learned the place-preference task. Overall, our findings argued that iHP plays a central role in encoding the integration of spatial locations and its motivational values, whereas dHP has a more specialty in representing the organism's accurate positions in the environment.

5.2. Limitation

In current studies, there are some limitations to understand the sophisticated questions of how the hippocampus processes the value signals. The main reason for limitations may come from the experimental manipulation of controlling the value by using food as a reward. This is because value driven by a reward will decrease over time as rats consume the reward. In our case, the motivational significance of sunflower seeds provided in block 3 might be lower than that in block 1 because rats already ate considerable foods. To overcome this limitation, using intracranial self-stimulation (ICSS) on the medial forebrain bundle (MFB) may be a substitute to replace the reward (Carlezon and Chartoff, 2007). Based on the results of previous literature and pilot experiments in our lab, ICSS has some advantages over food. First, motivation for ICSS could be stably maintained for more than 1 hour. Thus, by using ICSS, it will be possible to keep constant motivation from the beginning to the end of the experiment. In the case of our experiment, if the same motivational level could be maintained in blocks 1 and 3, it may be possible to observe the global remapping when changing from blocks 2 to 3. Second, it is possible to quantitatively control the level of motivational significance by precisely controlling the strength of the current. Such sophisticated manipulation is almost impossible in

experiments with food. By adjusting the magnitude of the current in this way, we can find the threshold of value changes to induce the global remapping of place cells in iHP. Ultimately, it might be tested whether the hippocampus involves in emotional pattern separation and completion (Kirk et al., 2017). Also, if rats are more demotivated in route 2 than route 1 by lowering the current intensity, we may observe global remapping from iHP in both routes.

In our studies, because few cells were recorded from the vHP, there is a limitation in interpreting the cell activities of the vHP in response to changes in reward value. Indeed, the vHP has been notorious for being a difficult area to record single-unit activities. For this reason, there are few studies to successfully record the single-cell response from the vHP (Ciocchi et al., 2015; Kjelstrup et al., 2008; Komorowski et al., 2013). Meanwhile, based on drug studies, the current prevailing function of the vHP is to mediate innate anxiety (Bannerman et al., 2003; Kjelstrup et al., 2002). Rats whose vHP was lesioned do not hesitate to visit open spaces. It is important to note that recurrent collaterals in CA3 were preserved along the dorsoventral axis (Li et al., 1994). Therefore, fundamental information processing (i.e., pattern completion) of the CA3 may be shared between dHP and vHP. This idea is supported by a study suggesting that the dentate gyrus of vHP is involved in pattern separation of reward value (Kirk et al., 2017).

5.3 Implication and perspective

Based on our results, one may conclude that the intermediate hippocampus may be involved in integrating spatial location and its value. In the wild, animals are required to update the value of place every time because the value of place can change from moment to moment. For them, visiting a place where they can get a maximum value (i.e., obtain the food as much as possible while avoiding the danger from the predator) is essential for survival (Jung et al., 2018). Therefore, they always decide on a goal location based on the value of locations. During this process, value-place associated information in iHP may be conveyed to mPFC and utilized to make value-based decision making (Verharen et al., 2020) (Figure 5-1). It implies that the hippocampus may serve as one of the neural substrates for decision-making.

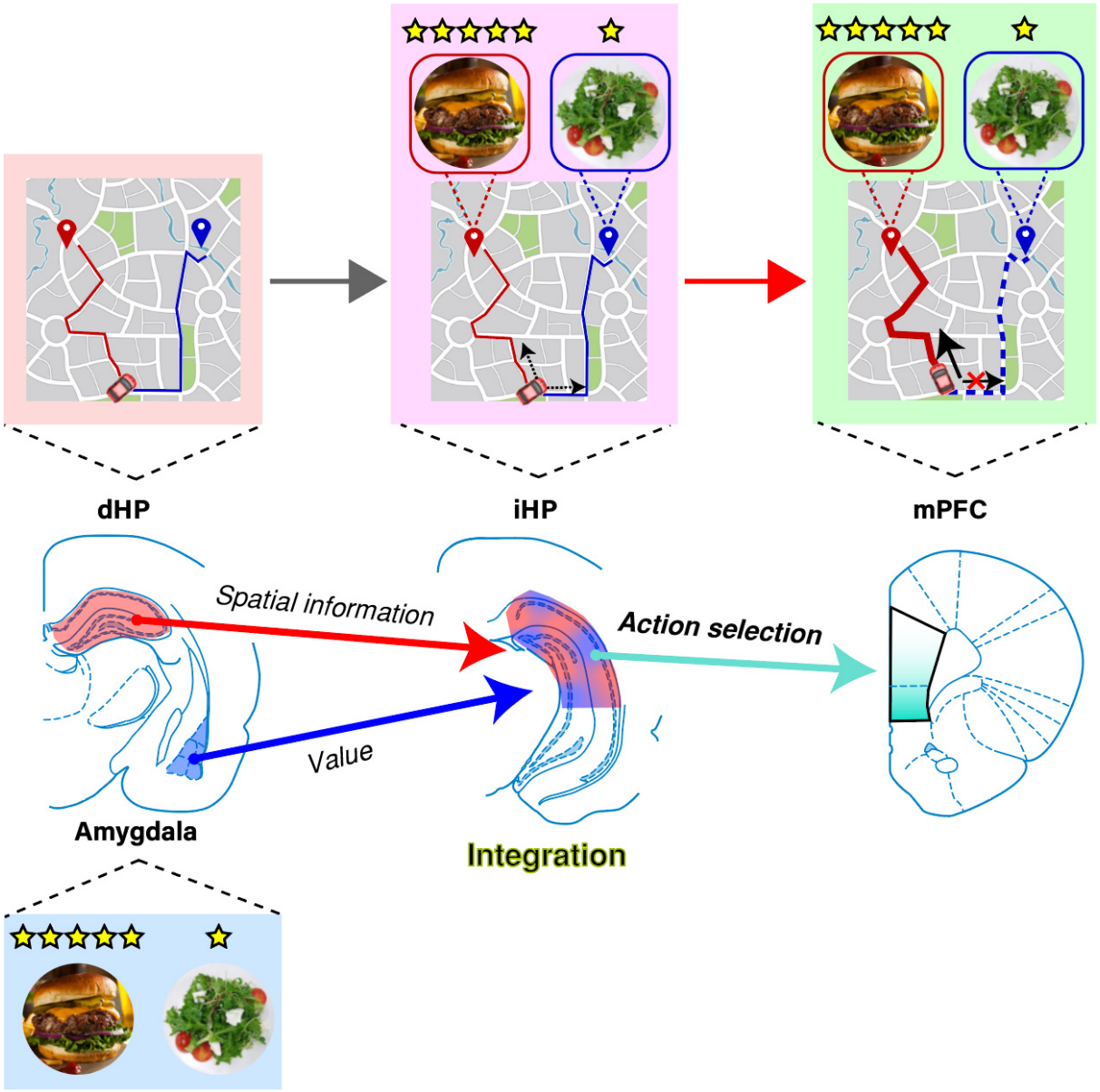

Figure 5-1. Graphical illustration of model in which hippocampus would involve in action selection process

Imagine that you are at the crossroads of choosing between two restaurants (chicken vs. vegetarian diet). In this situation, we assume the following information processing occurs inside the brain. First, the dorsal hippocampus represents the exact location of the restaurant, and the amygdala represents which food is more preferred. These two types of information were integrated within the intermediate hippocampus. Thus it can represent "where" there is a restaurant with "favorite" food. Then, this integrated information is going to be conveyed to the medial prefrontal cortex when you decide to visit the chicken restaurant, not the vegetarian restaurant.

In addition, our results imply that there are also differences in neuronal activities along the anteroposterior axis in the primate hippocampus. It has long been reported that cross-species anatomical connectivities were similar between the dorsoventral axis rodent and anteroposterior primate hippocampus. Specifically, hippocampus-to-cortical/subcortical connectivities (e.g., cingulate cortex, entorhinal cortex, nucleus accumbens, and amygdala) follow a similar topographical manner between rodent and primate (Aggleton, 1986, 2012; Aggleton et al., 2012; Friedman et al., 2002; Fudge et al., 2012; Mohedano-Moriano et al., 2008; Mohedano-Moriano et al., 2007; Petrovich et al., 2001; Saunders and Aggleton, 2007; Witter et al., 1989). In our study, cognitive rules and motivational value could differentially influence place cell activities in dHP and iHP. Thus, it may need to cautiously interpret the neuronal activities of the primate hippocampus if one has collected a single unit extensively across the anteroposterior axis (Mao et al., 2020; Sakon and Suzuki, 2020; Skaggs et al., 2007). If cells obtained from anterior and posterior parts were combined as "hippocampus" data, it may result in masking effects, which significant spatial signals recorded in the posterior parts would be overlooked due to strong non-spatial information from the anterior parts.

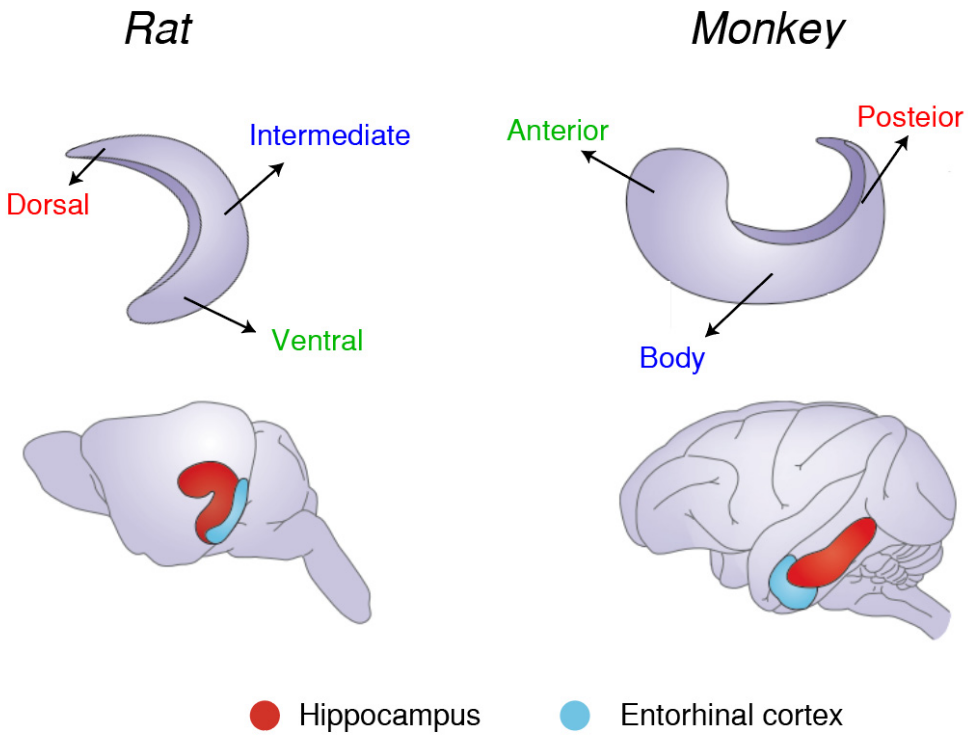

Figure 5-2. Comparing the cross-species of hippocampal formation anatomy

Schemetic illustration of the longitudinal structure of the hippocampal formation in rats and macaque

monkeys. The longitudinal axis is explained as dorsoventral in rodents and anteroposterior in primates. Note that the orientation of the hippocampal axis is vertical in rodents but lies horizontally in monkeys. The figure is adapted from Strange et al. (2014).

Although it has been well known that place field size becomes larger along the dorsoventral axis, it is largely unknown why the hippocampus had the differential scale of place cells. Are there any functional differences between them? In my speculation, evolutionally, it may be more effective to encode the precise locations by cells with small place fields and represent the value of locations by those with large place fields, respectively. When animals are chased by a predator, they should find a location of refuge at once, which requires great precision of place coding through focal place field. In contrast, a place's value in the environment exists in a wide range of zones. Thus, when encoding good places over a wide range, it is more effective to be represented by one large place cell than by multiple focal place cells.

Recently, Whittington et al. (2020) developed Tolman-Eichenbaum Machine in which suggests that place cells represented conjunctive codes of structural code from the medial entorhinal cortex (MEC) and sensory information from the lateral entorhinal cortex (LEC). They argued that factorizing the structural code and sensory information would help for the generalization of knowledge. Although authors focused on the place cells in dHP, it is possible to apply the same logic in iHP. It has been reported that cells in the intermediate band of MEC contained a larger scale of grid fields (Brun et al., 2008), and the intermediate band of LEC received direct inputs from the amygdala (Pikkarainen et al., 1999). Because the intermediate hippocampus was innervated by the intermediate band of MEC and LEC, it may receive larger structure code from MEC and sensory information mixed with the value from LEC, respectively. Therefore, our results could be interpreted that value-mixed inputs from LEC may induce place cells in iHP to be remap globally toward one of the large grid fields in response to changes in motivational significance.

Another important study insisted that cells in the anterior hippocampus could construct a three-dimensional abstract value map (Knudsen and Wallis, 2020). Specifically, when three cues were associated with a certain reward amount with dynamically changes in the amount of reward, the cells fired only when three cues were associated with certain value

relationships, and they became silent when the associated value was changed. In my opinion, although it is doubtful whether rodents have such abilities, if they could, it is possible that vHP has an abstract value map. This is because cells in the vHP fired in a non-spatial manner, which may enable cells to fire in abstract dimensions, not in spatial domains. Alternatively, the orbitofrontal cortex or ventral striatum in rodents is also a candidate for encoding abstract value maps because they have been known to represent the value of cues (Feierstein et al., 2006; Roesch et al., 2009).

5.4 Future research direction

Currently, up-to-date techniques, such as optogenetics and calcium imaging, have been developed to record and manipulate hippocampal neurons. And someone may seem to believe that advanced technologies are making new discoveries. However, if there are no appropriate behavioral paradigms, I am skeptical that high-tech methods could help to understand how the hippocampus involves in the memory process. That is, if rats randomly forage or go back and forth in linear track, no matter how up-to-date techniques were used, it may be impossible to understand how the hippocampus encodes and retrieves certain types of episodes. Therefore, I would like to focus on developing the appropriate behavioral paradigms to reveal the mechanisms of emotional memory. Recently, virtual reality environments are opening a new horizon that goes beyond the limits of animal experiments in the real environment. Thus, applying virtual reality in animal studies may be a candidate for developing the optimal behavior paradigm to investigate own research questions.

My motivation for brain research is to find the neuroscientific approach to help people suffered from psychological distress. One of the main reasons for such psychological suffers may stem from unforgettable memories. They ceaselessly induce the salient and negative emotions with associated episodes struck (e.g., witness dreadful car accident). How could neuroscientific research practically assist people who underwent such torments? Selectively eliminating these memories may be one option. If one can thoroughly understand the neural mechanisms of how certain episodes are associated with their negative emotions and where these memories are stored in the brain, there may be a hint to remove the painful memory. Ultimately, I wish that my future research will contribute to understand emotional memory.

BIBILOGRAPHY

Adolphs, R., Tranel, D., and Buchanan, T.W. (2005). Amygdala damage impairs emotional memory for gist but not details of complex stimuli. Nature neuroscience 8, 512-518.

Aggleton, J.P. (1986). A description of the amygdalo-hippocampal interconnections in the macaque monkey. Exp Brain Res 64, 515-526.

Aggleton, J.P. (2012). Multiple anatomical systems embedded within the primate medial temporal lobe: implications for hippocampal function. Neuroscience and biobehavioral reviews 36, 1579-1596.

Aggleton, J.P., Wright, N.F., Vann, S.D., and Saunders, R.C. (2012). Medial temporal lobe projections to the retrosplenial cortex of the macaque monkey. Hippocampus 22, 1883-1900.

Amaral, D.G., Dolorfo, C., and Alvarez-Royo, P. (1991). Organization of CA1 projections to the subiculum: a PHA-L analysis in the rat. Hippocampus 1, 415-435.

Amaral, D.G., and Witter, M.P. (1989). The three-dimensional organization of the hippocampal formation: a review of anatomical data. Neuroscience 31, 571-591.

Amarasingham, A., Harrison, M.T., Hatsopoulos, N.G., and Geman, S. (2012). Conditional modeling and the jitter method of spike resampling. Journal of neurophysiology 107, 517-531.

Aronov, D., Nevers, R., and Tank, D.W. (2017). Mapping of a non-spatial dimension by the hippocampal-entorhinal circuit. Nature 543, 719-722.

Bannerman, D., Grubb, M., Deacon, R., Yee, B., Feldon, J., and Rawlins, J. (2003). Ventral hippocampal lesions affect anxiety but not spatial learning. Behavioural brain research 139, 197-213.

Bannerman, D., Yee, B., Good, M., Heupel, M., Iversen, S., and Rawlins, J. (1999). Double dissociation of function within the hippocampus: a comparison of dorsal, ventral, and complete hippocampal cytotoxic lesions. Behavioral neuroscience 113, 1170.

Bannerman, D.M., Rawlins, J.N.P., McHugh, S.B., Deacon, R.M.J., Yee, B.K., Bast, T., Zhang, W.N., Pothuizen, H.H.J., and Feldon, J. (2004). Regional dissociations within the hippocampus—memory and anxiety. Neuroscience & Biobehavioral Reviews 28, 273-283.

Bast, T., Wilson, I.A., Witter, M.P., and Morris, R.G. (2009). From rapid place learning to behavioral performance: a key role for the intermediate hippocampus. PLoS biology 7, e1000089.

Bast, T., Zhang, W.-N., and Feldon, J. (2001). The ventral hippocampus and fear conditioning in rats. Exp Brain Res 139, 39-52.

Bermudez, M.A., and Schultz, W. (2010). Reward magnitude coding in primate amygdala

neurons. Journal of neurophysiology 104, 3424-3432.
Breese, C., Hampson, R.E., and Deadwyler, S.A. (1989). Hippocampal place cells: stereotypy and plasticity. The Journal of Neuroscience 9, 1097-1111.
Brun, V.H., Solstad, T., Kjelstrup, K.B., Fyhn, M., Witter, M.P., Moser, E.I., and Moser, M.B. (2008). Progressive increase in grid scale from dorsal to ventral medial entorhinal cortex. Hippocampus 18, 1200-1212.
Burton, B.G., Hok, V., Save, E., and Poucet, B. (2009). Lesion of the ventral and intermediate hippocampus abolishes anticipatory activity in the medial prefrontal cortex of the rat. Behavioural brain research 199, 222-234.
Buzsaki, G. (2004). Large-scale recording of neuronal ensembles. Nature neuroscience 7, 446-451.
Cacucci, F., Lever, C., Wills, T.J., Burgess, N., and O'Keefe, J. (2004). Theta-modulated place-by-direction cells in the hippocampal formation in the rat. The Journal of neuroscience : the official journal of the Society for Neuroscience 24, 8265-8277.
Cajal, R.y. (1909). Histologie du système nerveux de l'homme & des vertébrés, Vol v. 1, Ed. française rev. & mise à jour par l'auteur, tr. de l'espagnol par L. Azoulay. edn (Paris :: Maloine).
Canteras, N.S., and Swanson, L.W. (1992). Projections of the ventral subiculum to the amygdala, septum, and hypothalamus: a PHAL anterograde tract-tracing study in the rat. The Journal of comparative neurology 324, 180-194.
Carlezon, W.A., Jr., and Chartoff, E.H. (2007). Intracranial self-stimulation (ICSS) in rodents to study the neurobiology of motivation. Nature protocols 2, 2987-2995.
Cenquizca, L.A., and Swanson, L.W. (2007). Spatial organization of direct hippocampal field CA1 axonal projections to the rest of the cerebral cortex. Brain Res Rev 56, 1-26.
Chen, L., Lu, Y.-P., Chen, H.-Y., Huang, S.-N., Guo, Y.-R., Zhang, J.-Y., Li, Q.-X., Luo, C.-Y., Lin, S.-W., Chen, Z.-N.*, et al.* (2020). Ventral tegmental area GABAergic neurons induce anxiety-like behaviors and promote palatable food intake. Neuropharmacology 173, 108114.
Chiba, T. (2000). Collateral projection from the amygdalo–hippocampal transition area and CA1 to the hypothalamus and medial prefrontal cortex in the rat. Neuroscience research 38, 373-383.
Ciocchi, S., Passecker, J., Malagon-Vina, H., Mikus, N., and Klausberger, T. (2015). Brain computation. Selective information routing by ventral hippocampal CA1 projection neurons. Science 348, 560-563.

Colgin, L.L., Moser, E.I., and Moser, M.B. (2008). Understanding memory through hippocampal remapping. Trends in neurosciences 31, 469-477.

D'Hooge, R., and De Deyn, P.P. (2001). Applications of the Morris water maze in the study of learning and memory. Brain Research Reviews 36, 60-90.

de Hoz, L., Knox, J., and Morris, R.G. (2003). Longitudinal axis of the hippocampus: both septal and temporal poles of the hippocampus support water maze spatial learning depending on the training protocol. Hippocampus 13, 587-603.

De Saint Blanquat, P., Hok, V., Save, E., Poucet, B., and Chaillan, F.A. (2013). Differential role of the dorsal hippocampus, ventro-intermediate hippocampus, and medial prefrontal cortex in updating the value of a spatial goal. Hippocampus 23, 342-351.

Dolorfo, C.L., and Amaral, D.G. (1998). Entorhinal cortex of the rat: topographic organization of the cells of origin of the perforant path projection to the dentate gyrus. The Journal of comparative neurology 398, 25-48.

Dong, H.W., Petrovich, G.D., and Swanson, L.W. (2001). Topography of projections from amygdala to bed nuclei of the stria terminalis. Brain research Brain research reviews 38, 192-246.

Dougherty, K.A. (2020). Differential developmental refinement of the intrinsic electrophysiological properties of CA1 pyramidal neurons from the rat dorsal and ventral hippocampus. 30, 233-249.

Dougherty, K.A., Islam, T., and Johnston, D. (2012). Intrinsic excitability of CA1 pyramidal neurones from the rat dorsal and ventral hippocampus. The Journal of physiology 590, 5707-5722.

Dupret, D., O'Neill, J., Pleydell-Bouverie, B., and Csicsvari, J. (2010). The reorganization and reactivation of hippocampal maps predict spatial memory performance. Nature neuroscience 13, 995-1002.

Duvelle, E., Grieves, R.M., Hok, V., Poucet, B., Arleo, A., Jeffery, K., and Save, E. (2019). Insensitivity of place cells to the value of spatial goals in a two-choice flexible navigation task. The Journal of neuroscience : the official journal of the Society for Neuroscience.

Eichenbaum, H., Kuperstein, M., Fagan, A., and Nagode, J. (1987). Cue-sampling and goal-approach correlates of hippocampal unit activity in rats performing an odor-discrimination task. The Journal of Neuroscience 7, 716-732.

Eschenko, O., and Mizumori, S.J. (2007). Memory influences on hippocampal and striatal

neural codes: effects of a shift between task rules. Neurobiology of learning and memory 87, 495-509.

Feierstein, C.E., Quirk, M.C., Uchida, N., Sosulski, D.L., and Mainen, Z.F. (2006). Representation of Spatial Goals in Rat Orbitofrontal Cortex. Neuron 51, 495-507.

Ferbinteanu, J., and Shapiro, M.L. (2003). Prospective and retrospective memory coding in the hippocampus. Neuron 40, 1227-1239.

Fontanini, A., Grossman, S.E., Figueroa, J.A., and Katz, D.B. (2009). Distinct Subtypes of Basolateral Amygdala Taste Neurons Reflect Palatability and Reward. The Journal of Neuroscience 29, 2486-2495.

Friedman, D.P., Aggleton, J.P., and Saunders, R.C. (2002). Comparison of hippocampal, amygdala, and perirhinal projections to the nucleus accumbens: combined anterograde and retrograde tracing study in the Macaque brain. The Journal of comparative neurology 450, 345-365.

Fudge, J.L., deCampo, D.M., and Becoats, K.T. (2012). Revisiting the hippocampal-amygdala pathway in primates: association with immature-appearing neurons. Neuroscience 212, 104-119.

Fuhs, M.C., Vanrhoads, S.R., Casale, A.E., McNaughton, B., and Touretzky, D.S. (2005). Influence of path integration versus environmental orientation on place cell remapping between visually identical environments. Journal of neurophysiology 94, 2603-2616.

Fujisawa, S., Amarasingham, A., Harrison, M.T., and Buzsaki, G. (2008). Behavior-dependent short-term assembly dynamics in the medial prefrontal cortex. Nature neuroscience 11, 823-833.

Gasbarri, A., Packard, M.G., Campana, E., and Pacitti, C. (1994). Anterograde and retrograde tracing of projections from the ventral tegmental area to the hippocampal formation in the rat. Brain research bulletin 33, 445-452.

Gauthier, J.L., and Tank, D.W. (2018). A Dedicated Population for Reward Coding in the Hippocampus. Neuron 99, 179-193.e177.

Gilbert, P.E., Kesner, R.P., and DeCoteau, W.E. (1998). Memory for spatial location: role of the hippocampus in mediating spatial pattern separation. The Journal of neuroscience : the official journal of the Society for Neuroscience 18, 804-810.

Grasse, P. (1955). rait6 de zoologie: anatomie, systhatique, biolo- gie. Paris: Masson et Cie XVII premier fascicule.

Gray, C.M., Maldonado, P.E., Wilson, M., and McNaughton, B. (1995). Tetrodes markedly improve the reliability and yield of multiple single-unit isolation from multi-unit recordings in cat striate cortex. J Neurosci Meth 63, 43-54.

Grieves, R.M., Jenkins, B.W., Harland, B.C., Wood, E.R., and Dudchenko, P.A. (2016). Place field repetition and spatial learning in a multicompartment environment. Hippocampus 26, 118-134.

Groenewegen, H.J., der Zee, E.V.-V., te Kortschot, A., and Witter, M.P. (1987). Organization of the projections from the subiculum to the ventral striatum in the rat. A study using anterograde transport of Phaseolus vulgaris leucoagglutinin. Neuroscience 23, 103-120.

Groenewegen, H.J., Wright, C.I., and Beijer, A.V. (1996). The nucleus accumbens: gateway for limbic structures to reach the motor system? Progress in brain research 107, 485-511.

Hafting, T., Fyhn, M., Molden, S., Moser, M.B., and Moser, E.I. (2005). Microstructure of a spatial map in the entorhinal cortex. Nature 436, 801-806.

Hales, J.B., Schlesiger, M.I., Leutgeb, J.K., Squire, L.R., Leutgeb, S., and Clark, R.E. (2014). Medial entorhinal cortex lesions only partially disrupt hippocampal place cells and hippocampus-dependent place memory. Cell reports 9, 893-901.

Hampson, R.E., Simeral, J.D., and Deadwyler, S.A. (1999). Distribution of spatial and nonspatial information in dorsal hippocampus. Nature 402, 610-614.

Hodgkin, A.L., and Huxley, A.F. (1939). Action Potentials Recorded from Inside a Nerve Fibre. Nature 144, 710-711.

Hok, V., Lenck-Santini, P.-P., Roux, S., Save, E., Muller, R.U., and Poucet, B. (2007). Goal-Related Activity in Hippocampal Place Cells. The Journal of Neuroscience 27, 472-482.

Hollup, S.A., Molden, S., Donnett, J.G., Moser, M.-B., and Moser, E.I. (2001). Accumulation of Hippocampal Place Fields at the Goal Location in an Annular Watermaze Task. The Journal of Neuroscience 21, 1635.

Hoover, W.B., and Vertes, R.P. (2007). Anatomical analysis of afferent projections to the medial prefrontal cortex in the rat. Brain Structure and Function 212, 149-179.

Hubel, D.H., and Wiesel, T.N. (1959). Receptive fields of single neurones in the cat's striate cortex. The Journal of physiology 148, 574-591.

Insausti, R. (1993). Comparative anatomy of the entorhinal cortex and hippocampus in mammals. Hippocampus 3, 19-26.

Ishizuka, N. (2001). Laminar organization of the pyramidal cell layer of the subiculum in the

rat. The Journal of comparative neurology 435, 89-110.

Jadhav, S.P., Kemere, C., German, P.W., and Frank, L.M. (2012). Awake hippocampal sharp-wave ripples support spatial memory. Science 336, 1454-1458.

Jeffery, K.J., and Anderson, M.I. (2003). Dissociation of the geometric and contextual influences on place cells. Hippocampus 13, 868-872.

Jeong, Y., Huh, N., Lee, J., Yun, I., Lee, J.W., Lee, I., and Jung, M.W. (2018). Role of the hippocampal CA1 region in incremental value learning. Scientific reports 8, 9870.

Jung, M.W., Lee, H., Jeong, Y., Lee, J.W., and Lee, I. (2018). Remembering rewarding futures: A simulation-selection model of the hippocampus. Hippocampus.

Jung, M.W., Wiener, S.I., and McNaughton, B.L. (1994). Comparison of spatial firing characteristics of units in dorsal and ventral hippocampus of the rat. The Journal of neuroscience : the official journal of the Society for Neuroscience 14, 7347-7356.

Keinath, A.T., Wang, M.E., Wann, E.G., Yuan, R.K., Dudman, J.T., and Muzzio, I.A. (2014). Precise spatial coding is preserved along the longitudinal hippocampal axis. Hippocampus 24, 1533-1548.

Kennedy, P.J., and Shapiro, M.L. (2009). Motivational states activate distinct hippocampal representations to guide goal-directed behaviors. Proceedings of the National Academy of Sciences of the United States of America 106, 10805-10810.

Kirk, R.A., Redmon, S.N., and Kesner, R.P. (2017). The ventral dentate gyrus mediates pattern separation for reward value. Behav Neurosci 131, 42-45.

Kishi, T., Tsumori, T., Ono, K., Yokota, S., Ishino, H., and Yasui, Y. (2000). Topographical organization of projections from the subiculum to the hypothalamus in the rat. The Journal of comparative neurology 419, 205-222.

Kishi, T., Tsumori, T., Yokota, S., and Yasui, Y. (2006). Topographical projection from the hippocampal formation to the amygdala: a combined anterograde and retrograde tracing study in the rat. The Journal of comparative neurology 496, 349-368.

Kjelstrup, K.B., Solstad, T., Brun, V.H., Hafting, T., Leutgeb, S., Witter, M.P., Moser, E.I., and Moser, M.B. (2008). Finite scale of spatial representation in the hippocampus. Science 321, 140-143.

Kjelstrup, K.G., Tuvnes, F.A., Steffenach, H.A., Murison, R., Moser, E.I., and Moser, M.B. (2002). Reduced fear expression after lesions of the ventral hippocampus. Proceedings of the National Academy of Sciences of the United States of America 99, 10825-10830.

Knudsen, E., and Wallis, J. (2020). Hippocampal neurons construct a map of an abstract value space. bioRxiv, 2020.2012.2017.423272.

Kobayashi, Y., and Amaral, D.G. (2007). Macaque monkey retrosplenial cortex: III. Cortical efferents. The Journal of comparative neurology 502, 810-833.

Komorowski, R.W., Garcia, C.G., Wilson, A., Hattori, S., Howard, M.W., and Eichenbaum, H. (2013). Ventral hippocampal neurons are shaped by experience to represent behaviorally relevant contexts. The Journal of neuroscience : the official journal of the Society for Neuroscience 33, 8079-8087.

LaBar, K.S., and Cabeza, R. (2006). Cognitive neuroscience of emotional memory. Nature Reviews Neuroscience 7, 54-64.

LaBar, K.S., and Phelps, E.A. (1998). Arousal-Mediated Memory Consolidation: Role of the Medial Temporal Lobe in Humans. Psychological science 9, 490-493.

Lee, C.-H., and Lee, I. (2020). Impairment of Pattern Separation of Ambiguous Scenes by Single Units in the CA3 in the Absence of the Dentate Gyrus. 40, 3576-3590.

Lee, H.-W., Lee, S.-M., and Lee, I. (2018). Neural Firing Patterns Are More Schematic and Less Sensitive to Changes in Background Visual Scenes in the Subiculum than in the Hippocampus. The Journal of Neuroscience 38, 7392-7408.

Lee, H., Ghim, J.W., Kim, H., Lee, D., and Jung, M. (2012). Hippocampal neural correlates for values of experienced events. The Journal of neuroscience : the official journal of the Society for Neuroscience 32, 15053-15065.

Lee, I., Griffin, A.L., Zilli, E.A., Eichenbaum, H., and Hasselmo, M.E. (2006). Gradual translocation of spatial correlates of neuronal firing in the hippocampus toward prospective reward locations. Neuron 51, 639-650.

Lee, I., Yoganarasimha, D., Rao, G., and Knierim, J.J. (2004). Comparison of population coherence of place cells in hippocampal subfields CA1 and CA3. Nature 430, 456-459.

Lenck-Santini, P.P., Save, E., and Poucet, B. (2001). Evidence for a relationship between place-cell spatial firing and spatial memory performance. Hippocampus 11, 377-390.

Leutgeb, S., Leutgeb, J.K., Barnes, C.A., Moser, E.I., McNaughton, B.L., and Moser, M.B. (2005). Independent codes for spatial and episodic memory in hippocampal neuronal ensembles. Science 309, 619-623.

Leutgeb, S., Leutgeb, J.K., Treves, A., Moser, M.B., and Moser, E.I. (2004). Distinct ensemble codes in hippocampal areas CA3 and CA1. Science 305, 1295-1298.

Lever, C., Burton, S., Jeewajee, A., O'Keefe, J., and Burgess, N. (2009). Boundary vector cells in the subiculum of the hippocampal formation. The Journal of neuroscience : the official journal of the Society for Neuroscience 29, 9771-9777.

Li, X.G., Somogyi, P., Ylinen, A., and Buzsaki, G. (1994). The hippocampal CA3 network: an in vivo intracellular labeling study. The Journal of comparative neurology 339, 181-208.

Liu, D., Gu, X., Zhu, J., Zhang, X., Han, Z., Yan, W., Cheng, Q., Hao, J., Fan, H., Hou, R., *et al.* (2014). Medial prefrontal activity during delay period contributes to learning of a working memory task. Science 346, 458-463.

Louis, S., Borgelt, C., and Grün, S. (2010). Generation and Selection of Surrogate Methods for Correlation Analysis.

Mamad, O., Stumpp, L., McNamara, H.M., Ramakrishnan, C., Deisseroth, K., Reilly, R.B., and Tsanov, M. (2017). Place field assembly distribution encodes preferred locations. PLoS biology 15, e2002365.

Manns, J.R., Hopkins, R.O., and Squire, L.R. (2003). Semantic Memory and the Human Hippocampus. Neuron 38, 127-133.

Mao, D., Avila, E., Caziot, B., Laurens, J., Dickman, J.D., and Angelaki, D.E. (2020). Spatial representations in macaque hippocampal formation. bioRxiv, 2020.2010.2003.324848.

Maren, S. (1999). Neurotoxic or electrolytic lesions of the ventral subiculum produce deficits in the acquisition and expression of Pavlovian fear conditioning in rats. Behavioral Neuroscience 113, 283-290.

Maren, S., and Holt, W.G. (2004). Hippocampus and Pavlovian fear conditioning in rats: muscimol infusions into the ventral, but not dorsal, hippocampus impair the acquisition of conditional freezing to an auditory conditional stimulus. Behav Neurosci 118, 97-110.

Markus, E., Qin, Y., Leonard, B., Skaggs, W., McNaughton, B., and Barnes, C. (1995). Interactions between location and task affect the spatial and directional firing of hippocampal neurons. The Journal of Neuroscience 15, 7079-7094.

Masuda, A., Sano, C., Zhang, Q., Goto, H., McHugh, T.J., Fujisawa, S., and Itohara, S. (2020). The hippocampus encodes delay and value information during delay-discounting decision making. eLife 9.

McNaughton, B.L., Barnes, C.A., and O'Keefe, J. (1983a). The contributions of position, direction, and velocity to single unit activity in the hippocampus of freely-moving rats. Exp Brain Res 52, 41-49.

McNaughton, B.L., O'Keefe, J., and Barnes, C.A. (1983b). The stereotrode: a new technique for simultaneous isolation of several single units in the central nervous system from multiple unit records. J Neurosci Methods 8, 391-397.

Mehta, M.R., Quirk, M.C., and Wilson, M.A. (2000). Experience-dependent asymmetric shape of hippocampal receptive fields. Neuron 25, 707-715.

Miao, C., Cao, Q., Ito, H.T., Yamahachi, H., Witter, M.P., Moser, M.B., and Moser, E.I. (2015). Hippocampal Remapping after Partial Inactivation of the Medial Entorhinal Cortex. Neuron 88, 590-603.

Mohedano-Moriano, A., Martinez-Marcos, A., Pro-Sistiaga, P., Blaizot, X., Arroyo-Jimenez, M.M., Marcos, P., Artacho-Pérula, E., and Insausti, R. (2008). Convergence of unimodal and polymodal sensory input to the entorhinal cortex in the fascicularis monkey. Neuroscience 151, 255-271.

Mohedano-Moriano, A., Pro-Sistiaga, P., Arroyo-Jimenez, M.M., Artacho-Perula, E., Insausti, A.M., Marcos, P., Cebada-Sanchez, S., Martinez-Ruiz, J., Munoz, M., Blaizot, X.*, et al.* (2007). Topographical and laminar distribution of cortical input to the monkey entorhinal cortex. J Anat 211, 250-260.

Morris, R.G., Garrud, P., Rawlins, J.N., and O'Keefe, J. (1982). Place navigation impaired in rats with hippocampal lesions. Nature 297, 681-683.

Moser, E., Moser, M.-B., and Andersen, P. (1993). Spatial learning impairment parallels the magnitude of dorsal hippocampal lesions, but is hardly present following ventral lesions. The Journal of neuroscience 13, 3916-3925.

Moser, M.-B., Moser, E.I., Forrest, E., Andersen, P., and Morris, R. (1995). Spatial learning with a minislab in the dorsal hippocampus. Proceedings of the National Academy of Sciences 92, 9697-9701.

Moser, M.B., and Moser, E.I. (1998). Functional differentiation in the hippocampus. Hippocampus 8, 608-619.

Muller, R.U., Bostock, E., Taube, J.S., and Kubie, J.L. (1994). On the directional firing properties of hippocampal place cells. The Journal of neuroscience : the official journal of the Society for Neuroscience 14, 7235-7251.

Muller, R.U., and Kubie, J.L. (1987). The effects of changes in the environment on the spatial firing of hippocampal complex-spike cells. The Journal of neuroscience : the official journal of the Society for Neuroscience 7, 1951-1968.

Naber, P.A., and Witter, M.P. (1998). Subicular efferents are organized mostly as parallel projections: a double-labeling, retrograde-tracing study in the rat. The Journal of comparative neurology 393, 284-297.

Namburi, P., Beyeler, A., Yorozu, S., Calhoon, G.G., Halbert, S.A., Wichmann, R., Holden, S.S., Mertens, K.L., Anahtar, M., Felix-Ortiz, A.C., *et al.* (2015). A circuit mechanism for differentiating positive and negative associations. Nature 520, 675-678.

Narayanan, N.S., and Laubach, M. (2009). Methods for studying functional interactions among neuronal populations. Methods Mol Biol 489, 135-165.

Navawongse, R., and Eichenbaum, H. (2013). Distinct pathways for rule-based retrieval and spatial mapping of memory representations in hippocampal neurons. The Journal of neuroscience : the official journal of the Society for Neuroscience 33, 1002-1013.

O'Keefe, J., and Dostrovsky, J. (1971). The hippocampus as a spatial map. Preliminary evidence from unit activity in the freely-moving rat. Brain research 34, 171-175.

O'Keefe, J., and Recce, M.L. (1993). Phase relationship between hippocampal place units and the EEG theta rhythm. Hippocampus 3, 317-330.

Okeefe, J., and Nadel, L. (1978). The Hippocampus as a Cognitive Map.

Olton, D.S. (1987). The radial arm maze as a tool in behavioral pharmacology. Physiology & Behavior 40, 793-797.

Olton, D.S., and Werz, M.A. (1978). Hippocampal function and behavior: spatial discrimination and response inhibition. Physiol Behav 20, 597-605.

Ormond, J., and McNaughton, B.L. (2015). Place field expansion after focal MEC inactivations is consistent with loss of Fourier components and path integrator gain reduction. Proceedings of the National Academy of Sciences of the United States of America 112, 4116-4121.

Otto, T., and Eichenbaum, H. (1992). Neuronal activity in the hippocampus during delayed non-match to sample performance in rats: evidence for hippocampal processing in recognition memory. Hippocampus 2, 323-334.

Packard, M.G., and McGaugh, J.L. (1996). Inactivation of hippocampus or caudate nucleus with lidocaine differentially affects expression of place and response learning. Neurobiology of learning and memory 65, 65-72.

Park, A.J., Harris, A.Z., Martyniuk, K.M., Chang, C.-Y., Abbas, A.I., Lowes, D.C., Kellendonk, C., Gogos, J.A., and Gordon, J.A. (2021). Reset of hippocampal–prefrontal circuitry facilitates learning. Nature.

Parvizi, J., Van Hoesen, G.W., Buckwalter, J., and Damasio, A. (2006). Neural connections of the posteromedial cortex in the macaque. Proceedings of the National Academy of Sciences 103, 1563-1568.

Patel, J., Fujisawa, S., Berenyi, A., Royer, S., and Buzsaki, G. (2012). Traveling theta waves along the entire septotemporal axis of the hippocampus. Neuron 75, 410-417.

Petrovich, G.D., Canteras, N.S., and Swanson, L.W. (2001). Combinatorial amygdalar inputs to hippocampal domains and hypothalamic behavior systems. Brain research Brain research reviews 38, 247-289.

Phillips, R., and LeDoux, J. (1992). Differential contribution of amygdala and hippocampus to cued and contextual fear conditioning. Behavioral neuroscience 106, 274.

Pikkarainen, M., Ronkko, S., Savander, V., Insausti, R., and Pitkanen, A. (1999). Projections from the lateral, basal, and accessory basal nuclei of the amygdala to the hippocampal formation in rat. The Journal of comparative neurology 403, 229-260.

Poucet, B., and Buhot, M.C. (1994). Effects of medial septal or unilateral hippocampal inactivations on reference and working spatial memory in rats. Hippocampus 4, 315-321.

Quirk, G.J., Muller, R.U., and Kubie, J.L. (1990). The firing of hippocampal place cells in the dark depends on the rat's recent experience. The Journal of neuroscience : the official journal of the Society for Neuroscience 10, 2008-2017.

Ranck, J.J. (1973). Studies on single neurons in dorsal hippocampal formation and septum in unrestrained rats. Part I. Behavioral correlates and firing repertoires, Vol 41.

Richmond, M., Yee, B., Pouzet, B., Veenman, L., Rawlins, J., Feldon, J., and Bannerman, D. (1999). Dissociating context and space within the hippocampus: effects of complete, dorsal, and ventral excitotoxic hippocampal lesions on conditioned freezing and spatial learning. Behavioral neuroscience 113, 1189.

Risold, P.Y., and Swanson, L.W. (1996). Structural evidence for functional domains in the rat hippocampus. Science 272, 1484-1486.

Risold, P.Y., and Swanson, L.W. (1997). Connections of the rat lateral septal complex. Brain research Brain research reviews 24, 115-195.

Risold, P.Y., Thompson, R.H., and Swanson, L.W. (1997). The structural organization of connections between hypothalamus and cerebral cortex. Brain research Brain research reviews 24, 197-254.

Roberts, A.C., Tomic, D.L., Parkinson, C.H., Roeling, T.A., Cutter, D.J., Robbins, T.W., and

Everitt, B.J. (2007). Forebrain connectivity of the prefrontal cortex in the marmoset monkey (Callithrix jacchus): an anterograde and retrograde tract-tracing study. The Journal of comparative neurology 502, 86-112.

Robinson, N.T.M., Priestley, J.B., Rueckemann, J.W., Garcia, A.D., Smeglin, V.A., Marino, F.A., and Eichenbaum, H. (2017). Medial Entorhinal Cortex Selectively Supports Temporal Coding by Hippocampal Neurons. Neuron 94, 677-688.e676.

Roesch, M.R., Singh, T., Brown, P.L., Mullins, S.E., and Schoenbaum, G. (2009). Ventral Striatal Neurons Encode the Value of the Chosen Action in Rats Deciding between Differently Delayed or Sized Rewards. The Journal of Neuroscience 29, 13365-13376.

Royer, S., Sirota, A., Patel, J., and Buzsaki, G. (2010). Distinct representations and theta dynamics in dorsal and ventral hippocampus. The Journal of neuroscience : the official journal of the Society for Neuroscience 30, 1777-1787.

Sakon, J.J., and Suzuki, W.A. (2020). Neural evidence for recognition of naturalistic videos in monkey hippocampus. bioRxiv, 2020.2001.2003.894394.

Saunders, R.C., and Aggleton, J.P. (2007). Origin and topography of fibers contributing to the fornix in macaque monkeys. Hippocampus 17, 396-411.

Schlesiger, M.I., Boublil, B.L., Hales, J.B., Leutgeb, J.K., and Leutgeb, S. (2018). Hippocampal Global Remapping Can Occur without Input from the Medial Entorhinal Cortex. Cell reports 22, 3152-3159.

Schumacher, A., Vlassov, E., and Ito, R. (2016). The ventral hippocampus, but not the dorsal hippocampus is critical for learned approach-avoidance decision making. Hippocampus 26, 530-542.

Scoville, W.B., and Milner, B. (1957). Loss of recent memory after bilateral hippocampal lesions. Journal of neurology, neurosurgery, and psychiatry 20, 11-21.

Skaggs, W.E., and McNaughton, B.L. (1998). Spatial firing properties of hippocampal CA1 populations in an environment containing two visually identical regions. The Journal of neuroscience : the official journal of the Society for Neuroscience 18, 8455-8466.

Skaggs, W.E., McNaughton, B.L., Permenter, M., Archibeque, M., Vogt, J., Amaral, D.G., and Barnes, C.A. (2007). EEG sharp waves and sparse ensemble unit activity in the macaque hippocampus. Journal of neurophysiology 98, 898-910.

Skaggs, W.E., McNaughton, B.L., Wilson, M.A., and Barnes, C.A. (1996). Theta phase precession in hippocampal neuronal populations and the compression of temporal sequences.

Hippocampus 6, 149-172.
Markus, EJ; (1993). An Information-Theoretic Approach to Deciphering the Hippocampal Code. Advances in neural information processing systems.
Smith, A.C., Frank, L.M., Wirth, S., Yanike, M., Hu, D., Kubota, Y., Graybiel, A.M., Suzuki, W.A., and Brown, E.N. (2004). Dynamic Analysis of Learning in Behavioral Experiments. The Journal of Neuroscience 24, 447-461.
Sosa, M., Joo, H.R., and Frank, L.M. (2019). Dorsal and Ventral Hippocampal Sharp-Wave Ripples Activate Distinct Nucleus Accumbens Networks. Neuron.
Speakman, A., and O'Keefe, J. (1990). Hippocampal Complex Spike Cells do not Change Their Place Fields if the Goal is Moved Within a Cue Controlled Environment. The European journal of neuroscience 2, 544-555.
Spiers, H.J., Olafsdottir, H.F., and Lever, C. (2018). Hippocampal CA1 activity correlated with the distance to the goal and navigation performance. Hippocampus 28, 644-658.
Squire, L.R. (2009). The legacy of patient H.M. for neuroscience. Neuron 61, 6-9.
Squire, L.R., van der Horst, A.S., McDuff, S.G.R., Frascino, J.C., Hopkins, R.O., and Mauldin, K.N. (2010). Role of the hippocampus in remembering the past and imagining the future. Proceedings of the National Academy of Sciences 107, 19044-19048.
Steffenach, H.A., Witter, M., Moser, M.B., and Moser, E.I. (2005). Spatial memory in the rat requires the dorsolateral band of the entorhinal cortex. Neuron 45, 301-313.
Stephan, H., and Andy, O. (1970). The allocortex in primates. In: The pri- mate brain: advances in primatology, . New York: Appleton-Century-Crofts 1 (Noback CR, Montagna W, eds), 109-135.
Steward, O. (1976). Topographic organization of the projections from the entorhinal area to the hippocampal formation of the rat. The Journal of comparative neurology 167, 285-314.
Strange, B.A., Witter, M.P., Lein, E.S., and Moser, E.I. (2014). Functional organization of the hippocampal longitudinal axis. Nature reviews Neuroscience 15, 655-669.
Swanson, L.W., and Cowan, W.M. (1975). Hippocampo-hypothalamic connections: origin in subicular cortex, not ammon's horn. Science 189, 303-304.
Swanson, L.W., and Cowan, W.M. (1977). An autoradiographic study of the organization of the efferent connections of the hippocampal formation in the rat. The Journal of comparative neurology 172, 49-84.
Swanson, L.W., Wyss, J.M., and Cowan, W.M. (1978). An autoradiographic study of the

organization of intrahippocampal association pathways in the rat. The Journal of comparative neurology 181, 681-715.

Tabuchi, E., Mulder, A.B., and Wiener, S.I. (2003). Reward value invariant place responses and reward site associated activity in hippocampal neurons of behaving rats. Hippocampus 13, 117-132.

Tanila, H. (1999). Hippocampal place cells can develop distinct representations of two visually identical environments. Hippocampus 9, 235-246.

Taube, J.S., Muller, R.U., and Ranck, J.B., Jr. (1990). Head-direction cells recorded from the postsubiculum in freely moving rats. I. Description and quantitative analysis. The Journal of neuroscience : the official journal of the Society for Neuroscience 10, 420-435.

Thierry, A.M., Gioanni, Y., Dégénétais, E., and Glowinski, J. (2000). Hippocampo-prefrontal cortex pathway: anatomical and electrophysiological characteristics. Hippocampus 10, 411-419.

Tobler, P.N., Fiorillo, C.D., and Schultz, W. (2005). Adaptive coding of reward value by dopamine neurons. Science 307, 1642-1645.

Tolman, E.C. (1948). Cognitive Maps in Rats and Men.

Tye, K.M., and Janak, P.H. (2007). Amygdala neurons differentially encode motivation and reinforcement. The Journal of neuroscience : the official journal of the Society for Neuroscience 27, 3937-3945.

Vago, D.R., and Kesner, R.P. (2008). Disruption of the direct perforant path input to the CA1 subregion of the dorsal hippocampus interferes with spatial working memory and novelty detection. Behavioural brain research 189, 273-283.

Valenti, O., Mikus, N., and Klausberger, T. (2018). The cognitive nuances of surprising events: exposure to unexpected stimuli elicits firing variations in neurons of the dorsal CA1 hippocampus. Brain Structure and Function 223, 3183-3211.

Van Cauter, T., Poucet, B., and Save, E. (2008). Unstable CA1 place cell representation in rats with entorhinal cortex lesions. The European journal of neuroscience 27, 1933-1946.

van Groen, T., and Wyss, J.M. (1990a). The connections of presubiculum and parasubiculum in the rat. Brain research 518, 227-243.

van Groen, T., and Wyss, J.M. (1990b). Extrinsic projections from area CA1 of the rat hippocampus: olfactory, cortical, subcortical, and bilateral hippocampal formation projections. The Journal of comparative neurology 302, 515-528.

Van Groen, T., and Wyss, J.M. (2003). Connections of the retrosplenial granular b cortex in the rat. The Journal of comparative neurology 463, 249-263.

Verharen, J.P.H., den Ouden, H.E.M., Adan, R.A.H., and Vanderschuren, L.J.M.J. (2020). Modulation of value-based decision making behavior by subregions of the rat prefrontal cortex. Psychopharmacology 237, 1267-1280.

Vogt, B.A., and Miller, M.W. (1983). Cortical connections between rat cingulate cortex and visual, motor, and postsubicular cortices. The Journal of comparative neurology 216, 192-210.

Warburton, E.C., Baird, A., Morgan, A., Muir, J.L., and Aggleton, J.P. (2001). The conjoint importance of the hippocampus and anterior thalamic nuclei for allocentric spatial learning: evidence from a disconnection study in the rat. The Journal of neuroscience : the official journal of the Society for Neuroscience 21, 7323-7330.

Watts, A.G., Swanson, L.W., and Sanchez-Watts, G. (1987). Efferent projections of the suprachiasmatic nucleus: I. Studies using anterograde transport of Phaseolus vulgaris leucoagglutinin in the rat. The Journal of comparative neurology 258, 204-229.

Whittington, J.C.R., Muller, T.H., Mark, S., Chen, G., Barry, C., Burgess, N., and Behrens, T.E.J. (2020). The Tolman-Eichenbaum Machine: Unifying Space and Relational Memory through Generalization in the Hippocampal Formation. Cell 183, 1249-1263.e1223.

Wiener, S., Paul, C., and Eichenbaum, H. (1989). Spatial and behavioral correlates of hippocampal neuronal activity. The Journal of Neuroscience 9, 2737-2763.

Witter, M.P., and Groenewegen, H.J. (1990). The subiculum: cytoarchitectonically a simple structure, but hodologically complex. Progress in brain research 83, 47-58.

Witter, M.P., Van Hoesen, G.W., and Amaral, D.G. (1989). Topographical organization of the entorhinal projection to the dentate gyrus of the monkey. The Journal of neuroscience : the official journal of the Society for Neuroscience 9, 216-228.

Wixted, J.T., Goldinger, S.D., Squire, L.R., Kuhn, J.R., Papesh, M.H., Smith, K.A., Treiman, D.M., and Steinmetz, P.N. (2018). Coding of episodic memory in the human hippocampus. Proceedings of the National Academy of Sciences 115, 1093-1098.

Wood, E.R., Dudchenko, P.A., and Eichenbaum, H. (1999). The global record of memory in hippocampal neuronal activity. Nature 397, 613-616.

Wood, E.R., Dudchenko, P.A., Robitsek, R.J., and Eichenbaum, H. (2000). Hippocampal neurons encode information about different types of memory episodes occurring in the same location. Neuron 27, 623-633.

Wyass, J.M., and Van Groen, T. (1992). Connections between the retrosplenial cortex and the hippocampal formation in the rat: A review. Hippocampus 2, 1-11.
Wyss, J.M. (1981). An autoradiographic study of the efferent connections of the entorhinal cortex in the rat. The Journal of comparative neurology 199, 495-512.

ACKNOLEDGEMENT

오늘의 박사학위 논문을 작성하기까지 오랜 기간동안 제가 학문적으로 성장할 수 있도록 지도해주신 이인아 교수님께 고개 숙여 감사 인사를 드립니다. 평소 관심있었던 연구 주제를 선뜻 한번 해보라고 제안해주시고, 2~3 년 시행착오가 있음에도 불구하고 그 주제를 계속해서 연구할 수 있도록 믿고 지지해주셔서 오늘의 연구 성과를 얻을 수 있었던 것 같습니다. 연구뿐만 아니라 논문 작성, 학술 발표 등 연구자로써 피가 되고 살이 되는 많은 지식들을 배웠습니다. 다시 한번 감사드립니다. 그리고 2015 년도부터 끊임없이 제 연구에 관심가져주시고 연구에 대한 조언과 격려를 해주셨던 정민환 교수님께 감사인사를 드립니다. 마지막으로 다른 연구 활동으로 바쁘신 와중에도 박사 학위 심사에 참여해주셔서 연구 결과에 대한 깊이 있는 생각과 조언을 해주신 이석호 교수님, 정민환 교수님, 이상아 교수님, 이도윤 교수님께 감사드립니다.

박사 학위 기간 동안, 가족과 연구실 멤버들의 도움이 없었다면 무사히 박사 학위를 마치기 어려웠을 것 같습니다. 먼저, 7 년간 묵묵히 뒤에서 저를 믿고 기다려주신 부모님께 감사의 인사를 드립니다. 오랜 시간 지지해주신 덕분에 제가 연구에 매진하여 좋은 결과를 얻을 수 있었던 것 같습니다. 힘들 때마다 자식들을 위해 어떠한 일도 마다하지 않고 했던 부모님을 생각하면서 어려운 시기를 버텨낼 수 있었습니다. 그리고 낯선 타향인 서울에서 5 년간 함께 살며 서로 힘들때 의지하고 항상 힘이 되었던 저희 누나에게도 고맙다는 말을 전하고 싶습니다. 박사 과정을 밟고 있는 저한테 항상 '대단하다 내동생' 이라고 응원해주어서 많은 힘이 되었습니다. 그리고 제 삶의 나침판이 되어주고 힘든 시기에 삶의 지혜를 주시고 어려움을 헤쳐나가는데 도움을 주셨던 문규련, 이종문 선생님께 진심으로 감사드립니다. 1 학년때부터 같이 연구를 진행하며 힘든 시기를 함께 버텨내고 이겨냈던 요섭이형, 수술과 실험 분석등에 큰 도움을 주셨던 재롱이형, 전기생리학 데이터 분석에서 많은 도움을 주셨던 충희형, 수민이, 현우, 자전거를 함께 타며 힘들때마다 고민을 들어주고 큰 힘이 되어주셨던 승우형에게도 감사드립니다.

국문초록

장소와 그 가치를 저장하는 배측과 중간 해마의 차별적 역할

진승우

오래전부터 해마는 자신의 경험, 즉 일화 사건의 기억에 필수적인 영역으로 알려져왔습니다. 이러한 일화 사건에는 특정 장소에서 겪은 감정적 경험들이 기억으로 저장됩니다. 이러한 일화 기억의 특성을 고려하면, 해마는 감정 정보를 처리할 가능성이 매우 높고, 실제로 중간 해마와 복측 해마는 편도체로부터 해부학적으로 직접 연결되어 있습니다. 또한 중간 해마는 배측 해마로부터 많은 공간 정보를 받아드린다고 알려져있습니다. 따라서 중간 해마는 장소의 위치와 그 장소에서 경험한 감정정보를 연합할 가능성이 높습니다. 하지만, 중간 해마의 이러한 장소-감정 연합 기억의 역할은 거의 알려지지 않았다. 그래서, 저는 중간 해매가 특정 공간에서 발생하는 사건의 가치를 저장하는데 중요하고, 배측 해마는 정확한 위치 정보를 표상하는데 중요하다는 가설을 세웠습니다. 이를 검증하기 위해 쥐의 배측과 중간 해마의 개별 뉴런을 동시에 리코딩하였으며, 선호도가 다른 먹이를 이용해 장소의 가치 정보를 변화시키는 실험을 진행했습니다.

이 학위 논문의 첫 파트에서는 쥐가 2차원 공간에서 자유롭게 돌아다닐 때의 배측부터 복측해마의 장소 세포가 어떻게 달라지는지 살펴보았습니다. 구체

적으로, 중간해마보다 배측 해마에서 장소 선택적 활동이 더 강하게 나타났으며, 복측 해마에서는 장소 세포의 활동이 거의 관찰되지 않았습니다. 두번째 파트에서, 해마가 필요없는 간단한 과제에서 먹이의 가치가 바뀐 이후에, 배측과 복측 해마의 장소 세포의 공간 표상 변화를 살펴보았습니다. 주어진 공간에서 제공되던 맛있는 먹이가 맛없는 먹이로 바뀌고 나면, 중간 해마의 장소세포는 재빠르게 공간 표상을 재배열하게 됩니다. 하지만, 동일한 조작에서 배측 해마의 장소세포는 공간 표상을 일정하게 유지하였습니다. 마지막으로, 세번째 파트에서는 해마가 필요한 기억 과제에서 가치-의존적 공간 재배열을 추가적으로 알아보았습니다. T 모양의 미로에서 장소 선호 과제를 진행하는 동안, 중간 해마의 장소 세포는 맛있는 먹이가 나오는 공간을 집중적으로 표상하며, 이러한 집중된 표상은 맛있는 먹이의 위치가 바뀌어도 동일하게 관찰됩니다. 반면, 배측 해마 장소 세포의 공간 표상은 이러한 조작에 거의 영향을 받지 않습니다. 그리고 이 장소 선호 학습을 하는 동안, 배측 해마보다 중간 해마의 신경망 상태가 빠르게 변하는 모습을 보였습니다.

종합하자면, 위 결과들은 배측 해마와 복측 해마는 서로 다른 기능을 맡고 있다는 점을 보여줍니다. 즉, 배측 해마는 동물의 정확한 장소를 표상하는데 특화되어 있으며, 중간 해마는 장소와 그 가치 정보를 연합하는 역할을 맡고 있습니다. 이러한 발견은 중간 해마가 행동 선택과 밀접한 정보를 처리하며, 이러한 정보를 내측 전두엽을 통해 다른 뇌 영역과 소통하는 기능적으로 중요한 영역이라는 것을 시사합니다.